DUDLEY KNOX LIBRARY
NAVAL POSTGRADUATE SCHOOL
MONTEREY, CALIFORNIA 93943-5002

NAVAL POSTGRADUATE SCHOOL
Monterey, California

THESIS

MATHEMATICAL MODELS FOR THE S.D.I.

by

Yoram Ilan-Lipowsky

June 1987

Thesis Co-Advisors: Beny Neta
M.F. Platzer

Approved for public release; distribution is unlimited

T233076

UNCLASSIFIED
SECURITY CLASSIFICATION OF THIS PAGE

REPORT DOCUMENTATION PAGE

1a REPORT SECURITY CLASSIFICATION UNCLASSIFIED	1b RESTRICTIVE MARKINGS
2a SECURITY CLASSIFICATION AUTHORITY	3 DISTRIBUTION/AVAILABILITY OF REPORT Approved for public release; distribution is unlimited
2b DECLASSIFICATION/DOWNGRADING SCHEDULE	
4 PERFORMING ORGANIZATION REPORT NUMBER(S)	5 MONITORING ORGANIZATION REPORT NUMBER(S)
6a NAME OF PERFORMING ORGANIZATION Naval Postgraduate School 6b OFFICE SYMBOL (If applicable) Code 53	7a NAME OF MONITORING ORGANIZATION Naval Postgraduate School
6c ADDRESS (City, State, and ZIP Code) Monterey, California 93943-5000	7b ADDRESS (City, State, and ZIP Code) Monterey, California 93943-5000
8a NAME OF FUNDING/SPONSORING ORGANIZATION 8b OFFICE SYMBOL (If applicable)	9 PROCUREMENT INSTRUMENT IDENTIFICATION NUMBER
8c ADDRESS (City, State, and ZIP Code)	10 SOURCE OF FUNDING NUMBERS PROGRAM ELEMENT NO / PROJECT NO / TASK NO / WORK UNIT ACCESSION NO

11 TITLE (Include Security Classification)
MATHEMATICAL MODELS FOR THE S.D.I.

12 PERSONAL AUTHOR(S)
Ilan-Lipowsky, Yoram

13a TYPE OF REPORT	13b TIME COVERED	14 DATE OF REPORT (Year Month Day)	15 PAGE COUNT
Master's Thesis	FROM ____ TO ____	1987, June	153

16 SUPPLEMENTARY NOTATION

17 COSATI CODES			18 SUBJECT TERMS (Continue on reverse if necessary and identify by block number)
FIELD	GROUP	SUB-GROUP	Orbits; Railgun; Reentry; Homopolar Generator

19 ABSTRACT (Continue on reverse if necessary and identify by block number)

SDI technologies may affect the concepts of weapons systems and reshape the battlefields of the future. In this research a few of the SDI systems were analyzed and modeled mathematically. The different models were gathered in a software package that may be run on a personal computer. The intention was to produce a handy tool for preliminary studies and designs.

The following topics are covered: aerodynamic design of hypervelocity projectiles, flight simulation of hypervelocity projectiles, railgun simulation, ground track of orbits, guidance and homing.

A few case studies were analyzed to suggest and demonstrate potential use of these models.

20 DISTRIBUTION/AVAILABILITY OF ABSTRACT	21 ABSTRACT SECURITY CLASSIFICATION
☒ UNCLASSIFIED/UNLIMITED ☐ SAME AS RPT ☐ DTIC USERS	Unclassified

22a NAME OF RESPONSIBLE INDIVIDUAL	22b TELEPHONE (Include Area Code)	22c OFFICE SYMBOL
Professor Beny Neta	(408) 646-2235	Code 53Nd

DD FORM 1473, 84 MAR 83 APR edition may be used until exhausted
All other editions are obsolete

SECURITY CLASSIFICATION OF THIS PAGE
UNCLASSIFIED

Approved for public release; distribution is unlimited

Mathematical Models for the S.D.I.

by

Yoram Ilan-Lipowsky
Lt. Col., Israeli Air Force
B.SC., Technion Israel, 1969

Submitted in partial fulfillment of the
requirements for the degree of

MASTER OF SCIENCE IN AERONAUTICAL ENGINEERING

from the

NAVAL POSTGRADUATE SCHOOL
June 1987

ABSTRACT

SDI technologies may affect the concepts of weapons systems and reshape the battlefields of the future. In this research a few of the SDI systems were analyzed and modeled mathematically. The different models were gathered in a software package that may be run on a personal computer. The intention was to produce a handy tool for preliminary studies and designs.

The following topics are covered: aerodynamic design of hypervelocity projectiles, flight simulation of hypervelocity projectiles, railgun simulation, ground track of orbits, guidance and homing.

A few case studies were analyzed to suggest and demonstrate potential use of these models.

TABLE OF CONTENTS

I. INTRODUCTION ---------- 8

II. THE DRAG MODEL (AERODYNAMICS COEFFICIENT ESTIMATION) ---------- 11

A. GENERAL ---------- 11

B. THE MATHEMATICAL MODEL ---------- 11

C. THE COMPUTER CODE ---------- 20

D. USING THE MODEL ---------- 21

III. THE RAILGUN MODEL ---------- 25

A. GENERAL ---------- 25

B. THE MATHEMATICAL MODEL ---------- 31

C. THE COMPUTER CODE ---------- 61

D. USING THE MODEL ---------- 62

IV. THE FLIGHT SIMULATION MODEL ---------- 71

A. GENERAL ---------- 71

B. THE MATHEMATICAL MODEL ---------- 72

C. THE COMPUTER CODE ---------- 84

D. USING THE MODEL ---------- 85

V. THE GROUND TRACK MODEL ---------- 94

A. GENERAL ---------- 94

B. THE MATHEMATICAL MODEL ---------- 94

C. THE COMPUTER CODE ---------- 99

D. USING THE MODEL ---------- 101

VI. THE GUIDANCE MODEL ---------- 104

A. GENERAL ---------- 104

B. THE MATHEMATICAL MODEL ---------- 105

C. THE COMPUTER CODE ---------- 111

D. USING THE PROGRAM ---------- 111

VII. THE COMPUTER AND THE PROGRAMMING LANGUAGE ------- 114

A. THE COMPUTERS ---------- 114

B. THE PROGRAMMING LANGUAGE ---------- 114

C. RUNNING THE MODEL ON THE MAINFRAME ---------- 115

VIII. CASE STUDIES ---------- 119

A. GENERAL ---------- 119

B. CASE STUDY 1--PARAMETRIC STUDY OF THE PERFORMANCE OF A RAILGUN SYSTEM ---------- 119

C. CASE STUDY 2--SENSITIVITY OF THE RANGE TO ERRORS IN LAUNCH CONDITIONS ---------- 125

D. CASE STUDY 3--SEABORNE SYSTEM ---------- 128

E. CASE STUDY 4--AIRBORNE SYSTEM ---------- 135

IX. RECOMMENDATIONS ---------- 147

APPENDIX: THE ATARI ST-1040 COMPUTER ---------- 149

LIST OF REFERENCES ---------- 151

INITIAL DISTRIBUTION LIST ---------- 152

ACKNOWLEDGEMENTS

This research was conducted in conjunction with the research program being conducted by Prof. Neta in coordination with Dr. D. Parks of the Naval Surface Weapons Center.

This work would not have been possible without the continued guidance and excellent cooperation shown me by my thesis advisors: Prof. Neta of the Department of Mathematics and Prof. Platzer of the Department of Aeronautical Engineering. I also want to thank Prof. Woehler of the Physics Department for his constructive remarks on the chapter on the railgun simulation.

I would like to thank the library staff and especially the research group under Mrs. Candas Walker for their invaluable support in locating references.

I also want to thank my family for their unlimited patience in allowing me to spend so many uninterrupted nights working on the computer. I'd especially like to thank my son Oded (age 10) for his contribution in using the full capabilities of the ATARI-ST Computer due to his amazing level of familiarity with the machine.

I want to thank the entire staff of the Naval Postgraduate School for the high level of teaching and for

providing such an excellent environment for creative thought.

I am most grateful to my commanders in the IDF for allowing me to choose the Naval Postgraduate School for advanced study.

Many thanks to Miss Laura Deeriack, my English teacher, for guiding me through the labyrinth of the English language.

Finally, my appreciation to my typist, Bob Lande, for overcoming my unreadable manuscript.

I. INTRODUCTION

In March 23, 1983 the President of the United States announced he was:

> directing a comprehensive and intensive effort to define a long-term research and development program to achieve our ultimate goal of eliminating the threat posed by strategic nuclear missiles.

In 1984 the Department of Defense established an organization to expand and accelerate research in this area. The research program was called the "Strategic Defense Initiative," better known as the SDI.

Since that day, research and studies on the subject continue at an accelerated rate. There is also a growing controversy over the potential of various SDI technologies and the possibilities for applying them in affordable weapon systems that would be effected when needed.

Despite the controversy over the SDI system's ability to achieve its strategic role, there is a wide acceptance that SDI technologies may also affect the concepts of weapons systems and reshape the battlefields of the next century. It is therefore important to study the additional non-SDI contributions that SDI technologies could make on the future.

In this research a few of the SDI weapon systems were analyzed and modeled mathematically. The various models were gathered in a software package that may be run on an

inexpensive desk-mounted personal computer. This analytical tool was built to assure an easy access system. It will allow the user to learn, to study and even to perform a preliminary design of future weapon systems based on these technologies. The emphasis was to provide a system that will allow a very quick, interactive and easy-to-operate working tool.

Most models were written in ST-Basic. They make use of the rich graphics capabilities of the ATARI ST-1040 computer. The machine-language version was compiled for most models. A Fortran version of the orbit model was produced and run on the IBM mainframe. This version is used whenever very long cases are run, and the graphic presentation is not needed.

The system was built in modules. By using this approach, it became easier to add more modules or to improve the existing ones, easily. In the process of this research, models were designed on the following topics:

a. Aerodynamic design of hyper-velocity projectiles.

b. Flight simulation of hyper-velocity projectiles.

c. Evaluation of the railgun performance.

d. Ground track of orbits.

e. Guidance and homing.

Other models for study of these topics do exist. However, most of them are very sophisticated and complex. The majority of them were written to be operated on large

mainframes. Some of them can be used only by experts in those specific fields.

The approach of this work was to create a very simple and handy tool to use. It was prepared for use by system engineers and weapons designers that need to know the "big picture" without going deeply into the fine details of each component. This approach is very important in the preliminary design phase, in which many iterations are done until a well-balanced preliminary design is achieved.

Whenever a more accurate and refined study is needed, a more sophisticated model has to be used. The use of this simple model will assure the efficient use of the sophisticated models because the tasks will be better defined and the user will have previous experience with the topics.

In the following chapters each module of the mathematical models will be explained. A few case studies will be given in order to suggest and demonstrate potential use of these models. Conclusions and recommendations will close this research report.

II. THE DRAG MODEL (AERODYNAMIC COEFFICIENTS ESTIMATION)

A. GENERAL

The purpose of the Aerodynamic Coefficients Estimation model is to provide initial values for the preliminary design. The designer gives as an input the value of the main geometrical parameters that determine the shape of the body. The model, based on double interpolation of aerodynamic graphs produce as an output the values relevant to the chosen shape. The program also provides a scaled scheme of the body and the limitations of the center of gravity location to assure stability.

After studying the output the designer may either decide to change the input parameters and to start a new design iteration, or if he is satisfied with the results, he may proceed to the next phase of the design.

B. THE MATHEMATICAL MODEL

1. List of Constants

The list of constants used in this model is given in Table 2.1. The following description is given for each constant:

a) The text symbol

b) The definition

c) The value

d) The units.

TABLE 2.1

LIST OF CONSTANTS

SYMBOLS	MEANINGS	VALUES	UNITS
PI	PI	3.14	Non Dimen.
F	SCREEN RATIO	79/33	Non Dimen.

2. List of Variables

The list of variables used in this model is given in Table 2.2. The following is given for each variable:

a) The program code symbol

b) The text symbol

c) The definition

d) The units.

TABLE 2.2

LIST OF VARIABLES

SYMBOLS		MEANINGS	UNITS
Computer Code	Text		
X1	X_1	X coordinate of point 1	Non Dimen.
X2	X_2	X coordinate of point 2	Non Dimen.
X3	X_3	X coordinate of point 3	Non Dimen.
YA1	Y_{A1}	Y coordinate of point 1, Curve A	Non Dimen.
YA2	Y_{A2}	Y coordinate of point 2, Curve A	Non Dimen.

TABLE 2.2 (CONTINUED)

SYMBOLS		MEANINGS	UNITS
Computer Code	Text		
YA3	Y_{A3}	Y coordinate of point 3, Curve A	Non Dimen.
YB1	Y_{B1}	Y coordinate of point 1, Curve B	Non Dimen.
YB2	Y_{B2}	Y coordinate of point 2, Curve B	Non Dimen.
YB3	Y_{B3}	Y coordinate of point 3, Curve B	Non Dimen.
YC1	Y_{c1}	Y coordinate of point 1, Curve C	Non Dimen.
YC2	Y_{c2}	Y coordinate of point 2, Curve C	Non Dimen.
YC3	Y_{c3}	Y coordinate of point 3, Curve C	Non Dimen.
YD1	Y_{d1}	Y coordinate of point 1, Curve D	Non Dimen.
YD2	Y_{d2}	Y coordinate of point 2, Curve D	Non Dimen.
YD3	Y_{d3}	Y coordinate of point 3, Curve D	Non Dimen.
CD	C_d	Coefficient of drag	Non
AD	d	Cone half angle	Deg
AR	θ	Cone half angle	Rad
RNRB	R_r	Ratio of radii	Non Dimen.
L	L	The cone length	m
RP	R	The radius of cone base	m
XCP	X_{cp}	Location of C.g. (measured from nose tip)	m

TABLE 2.2 (CONTINUED)

SYMBOLS		MEANINGS	UNITS
Computer Code	Text		
VP	V_p	The cone volume	in^3
MP	M_p	The cone mass	kg
XS	X_s	X coordinate selected	Non Dimen.
YS	Y_s	Y coordinate selected	Non Dimen.
ZS	Z_s	Z value at X_s, Y_s	Non Dimen.
X		X coordinate	Non Dimen.
Y		Y coordinate	Non Dimen.
Z		The function value	Non Dimen.

3. Basic Assumptions and Relations

The construction of this model is based upon the following basic assumptions and relations:

a. For this preliminary design, only the particle dynamics of the projectile are relevant. In reality vehicular angular motions exist, and alter the new flow field, and hence also affect the heat transfer mechanism. In this model it was assumed that a single average value of the coefficient of drag may properly represent the aerodynamic characteristics of a non-maneuvering projectile during launch and reentry, and the earth's atmosphere.

b. Since most of the cases of interest are related to hypersonic flight, the value of the drag coefficient is independent of the Mach number.

c. It is also assumed that most relevant reentry bodies may approximate a blunt cone. (Atmospheric flights of hypersonic speeds demand that frictional drag be smaller relative to the pressure drag to prevent overheating.) The engineering implications of this demand are that reentry and high hypersonic launched

projectiles must have large pressure drag, i.e., blunt shape.

d. The shape of blunt-cone (see Figure 1.1) may be satisfactorily defined by the following two parameters:

   a. The cone half angle (θ)

   b. The ratio of cone nose radius to base radius (R_r).

e. The function of the drag coefficient vs. cone bluntness (for a constant value of cone half angle) may be approximated by polynomials (fourth degree polynomials were used in this version).

f. The graph of cone drag vs. cone bluntness of [Ref. 1] was chosen to represent the data base for this model.

g. The function of the drag coefficient (C_d) vs. the cone half angle (for any given value of cone nose radius to base radius ratio) may be approximated by a polynomial.

h. The calculation of the location of the center of pressure is based on [Ref. 2] where an analysis was described for conical noses. Based on this analysis it is assumed that the location of the center of pressure is:

$$X_{cp} = (L)(2/3)\sec^2\theta$$

where:

X_{cp} is the location of the center of pressure measured from the nose tip

L is overall length of the nose

θ is the cone, half angle.

This is considered a conservative approach that includes a safety factor, whenever the projectile includes, besides the nose, also tail and/or fins.

i. An estimate of the projectile volume and mass is given. The estimate is based on the volume of a blunt cone. The mass estimate is based on a typical value for a specific weight for guided warheads [Ref. 3].

4. Method of Solution

The data base for this program was provided as a 4 curve-graph (see Figure 2.1). Each curve represents the function of the drag coefficient (C_d) vs. the ratio of the cone nose radius to the base radius for a known value of cone half angle (θ). These curves are typical of other aerodynamic curves that represent the value of an aerodynamic variable as a function of one geometric variable while other geometric values are held constant. This is the common method of presenting the empirical results of aerodynamic tests that normally are done in a similar method (running over values of one parameter while holding the value of other parameters constant). In more general terms, it is a case of function f that relates the value of a variable z to the values of two others, x,y (see Figures 2.2 and 2.3). The values of z = z(x) are given for a few values of constant value of y (y serving as a parameter).

The aerodynamic data in this specific case consists of 3 curves: Curves A, B, and C. Every curve is represented by a set of values of the drag coefficient (z) versus the cone angle (y) and the radius ratio (x). For each point:

$$Z_{Mn} = f(X_{Mn}, Y_{Mn})$$

where the notations are:

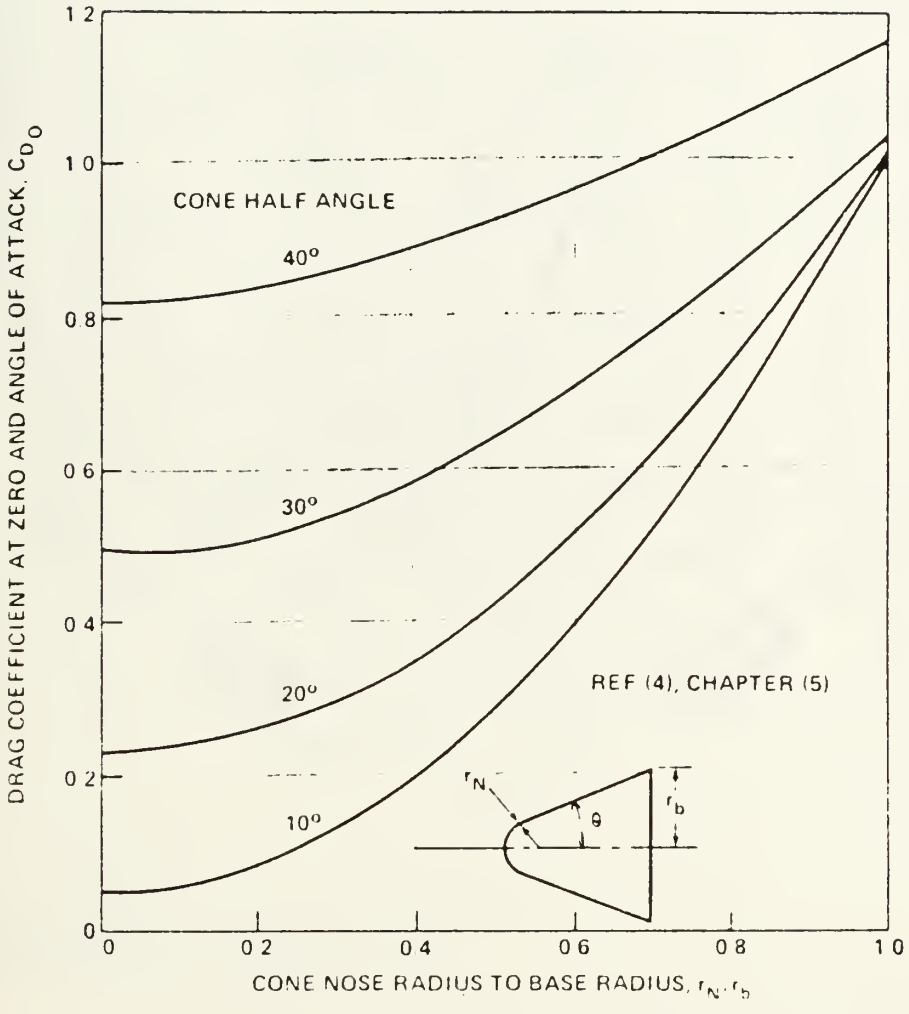

Figure 2.1 C_d vs Cone Bluntness

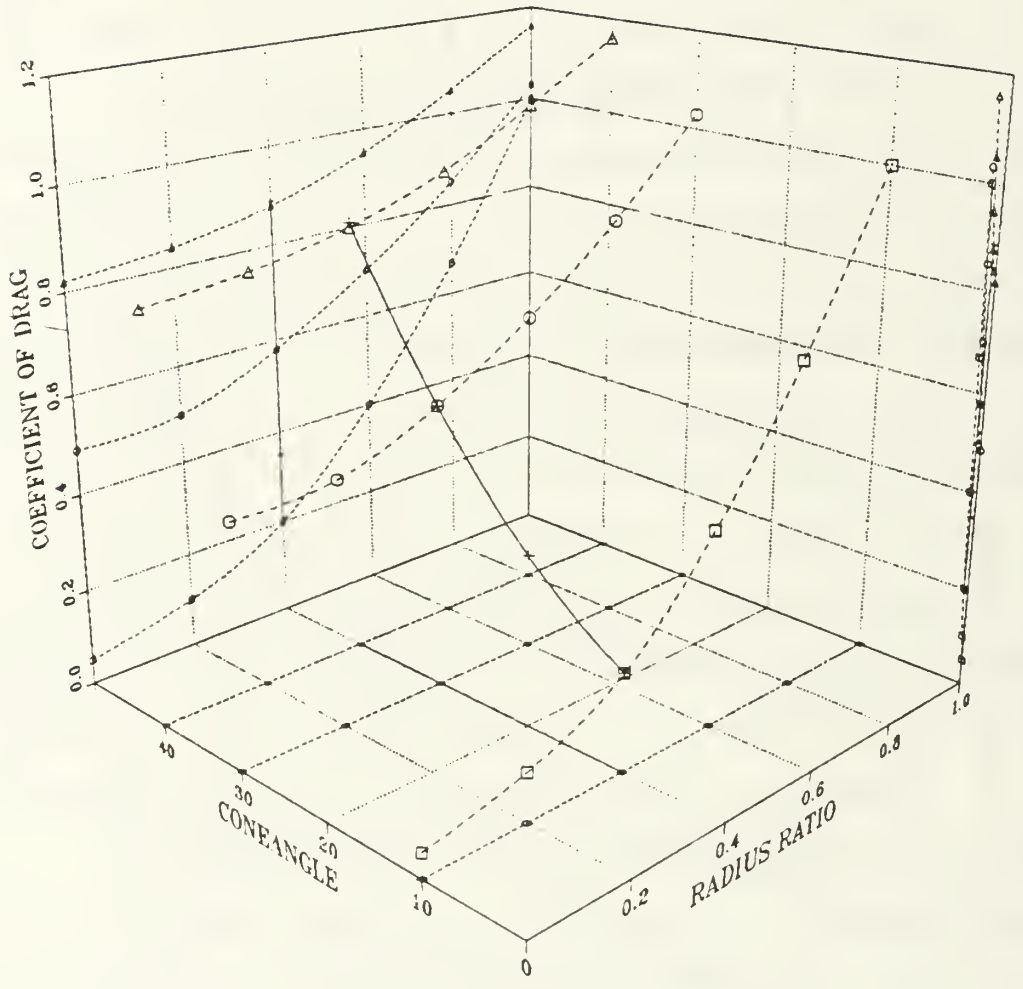

CD VS CONE ANGLE, RADIUS RATIO

Figure 2.2 Three Dimensional Presentation of $C_d = C_d(\theta, R_n)$

Z=Z(X,Y)

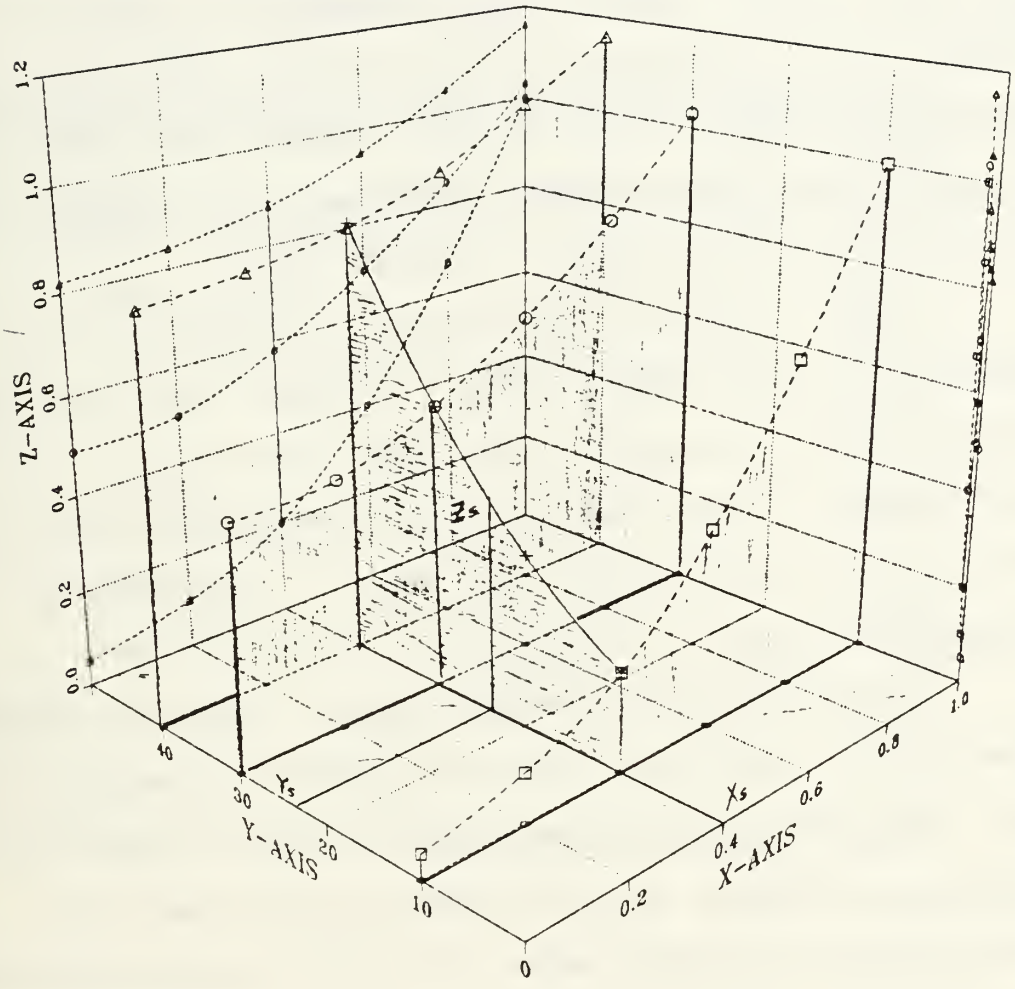

AT POINT XS,YS ZS=Z(XS,YS)

Figure 2.3 Three Dimensional Presentation of z = z(x,y)

M = the curve (A, B, or C)

n = Serial number of the point.

The first module of this model is responsible to produce for each function (represented by values of z vs. values of x) an interpolating polynomial. The interpolating polynomials were given in the Lagrangian form. (The Lagrangian form was selected because it is suitable for the general nonuniformly-spaced x values case).

When a specific value of $Z_S = f(X_S,Y_S)$ for a given value of $x = X_S$ and $y = Y_S$ is needed, the next module (first-interpd) produces first the functions of $z = f(y)$ (see Figure 2.3) for the selected value of $x = X_S$. This is done by interpolation of all the $Z = Z(x)$ curves at the value of $x = X_S$.

The next module (second-interpd) takes the different values of Z's as a function of y (x held constant, $x = f(X_S)$ and constructs a new polynomial $z = z(y)$. For the same reason as before, the Lagrangian form was used. By interpolation the approximate value of z at the selected $y = Y_S$ is found. This is the value of $Z_S = Z(X_S,Y_S)$ at the selected X's and Y's.

C. THE COMPUTER CODE

1. General

The computer code was written originally in ST-BASIC. The code includes the following modules:

a) START--starts the program, defines values of parameters and gets input

b) CDCURVE--defines the function of $C_d = C_d(\theta, R_r)$

c) DEWCRW--draws the curves on the screen

d) CDCALC--calculates the value of C_d by double interpolation

e) NewCon--presents the results and draws the shape of the new cone

f) Weight--calculates and presents estimates of the cone weight and volume.

2. Flow Charts

Flow charts of the program code are shown in Figure 2.4.

D. USING THE MODEL

1. Input

As input to the program the following variables are needed:

a. The cone half angle

b. The ratio of cone nose radius to base radius.

To assist the user the input screen represents the data base and the meaning of the input, graphically.

2. Output

a. General

The output of this model is given by graphic representations and numerical values on the screen. A typical output is shown in Figure 2.5.

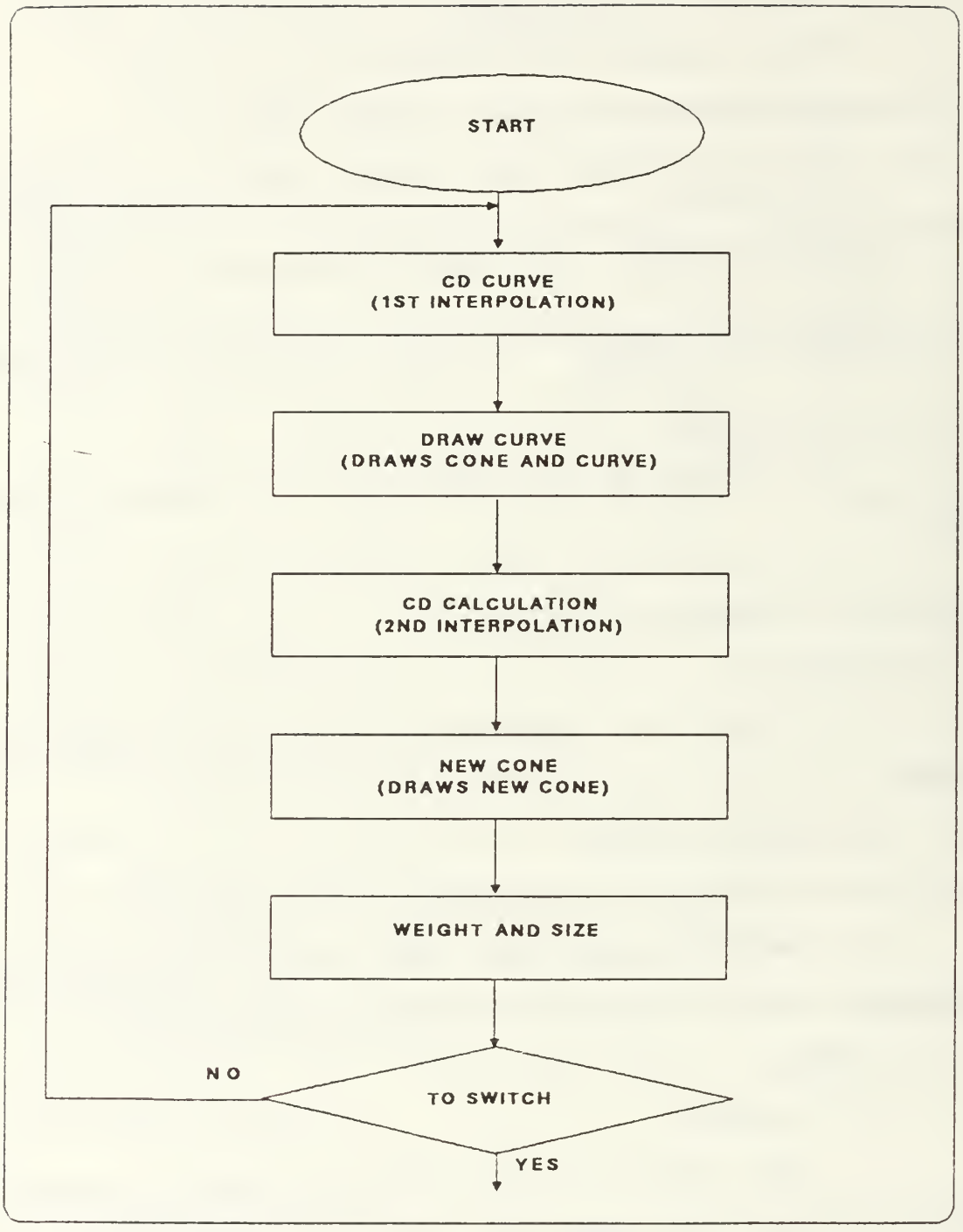

Figure 2.4 Flowchart of CD Cone Program

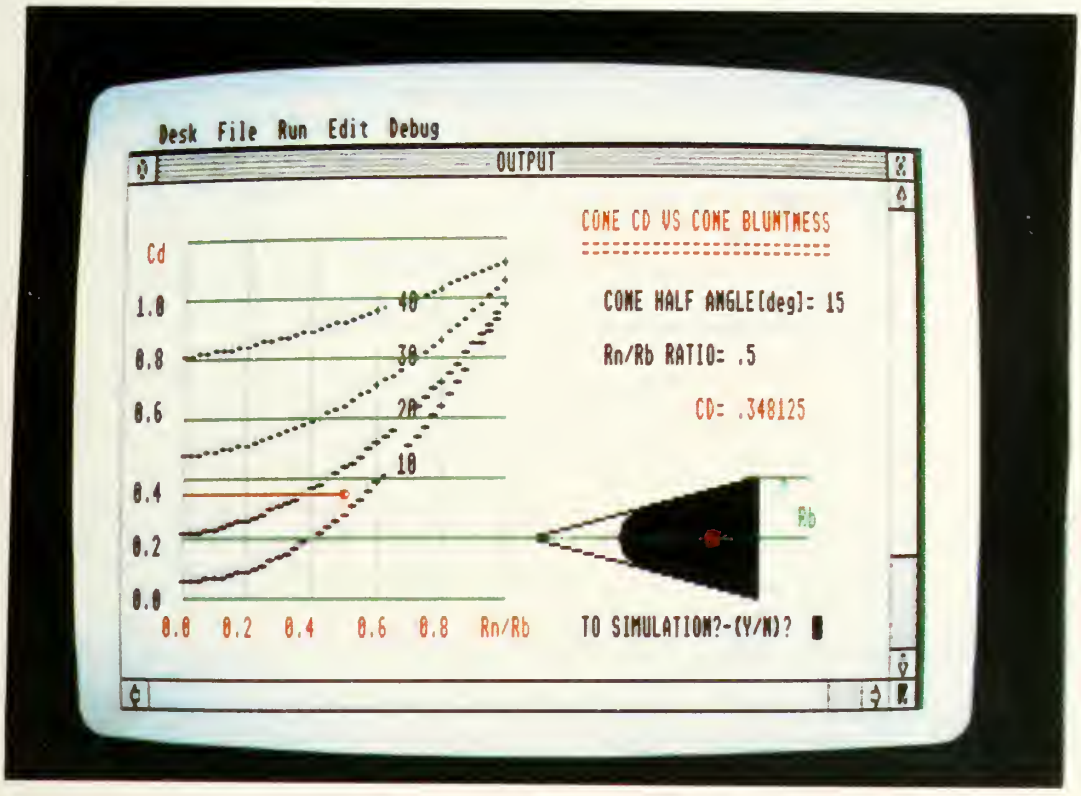

Figure 2.5 Typical Output

b. Graphics

The graphical representation includes the following elements:

1) The graph of $z = z(x,y)$

2) On the graph the values of the selected variables X_s, Y_s are shown beside the value of the dependent variable ($Z_s = Z(X_s,Y_s)$).

3) A scale scheme of the body is drawn. The scheme provides the designer with a graphic representation. The location of the center of pressure ($X_{c.p.}$) is marked clearly on the symmetric axis of the body.

c. Numerical Results

The values of the following parameters are shown digitally on the output screen:

1) Coefficient of drag (C_d)

2) The cone mass (M_p)

3) The cone volume (V_p).

Estimated values of the projectile volume and mass are calculated if desired. The calculation is based upon the measure of the projectile base radius.

III. THE RAILGUN MODEL

A. GENERAL

1. Background

Electromagnetic rail launcher concepts (railguns) have existed since the early 1900's. The work of Rashleigh and Marshall (1978) and Barber (1972) gave credence to the potential of railgun accelerators. The research was revived at the Australian National University (1972) using a single large inductor as the power source. More recently a Lawrence Livermore National Laboratory/Los Alamos National Laboratory team has successfully demonstrated the use of explosively driven magnetic flux compression generators to power a variety of rail launchers. Theoretical and practical researches and works are continuing in several directions, predominantly in the United States. This model is based mainly on the open literature about railgun studies. The studies sponsored by NASA concerning the feasibility assessment of earth-to-space railgun launchers for launching nuclear waste disposal into space were found to be valuable references. They were also used to examine and validate this model.

2. Railgun--The Basic Principles

An electromagnetic railgun consists of two conducting rails (electrodes), between which a conducting

element with an attached projectile is placed. Electric current is passed along one electrode through the conducting portion (armature) of the conductor/projectile and back along the other electrode (see Figure 3.1). The current, I, flowing through the projectile armature, interacts with the magnetic flux generated by the current loop, resulting in an I x B force in the direction parallel to the rails (as indicated on Figure 3.1). The projectile is free to slide along the rails. The I x B force accelerates the projectile as long as the current continues to flow and the conductor remains in electrical contact with the rails.

3. Power Supply and Conditioning

In order to fire the projectile from the railgun, power has to be supplied from a power source. A conditioning system has to transfer this power to suitable wave form that will assure maximum efficiency.

The demand from the power supply system is dependent both on the total input energy needed per shot and the rate of shooting. The power supply system must be suitable to the carrier of a railgun. Basically the following main options for power supply exist:

a. Static ground system--in this case power may be supplied either from the local power grid or from a special system designed for this purpose.

b. Movable terrain system--this system would rely on a self-contained power system that would assure continuous operation of the weapon system.

c. Seaborne system--in this case the power supply would originate either from the vessel (ship/submarine)

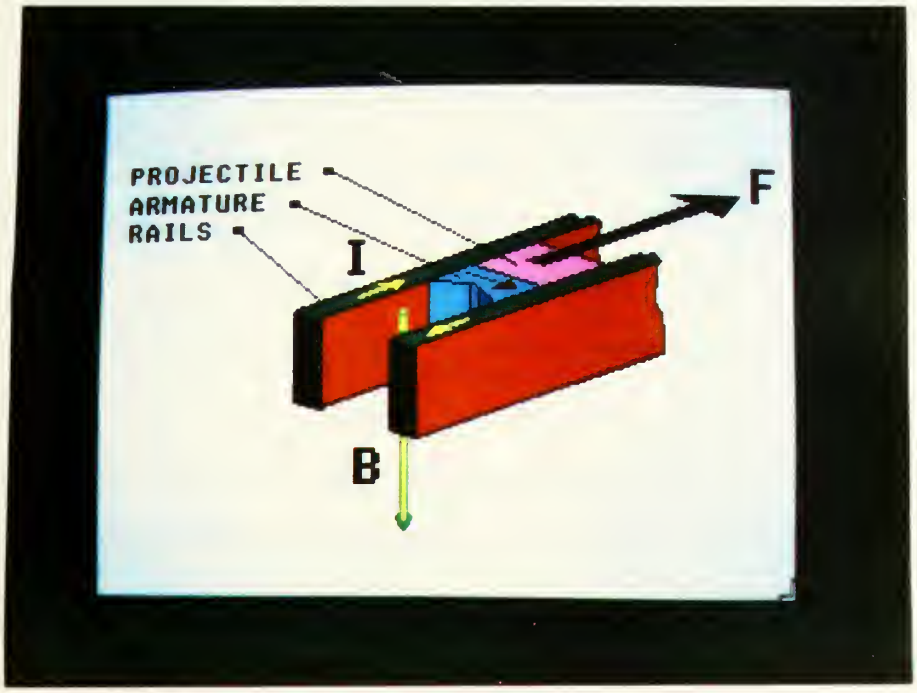

Figure 3.1 The Railgun

power system or from a special power supply system dedicated to this mission.

d. Airborne system--same options as in the seaborne case. In addition, the power system has to be light and comply with the standards and demands for airborne systems.

e. Space system--power supply is difficult to achieve and expensive to produce. The magnitude of power needed to fire a railgun would require an enormous solar panel or a large nuclear power source.

The power supply from the primary source is not in a suitable form to be used by the railgun. A power conditioning system is needed in order to produce the huge pulse of power for such a short duration.

The power conditioning system is demonstrated in Figure 3.2. The power from the primary supply unit is transformed by a power transmission bus to a DC-DC converter that regulates the voltage in order to transfer it to the energy storage device. The energy is kept for a short period in the energy storage unit until the moment when the gun is fired and the switch is closed.

A pulse forming network creates the final shape of the power and sends it to the rails.

The short-time storage contains the high energy just before sending it in its suitable form to the railgun. It may be either an electric system (capacitive system based on energy storage by capacitors) or an inductive system (in which the energy is stored in a mechanical form as a rotational speed of a heavy flywheel of a homopolar generator).

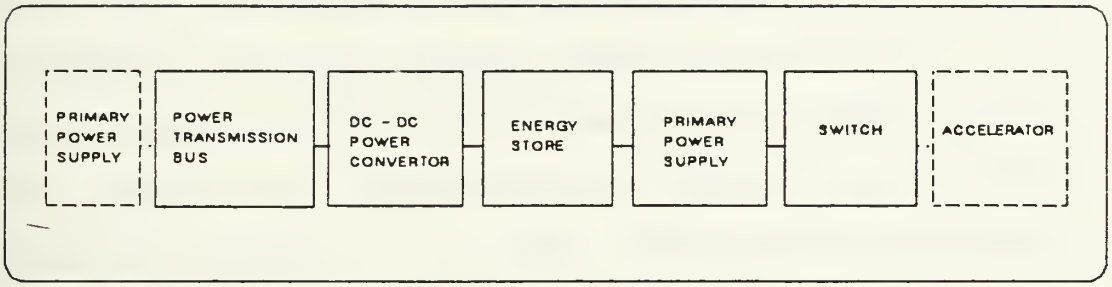

Figure 3.2 Power Conditioning System

The inductive based systems are much more efficient for storing energy and producing the suitable waveform for the railgun. Most efforts in recent years were aimed at improving those systems and to make them suitable for airborne and space operation. The main interest is now focused on the distributed energy railguns.

In the distributed energy store railguns the energy sources required to power the gun are distributed along the length of the barrel. When firing, a traveling wave of current accelerates the projectile by sequential switching of energy sources distributed along the rails.

The first major demonstration of this idea was the construction of the homopolar generator (HPG) at the Australian National University (ANU) in Canberra. This machine demonstrated that it was possible to make very large electromechanical energy stores in the range of 1 Gj range. The energy is stored in the form of rotational kinetic energy of heavy (ten tons) rotors. When needed the full energy can be extracted electrically into a suitable circuit.

It was also demonstrated by the Canberra HPG that solid brushes can be used to carry the huge currents for the short acceleration-time involved.

The success of the Canberra HPG led other groups to apply the same techniques.

At the University of Texas at Austin, a 10 M_j machine was operated in 1981. It was found that these machines were not efficient enough and only about 6 percent of the mass of the energy was actually used for energy storage. This situation led to a new concept in inductive-based power conditioning systems in which all the mass of the magnetic circuit can be used as a rotational energy device. This model is based on the most recent data about these machines that were available in the open literature. Other new concepts of inductive systems, like the reverse railgun concept (fast moving armature is producing the current wave) and the explosive driven flux compression concept were not modeled in this work.

B. THE MATHEMATICAL MODEL

1. List of Constants

The list of constants used in this model is given in Table 3.1. The following description is given for each constant:

a) the program code symbol
b) the text symbol
c) the definition
d) the value
e) the units.

2. List of Variables

The list of variables used in this model is given in Table 3.2. The following is given for each variable:

TABLE 3.1

LIST OF CONSTANTS

SYMBOLS		MEANING	VALUES	UNITS
Computer Code	Text			
PI	π	Pi	3.14	Non Dimen.
F	f	Screen ratio	79/33	Non Dimen.
Lo	L_o	Inductance	3	
Uo	μ_o	Mag. permeability	$1.26*10^{-6}$	H
Ur	μ_r	Resistivity coper.	$20*10^{-9}$	Ohm's/m
AMAX	A_{max}	Max acceleration of the projectile	100,000	g's
SPCWP	ρ_p	Specific weight of the projectile	3000	KG/m^3
SPCWR	ρ_r	Specific weight of the rails	9000	KG/m^3
SPCWS	ρ_s	Specific weight of the structure	2000	KG/m^3
RYIELD	σ_y	Yield stress of the rails	600,000,000	N/m^2
KGKW1	ρ_{pA}	Specific weight per power-- airborne	0.2	Kg/KWATT
KGKW2	ρ_{pm}	Specific weight per power-- maritime	0.4	Kg/KWATT
KGKW3	ρ_{ps}	Specific weight per power--solar	5.3	Kg/KWATT
EDC	ε_{dc}	Efficiency of the DC-DC converter	0.92	Non Dimen.
EC	ε_c	Efficiency of the capacitive storage	0.97	Non Dimen.

TABLE 3.1 (CONTINUED)

SYMBOLS		MEANING	VALUES	UNITS
Computer Code	Text			
E	ε_{in}	Efficiency of the inductive storage	0.99	Non Dimen.
EL	ε_{L}	Efficiency of the pulse forming network	0.99	Non Dimen.
Ehp	ε_{hp}	Efficiency of the homopolar generator	0.8	Non Dimen.
TLN	T_{LN}	Temperature of liquid nitrogen	77	^{o}K
TACM	T_{rm}	Max rail temp.	45^{o}	^{o}K
	$\rho_{s.l.}$	Density of air at sea level	1.25	Kg/m^3
FAIR	F_{cl}	Ratio of cooling area to surface area	10	Non Dimen.

TABLE 3.2

LIST OF VARIABLES

SYMBOLS		MEANING	UNITS
Computer Code	Text		
T	t	Time from the start of acceleration	Sec
X	X	X coordinate along the barrel length	m
VP	V_p	Velocity of the projectile (along X)	M/sec

TABLE 3.2 (CONTINUED)

SYMBOLS		MEANING	UNITS
Computer Code	Text		
Vmax	V_{max}	Max velocity of the projectile (along X)	m/sec
L	L	Inductance per unit length of rails	Henry
Lp	L'	Inductance per unit length of rails	Henry/m
Lo	L_o	Inductance of the storage and wiring	Henry
R	R	Resistance	Ohms
Lmax	L_{max}	Max allowable value of barrel length	m
Rp	R_p	Resistance per unit length of rails	Ohm/meter
Ro	R_o	Resistance of the storage and wiring	Ohm
I	I	Electric current	Amp
Io	I_o	Electric current time T = 0	Amp
F	F	Force	Newton
E	E	Energy	Joule
Eres	E_r	Resistance energy	Joule
Eloss	E_l	Energy loss	Joule
Einduc	E_i	Inductance energy	Joule
DPI	E_{pi}	Energy for power inputing	Joule
Ek	E_k	Kinetic energy of the projectile	Joule
Es	E_s	Energy storage	Joule

TABLE 3.2 (CONTINUED)

SYMBOLS		MEANING	UNITS
Computer Code	Text		
EFRrg	ε	Efficiency of the railgun	Non Dimen.
EFc	ε_c	Efficiency of the capac. energy store	Non Dimen.
EFpc	ε_{PC}	Total power conditioning efficiency	Non Dimen.
B	B	Coefficient of rail drag	N/(m/S)
H	h	Height of rails	m
W	w	Distance between rails	m
Ar	AR	Rails cross area	m^2
dS	ds	The structure width	m
AS	AS	Structure cross area	m^2
MB	M_B	Mass of the barrel	Kg
Mr	M_r	Mass of the rails	Kg
Mpwrs	M_{pg}	Mass of the power supply system	Kg
Mpwrc	M_{pc}	Mass of the total conditioning system	Kg
Epc	ε_{pc}	Efficiency of conditioning system	Non Dimen.
Mbc	M_{bc}	Mass of the power transmission bus	Kg
Mc	M_c	Mass and efficiency of the capac. energy stor.	Kg
Msw	M_{SW}	Mass and efficiency of the switch of the rails	Kg
Mdc	M_{dc}	Mass and efficiency of the DC-DC converter	Kg

TABLE 3.2 (CONTINUED)

SYMBOLS		MEANING	UNITS
Computer Code	Text		
Mpf	M_L	Mass and efficiency of the pulse forming system	Kg
Mhpg	M_{hp}	Mass of the homopolar generator	Kg
Mind	M_{in}	Mass of the inductance power storage	Kg
MSW	M_{sw}	Mass of the switching network	Kg
Mgnt	M_g	Mass of the quantity of ammunition	Kg
Mstro	M_{st}	Mass of railgun structure	Kg
Mtotal	M_t	Total mass of the full railgun system	Kg
V	V	Volume	m^3
Vind	V_{in}	Volume of the inductance power storage	m^3
Vhpg	V_{hg}	Volume of the homopolar generator	m^3
Vind	V_{ind}	Volume of the inductance power storage	m^3
VSW	V_{sw}	Volume of the switching network	m^3
PPS	f	Rate of fire	Pulse/sec
PWR	P_{wr}	Average power supply to rails	Watts
KGPKW	W_p	Specific weight per power	Kg/KW
FE	F_m	Electromagnetic force	N
FF	F_f	Friction force	N

TABLE 3.2 (CONTINUED)

SYMBOLS		MEANING	UNITS
Computer Code	Text		
Mp	M_p	Total mass (projectile--sabot)	Kg
ESD	δ	Electrical skin depth	m
ta		Acceleration time	sec
R1	R_1	Long radius of ellipse	m
R2	R_2	Short radius of ellipse	m
TINDUC	T_{in}	Temperature of inductor	^oK
TRAD	T_r	Temperature of radiator	^oK
TAIR	T_{air}	Temperature of air	^oK
TWTR	T_{wtr}	Temperature of sea water	^oK
TR	T_r	Temperature of rails	^oK
DETEMP	DT	Temperature difference	^oK
FAIR	$\rho h/\rho s.l$	Density ratio	
VAIR	V_{air}	Airspeed	m/s
MTOTAL	K_t	Coefficient of heat (TOTAL)	W/K^oCm^2
KWTR	K_{wtr}	Coefficient of heat transfer to water	W/K^oCm^2
KCOPPER	K_{cp}	Coefficient of heat of copper	W/K^oCm^2
KAIRW	K_{air}	Coefficient of heat transfer to air	W/K^oCm^2
KAlUM	K_{al}	Coefficient of heat of aluminum	W/K^oCm^2
TALUM	K_{Al}	Temperature of aluminum plates	^oK
TCOPPER	T_{cp}	Temperature of copper plates	^oK

TABLE 3.2 (CONTINUED)

SYMBOLS		MEANING	UNITS
Computer Code	Text		
MCOOL	M_{cl}	Mass of the cooling system	Kg
VCOLL	V_{cl}	Volume of the cooling system	m^3

a) The program code symbol

b) The text symbol

c) The definition

d) The units.

3. Basic Assumptions and Relations

a. General

The assumptions and relations that are used to conduct this model are described below. They were gathered in groups. Each group is related to one of the different physical aspects of the model. The description of the following groups of assumptions is given in this chapter:

1) The railgun model

2) The railgun structure and mass estimation

3) The power supply

4) Capacitive based power conditioning system

5) Inductive based power conditioning system

6) The cooling system

7) The system efficiency.

b. The Railgun Model

(1) The Equation of Motion. The electromagnetic force (F_{EM}) acting on the projectile is given by [Ref. 4]:

$$F_{EM} = L'I^2/2$$

where:

L' is the inductance per unit length of the rails

I is the current.

The equation of motion of the projectile in the barrel is:

$$M \frac{dV_p}{dt} = F_{EM} - F_f$$

where:

M is the mass of the project (plus the sabot)

V_p is the projectile velocity

F_{EM} is the electromagnetic force

F_f is the friction and drag force.

The electromagnetic force in the railgun is rising to huge values. In order to achieve good conductivity with low friction the projectile is mounted during the acceleration process in a specially designed sabot. If the railgun is located in low altitude (on a ship on land or on a low flying airplane) and the dense air may cause aerodynamic drag on the projectile, a specially

designed pumping system may be installed in order to achieve a low pressure at the barrel before shooting. Therefore, it may be assumed that the electromagnetic accelerating force is much larger than the friction force. As a result, the friction and drag forces may be considered negligible on this model:

$$F_{EM} >> F_f$$

Under these assumptions the equation of motion has the following form:

$$M \frac{dV_p}{dt} = L \cdot I^2$$

The mass, M, is the total mass accelerated by the railgun. It includes the projectile and the sabot. For the purpose of this model it was assumed that the sabot mass is about 25% of the projectile mass. [Ref. 5] Once the projectile leaves the muzzle, the sabot is detached from the projectile and decelerates because of its high aerodynamic drag.

(2) The Electrical Circuit. The electrical circuit of the railgun is shown schematically in Figure 3.3. This circuit may be presented in the form:

$$V - \frac{d}{dt}(LI) - RI = 0$$

The inductance L may be represented as a function of the projectile location along the barrel (x).

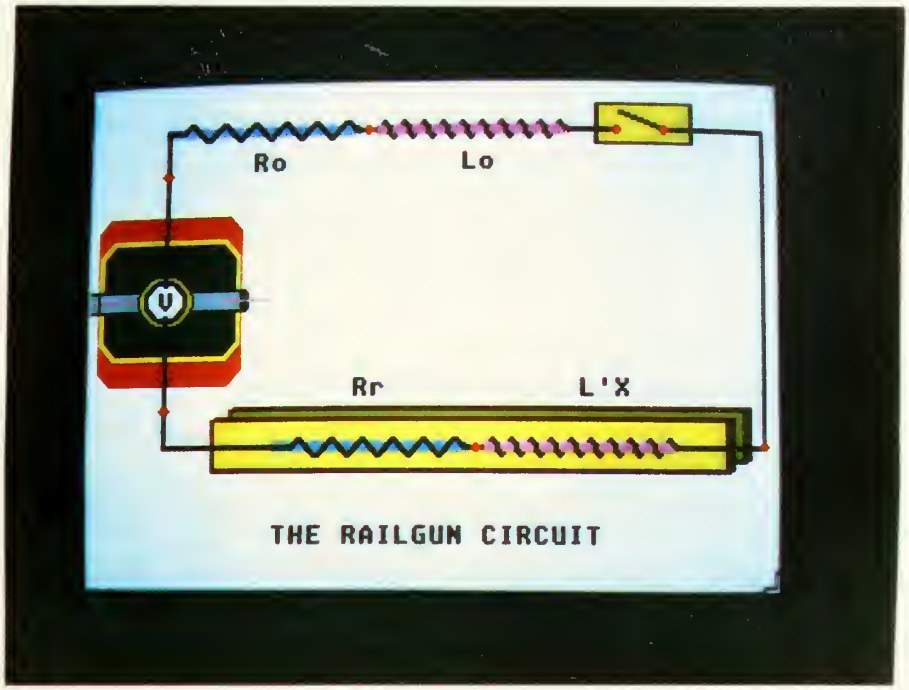

Figure 3.3 The Electric Circuit

$$L = L'x$$

By using this relation we get:

$$\begin{aligned}\frac{d}{dt}(LI) &= \frac{dL}{dt} I + L \frac{dI}{dt} \\ &= L'I \frac{dx}{dt} + L \frac{dI}{dt} \\ &= L'IV_p + L \, dI/dt\end{aligned}$$

and the circuit equation now has the form:

$$V - L'IV_p - L \frac{dI}{dt} - RI = 0 .$$

(3) The Railgun Cycle. In order to fire a series of projectiles the railgun must be operated cyclically. The cycle involves: charging of intermediate storage devices by the main power supply, loading a projectile, accelerating it through the barrel, and finally restoring the system to the initial conditions.

This firing cycle is repeated at a rate determined by the rate of fire. In this model it is assumed that an analysis of a single cycle may represent all cycles in a series of repetitive shots.

The process of transferring the electrical power generated by the primary source to kinetic energy of the projectile is involved with considerable energy losses. The main mechanisms and magnitudes of energy losses during the process were modeled here.

For an inductive driven railgun the process starts by accelerating the homopolar generator by an electric motor, a gas turbine or any other device. During the charging of the inductor energy is dissipated in the inductive store and the charging circuits due to resistive losses. When the switch is operated current flows into the accelerator. Most of the energy is imparted into the pellet, the rest is dissipated resistively in the rails. After the process is over, some residual magnetic energy may still be stored in the inductor and the accelerator. A large fraction of this energy may be dissipated by arcing at the muzzle. The energy is deposited in the thermal and kinetic energy of plasma.

(4) The Resistive Losses. The resistive losses during a cycle of acceleration may be divided into two parts: circuit resistance and rail resistance. The resistance of the circuit and therefore the losses can be reduced by increasing the cross sectional area of the conductor or by use of the superconductors techniques. For the purpose of this model it is assumed that circuit resistive losses may be considered negligible compared to the rail resistance losses. [Ref. 6]

The current flows in the rails during the acceleration phase. The process is very fast and the resistance of the rails changes continuously during acceleration as the current propagates through the rails.

The resistance is further affected by the "velocity skin effect" which confines the current to a thin sheet on the rail surface. [Ref. 4] The finite rate of current diffusion into the rails must be considered in order to properly evaluate the rail resistance. The incremental resistance equation for the rails is:

$$\frac{dR_r}{dt} = 2\,\eta_r V/h\,\delta$$

where:

R_r is the rail resistance

η_r is the rail resistivity.

V_p is the projectile velocity

h is the height of the rails

δ is the electrical skin depth.

The electrical skin depth (δ) was derived [Ref. 7] from the diffusions of a step function of a current into a conductor as:

$$\delta = (\pi \eta_r t/\mu_o)^{1/2}$$

where:

t is the time after the start of application of the current.

The equations were combined to give the rail resistance as a function of time.

$$R_r = (2(\mu_o \mu_r/\pi)^{1/2}/h) \int_0 \frac{V_p}{t^{1/2}} \, dt \, .$$

(5) Inductive Losses. The inductive energy stored in the circuit is given by:

$$E_{ind} = (L_o + L'x)I^2/2$$

where:

L_o is the storage inductance

L' is the inductance per unit length of the accelerator

X is the position of the projectile

I is the current.

At the beginning of the process (X = 0) all the energy is stored in the storage inductor

$$E_{ind(X=0)} = L_o \, I^2/2$$

During the acceleration process x increases and some energy begins to be stored inductively in the rail. At the end of the process the residual energy in the storage inductor is conserved. The inductive energy on the rails is lost. As a result the loss of inductive energy per cycle may be considered to be:

$$E_{ind} = L'xI^2/2$$

c. Railgun Mass Estimation

The estimation of the railgun mass is based on a barrel configuration as illustrated in Figure 3.4. It is a

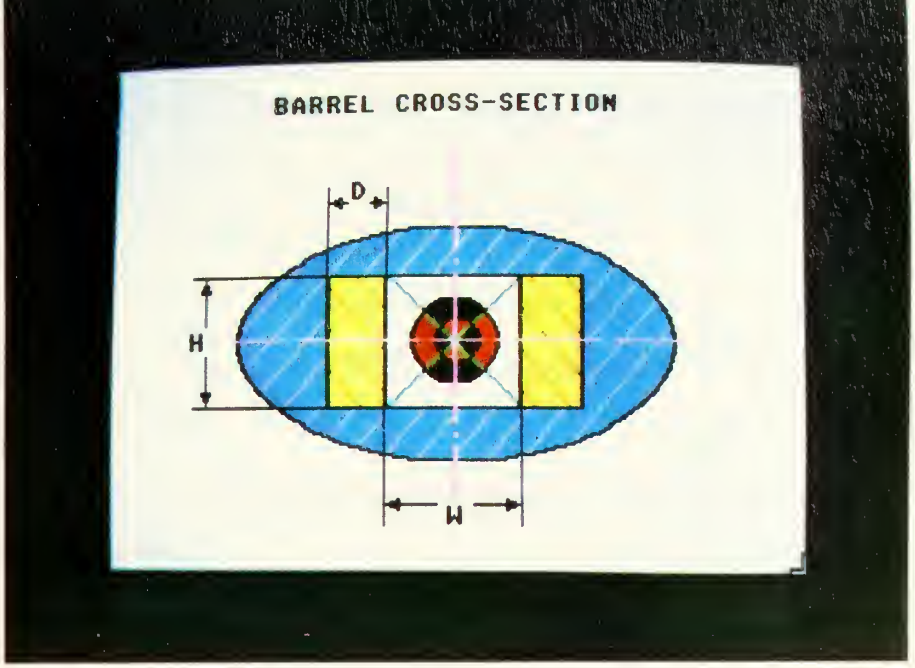

Figure 3.4 The Barrel Cross Section

simple rectangular copper bar embedded in a plastic structure reinforced by fiber. The plastic cover serves also as an insulation material for the barrel.

The cross section area of the rails (A_r) is given by:

$$A_r = 2h\ dr$$

Rail thickness (dr) must be at least equal to the electric skin depth of copper for the acceleration time (τ). Thicker rails do not result in lower resistive losses! From weight consideration in this model the rail thickness was assumed to be the minimum necessary--equal to the skin depth.

The mass of the rails depends on their cross section (A_r), their density (ρ_r) and their length (X):

$$M_r = \rho_r A_r X$$

The pressure stress on the barrel is carried mainly by the barrel structure. From conservative considerations it is assumed that the full recoil force is acting on the fiber reinforced plastic in which the rails are embedded.

The typical yield stress (σ_s) of such materials is about 600,000,000 N/m^2. The recoil force (F_r) is given by:

$$F_r = M \cdot a$$

The minimal cross section area (A_s) needed to withstand the load is given by:

$$A_s = F_r/\sigma_s = M \cdot a/\sigma_s$$

The mass of the structure (M_s) is given by:

$$M_s = \rho_s A_s X$$

where ρ_s is the density of the fiber-reinforced plastic (typical value of density might be around 3000 Kg/m^3).

The mass of the total barrel (M_B) is, therefore, the sum of the rails' mass (M_r) and the structure mass (M_s):

$$M_B = M_r + M_s \ .$$

A very important constraint for the design of the system is imposed by the maximum value of acceleration in which the projectile and its internal systems can withstand safely. The model does include a check on this value wherein the calculated value of the acceleration exceeds the maximum value permitted, the model sends a warning.

The height of the rails is primarily a function of the dimensions of the projectile. For this purpose it was assumed that the mass of the projectile plus the sabot may be represented by a prism with a square cross section. The length of the prism is about five times the side of the square section.

If the average density of the accelerated mass is ρ_a (typical value of 1500 Kg/m^3) is used, the total mass is given by:

$$M_a = M_p + M_s = \rho_a V_a = \rho_a 5 h_r^3$$

where:

M_a is the total mass accelerated

M_p is the projectile mass

M_s is the sabot mass

h_r is the rail height.

The value of the rail height is therefore given by:

$$h_r = [(M_p + M_s)/5\ _a]^{1/3}$$

If an elliptical cross section is chosen for the barrel, the net structural area of the barrel cross section is given by:

$$A_s = \pi R_1 R_2 - h_r\ (2dr + w)$$

where:

R_1, R_2 are the two radii of the ellipse

h_r is the rail height

d_r is the rail width

w is the distance between rails.

d. Power Supply

The model of the power supply system is based upon the following assumptions and relations:

(1) The total power supply needed is a function of both the amount of energy needed per cycle and the number of cycles per time unit (rate of fire):

$$PWR = E_k * f/\varepsilon$$

where:

PWR is the energy per cycle
f is the rate of fire (pulses per second)
ε is the overall efficiency of the process.

(2) The weight of the power supply system is dependent on the power required and the type of the power supply system. Typical values of specific weight per power (W_p) were chosen to represent the following types of systems:

(a) For airborne systems (f_2)--0.5 Kg/KWatts
(b) For seaborne systems (f_m)--1.0 Kg/KWatts

(c) For solar spatial based systems (f_S)--5.3 Kg/KWatts

Land based systems may get their supply either from military type generators or from a local electric grid.

The weight of nuclear spatial based power systems is a more complex function of the power produced. The specific weight per power of the system is given by [Ref. 7]:

$$W_p = 5.3 - (PWR/1000 - 2000) * 17 \quad [Kg/Kw]$$

The value of the specific weight per power does not decrease beyond the value of 1.0 [Kg/Kw] no matter how high the value of PWR will be.

e. Capacitive Based Power Conditioning System

The mass and volume of the capacitive based power conditioning are the sum of masses and volumes of the major elements. The models of the subsystem are based on [Ref. 8]. The main parameters that affect the size of the power conditioning system are: the stored energy (per shot), the power needed, the various efficiencies of the subsystems, and the characteristic acceleration time.

The capacitive based system mass is therefore:

$$M_{pc} = M_{BC} + M_{DC} + M_C + M_L + M_{SW}$$

where:

$$M_{BC} = 7.7 * 10^{-8} P^{3/2}$$

$$M_{DC} = 10 + 0.057 P_{PC}^{1/2} + 0.014 P_{PC}^{3/4} + 1 * 10^{-4} P_{PC}$$

$M_C = 0.011\ E_s$

$M_{SW} = 1.74 * 10^{-6}\ E_s / a$

$ML = 3.08 * 10^{-4}\ E_s$

The overall capacitive based system efficiency is given by the relations [Ref. 8]:

$$\varepsilon_{pc} = \varepsilon_{BC}\ \varepsilon_{DC}\ \varepsilon_C\ \varepsilon_L$$

where:

$\varepsilon_{BC} = 1 - .66 * 10^{-6}\ P^{1/2}$

$\varepsilon_{DC} = 0.082$

$\varepsilon_C = 0.97$

$\varepsilon_L = 0.99$

where:

M_{PC}, ε_{PC} are the total power conditioning mass and efficiency

M_{BC}, ε_{BC} are power transmission bus mass and efficiency

M_{DC}, ε_{DC} are the DC-DC converter mass and efficiency

M_C, ε_C are the capacitive energy store mass and efficiency

M_L, ε_L is the pulse forming network mass and efficiency

M_S ε_s is the switch mass and efficiency

P is the total average power output of the source

P_C $= \varepsilon_{BC}\ P$

P_{DC} is the input power to the DC converter

E_s is the stored energy (for one shot)

τ_a is the characteristic projectile acceleration time.

f. Inductive Based Power System

The system concept is illustrated in Figure 3.5. A gas turbine was chosen as the primary power source for this model. The turbine shaft is connected to the homopolar generator which charges an inductive energy storage. A repetitive switch is used to connect and disconnect the railgun from the inductive energy storage and the generator circuit.

The turbine might be a typical turbo-shaft engine (like those used in turboprop engines or helicopters) or a specially designed turbine activated by a gas generator.

The modeling of the inductive based power conditioning system is founded mainly on recent information gathered from publications and the literature. Most data came from the IEEE Transactions on Magnetics dedicated to the third symposium on Electromagnetic launch technology [Ref. 8].

In this model, the volume and the weight of the system were estimated to be as follows: the system volume and mass are the sum of its three major components:

a) the homopolar generators,

b) the inductor, and

c) the switching network.

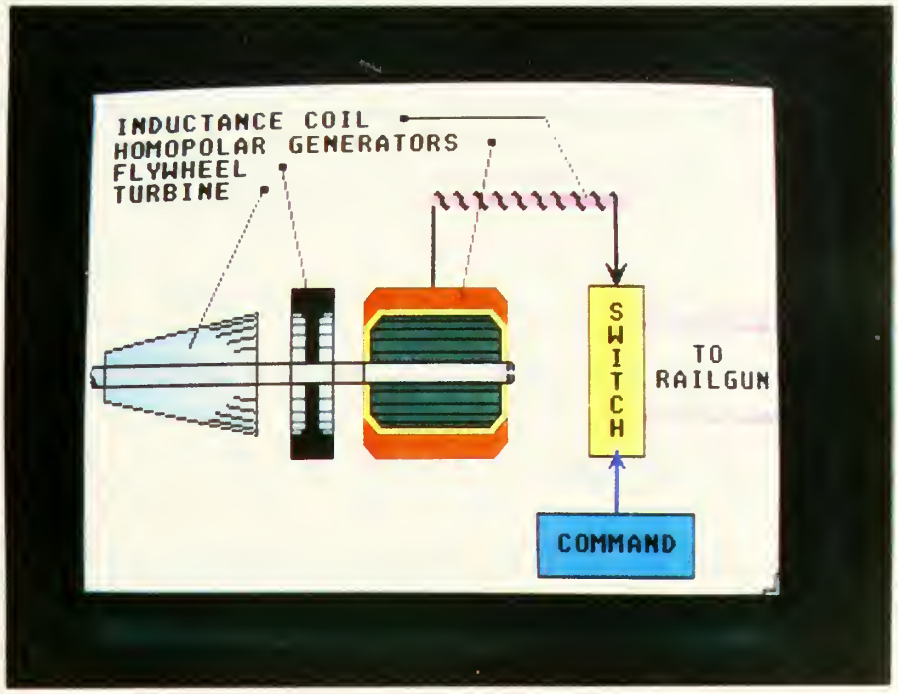

Figure 3.5 Inductive Power System

Hence:

$$M = M_{HP} + M_{IN} + M_{sw}$$

$$V = V_{HP} + V_{IN} + V_{sw}$$

where:

M_{HP}, V_{HP} are the mass and volume of the homopolar generator

M_{IN}, V_{IN} are the mass and volume of the inductance

M_{sw}, V_{sw} are the mass and volume of the switching network.

The volume and mass of the homopolar generation are proportional to the energy stored (for one shot).

$$M_{HP} = K_{MHP}\, E_s = K_{MHP}\, E_k / \text{ hp}$$

$$V_{HP} = K_{VHP}\, E_s = K_{VHP}\, E_k / \text{ hp}$$

where:

E_s is the maximum energy storage (per shot)

K_{MHP} is the specific volume (per energy unit)

K_{VMP} is the specific volume (per energy unit)

ε_h is the efficiency of the homopolar generator.

The values of K_{MHPG} and K_{VHPG} [Ref. 8] are:

K_{MHP} = 0.178 ton/mg (10 ion/56 mg)

K_{VHP} = 0.068 cubic m/mg (0.9^2 hs/56 mg)

The estimate for the volume and the mass of the inductor system is based on [Ref. 8]. The estimate is done for inductors of the coaxial type. These inductors are chosen because they produce no external magnetic fields that may damage the conveyor (orbiter, airplane, ship or submarine). Their mass and volume are dependent linearly on their temperature. A 48 Mg aluminum inductor cooled by liquid nitrogen has a mass of 1.5 tons and its dimensions are: 1.8 m--diameter and 1.5 m--length. At 151° room temperature (15° C) the same amount of energy may be stored in inductor having 10 times more mass and about twice the size. The temperature dependent model for estimating the inductor mass and volume is therefore:

$$M_{IN} = 1.5 + \frac{(15-1.5)}{(288-T_{in})}(T_{in} - T_{LN})$$

$$V_{IN} = [\pi(0.9)^2 1.5][1 + 7(T_{in}-T_{LN})]$$

where:

M_{IN} is the inductor mass [Kg]

V_{IN} is the inductor volume [cubic meter]

T_{in} is the inductor temperature [Kelvin]

T_{LN} is the liquid nitrogen boiling temperature.

The bus and the switching network of the inductive system are about one to two orders of magnitude smaller than similar devices of a capacitive based [Ref. 8]

conditioning system. Therefore a good estimate for their mass and volume is given by:

$$M_{sw} = [1.74 * 10^{-6} E_s / a]/30$$

$$V_{sw} = M_{sw}/S_{sw}$$

$$S_{sw} = 7,500 \text{ Kg/m}^3$$

where:

M_{sw} is the mass of the bus and the switching network

V_{sw} is the volume of the bus and the switching network

S_{sw} is the specific weight of the bus and the switching network.

g. The Cooling System

The low efficiency of the railgun system implies that large amounts of wasted heat must be rejected. For an efficient operation and in order to prevent structural problems, the rails temperature must be kept under 450^{o} K [Ref. 8]. A cooling system is needed in order to reject the wasted heat and to prevent the temperature from rising above the permitted limit.

For space-based systems the most promising cooling device is derived from the heat pipe concept. The estimated mass of the heat pipe system is the following function of the cooling power and the radiator temperature:

$$M_r = 1.95 * 10^8 \, Tr^{-4} \, P_r$$

where:

M_r is the mass of the heat pipe system

T_r is the temperature of the radiator

P_r is the radiated power.

To estimate the size and the weight of an airborne cooling system, the standard methods of heat transfer calculation were applied [Ref. 8]. The air approaches the cooling fins in its ambient temperature and density. The wasted heat flows through the fins and is transferred to the passing air. This model accounts for the following relevant parameters: airspeed, altitude, fin size and fin thermal characteristics.

The overall conductance of the heat (Kt) has the following relation with the metal conductance (Kal) and the metal-to-air conductance (K_{air}):

$$\frac{1}{K_t} = \frac{1}{K_{air}} + \frac{1}{K_{al}}$$

The value of the metal-to-air conductance is the following function of the airspeed and relative density affected by the altitude:

$$K_{air} = [4 + 80/500(V_{air}-100)](\rho_{air}/\rho_{s.l.})$$

The railgun temperature is limited to 450^{o} K. The ambient temperature of the air is a function of the altitude. The same model of the atmosphere as for the

flight simulation was used. The difference between these two temperatures is therefore:

$$DT = T_r - T_{air}$$

where:

DT is the temperature difference

T_{air} is the ambient temperature of the air
$T_{air} = T_{air}(H)$

T_{rm} is the maximum rail temperature (450° K).

The estimate of the surface area of the cooling system is given by:

$$M_{cl} = A_{cl} * W_{cl} * \rho_{cl}$$

where:

M_{cl} is the mass of the cooling surface

W_{cl} is the average width of the cooling surface

ρ_{cl} is the specific weight of the fins material (aluminum alloys)

A_{cl} is the cooling system "surface area"

where:

K_{air} is the metal to air conductance

V_{ar} is the airspeed

$\rho_{air}/\rho_{s.c}$ is the relative density.

The amount of wasted heat is a function of the power and the efficiency of the whole railgun system. Therefore:

$$P_{cl} = P_{wr}(1 - \varepsilon)$$

where:

P_{cl} is the cooling power

P_{wr} is the input power

ε is the railgun efficiency.

The cooling power on the other hand is given by:

$$P_{cl} = K_T * DT * A_{cl} * F_{cl}$$

where:

K_T is the heat conductance

DT is the temperature difference

A_{cl} is the surface area of the cooling system

F_{cl} is the ratio of cooling area (including the fins) to the surface area.

The estimate of the size and the weight of the seaborne cooling system was done in a similar way.

The following differences between the air-cooling system and the water cooling system were taken into account:

a) The heat transfer is from the fins to the flowing water (dependent on the ship speed)

b) The temperature of the sea (assumed to be 10^{o} C--283^{o} K)

c) The fins being made of copper.

h. System Efficiency

In order to evaluate the overall efficiency (ε) of the accelerating process, an efficiency factor is defined. The factor is the ratio of the kinetic energy of the projectile at the muzzle (E_M) to the input energy (E_{pi}) that was supplied to the railgun by the primary power source. Therefore:

$$\varepsilon = \frac{E_k}{E_{pi}}$$

The input energy that is supplied to the system during one cycle either diverted to kinetic energy of the projectile or is lost in the process. So:

$$E_{pi} = E_k + E_l$$

where:

E_{pi} is the total energy input

E_k is the kinetic energy of the projectile at muzzle

E_l is the energy loss.

4. Method of Solution

The numerical solution of the differential equations is achieved by a modified Euler method. According to this method, in order to improve the accuracy of the results, the values of the variables are taken as the sum of their value at the start of the interval plus half the value of their differential in the interval dt. According to this method

the differential equations of the model take the following form:

$$\Delta V = LI^2 \, \Delta t/2 \, M_p$$

$$\Delta X = (V + \Delta V/2) \, t$$

$$\Delta R_r = 2(\eta_r \eta_o/\pi(t+\Delta t/2))^{1/2}(V+\Delta V/2)\Delta t/h$$

$$\Delta I = -(L'(V+\Delta V/2) + R_o + (R_n+\Delta R_r/2))I\Delta t/(L_o+L_1(X+\Delta X/2)$$

$$V = V + \Delta V$$

$$X = X + \Delta X$$

$$R_r = R_r + \Delta R_r$$

$$I = I + \Delta I$$

$$t = t + \Delta t.$$

C. THE COMPUTER CODE

1. General

The computer code was written in ST-BASIC. The code includes the following modules:

a) Input--defines the values of the parameters and receives input

b) Simulation--numerical solutions of the model. The simulation stops when one of these conditions is met, for example desired speed reached, length of barrel exceeds maximum value

c) Railgun--designs and presents the railgun structure according to the simulation results

d) Power system--calculates and presents the main parameters of the electrical components (primary power supply, conditioning system, switches, etc.)

e) Weight and volume--gives an estimate of the weight and volume of all major components

f) Cooling system--gives an estimate of the weight and size of the cooling system. The estimate is based on the wasted heat power and on the environmental conditions

g) Weight and volume--summarizes the estimates of the weight and size of all major components of the system. The sum of the weight and the volume of the whole system is shown numerically on the screen.

h) End--this module controls the communication with the user. Decisions can be made either to run the code again or to chain directly to the flight simulation program.

2. Flowcharts

Flowcharts of the program code are given in Figure 3.6.

D. USING THE MODEL

1. Input

The input to the computer includes the following parameters and initial conditions:

a) The projectile mass (MP)

b) The initial current (I_o) at time t = 0

c) The desired velocity

d) The maximum value of the barrel's length permitted.

The code includes many values of parameters. These values can be altered by standard editing of the code. In addition, the cooling system module asks for input about the environmental conditions.

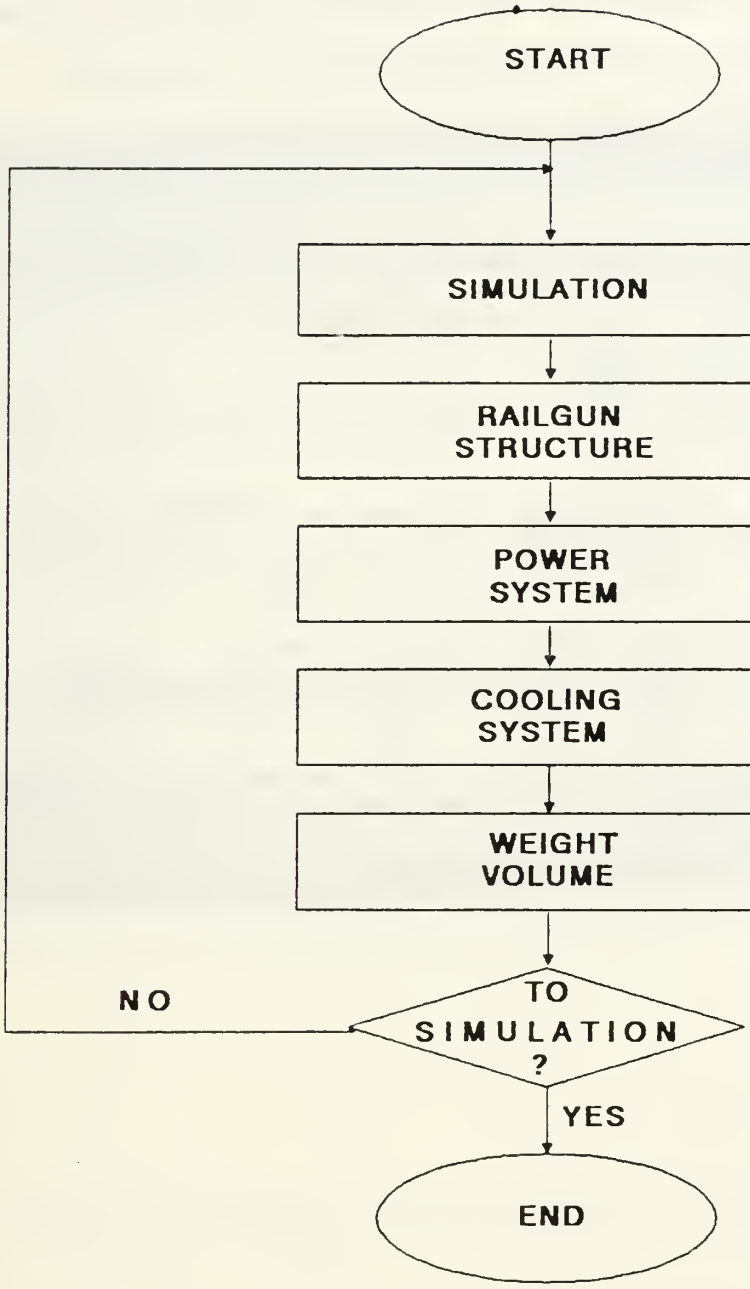

Figure 3.6 Flowchart of the Railgun Program

2. Output

The output of the program code is given on the monitor screen. The following layouts are used:

a) Simulation--the dynamic development of the acceleration process is shown both graphically and numerically on the screen (Figure 3.7).

b) Railgun structure--the main design parameters based on the simulation results are shown both graphically and numerically on the screen (Figure 3.8).

c) Power system design--main results of the power system estimates are shown numerically on the screen (Figure 3.9).

d) Cooling system--the estimates of the cooling system size and weight are shown numerically on the screen (Figure 3.10).

e) Power conditioning--main results of the power conditioning system are shown numerically on the screen (Figure 3.11).

f) Weight and site--summary of the weight and size of the main components and the whole system is given on the screen (Figure 3.12).

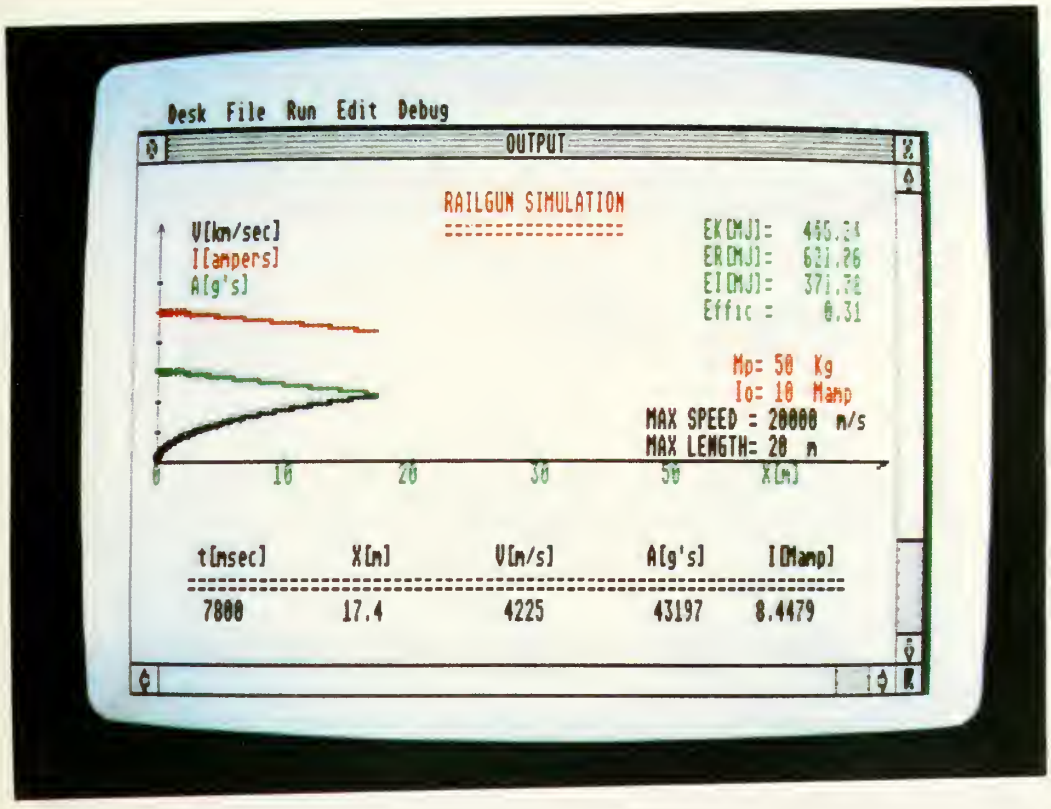

Figure 3.7 Output 1--The Railgun Simulation

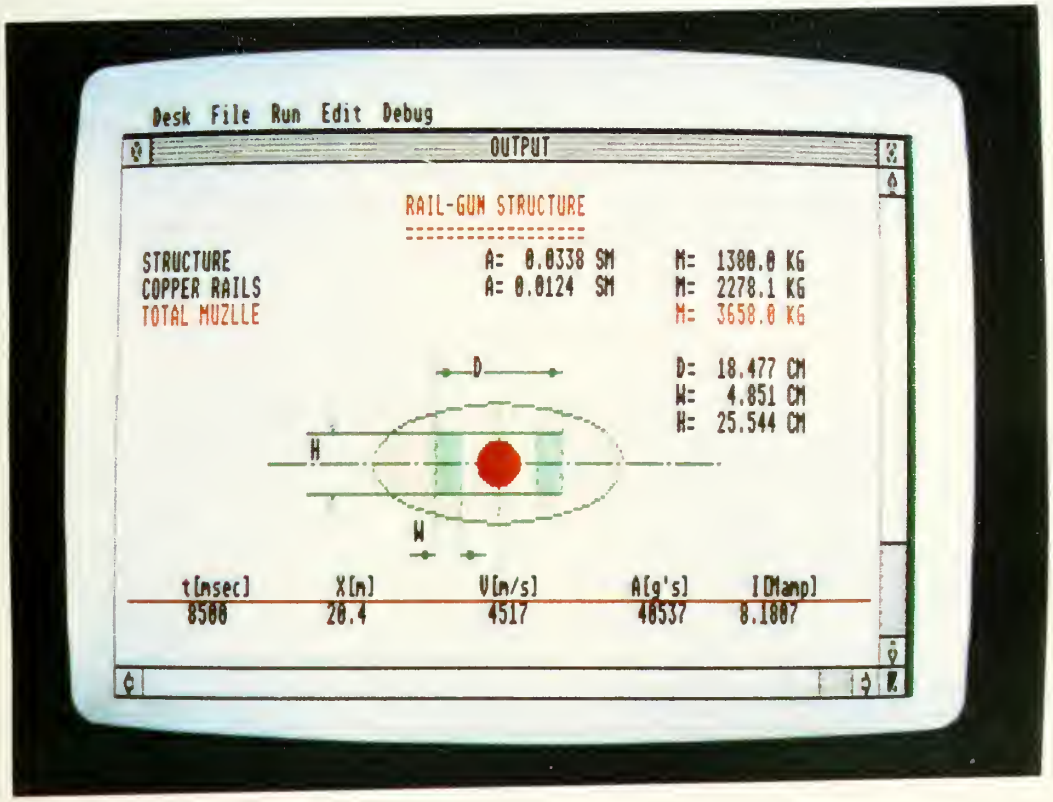

Figure 3.8 Output 2--The Railgun Structure

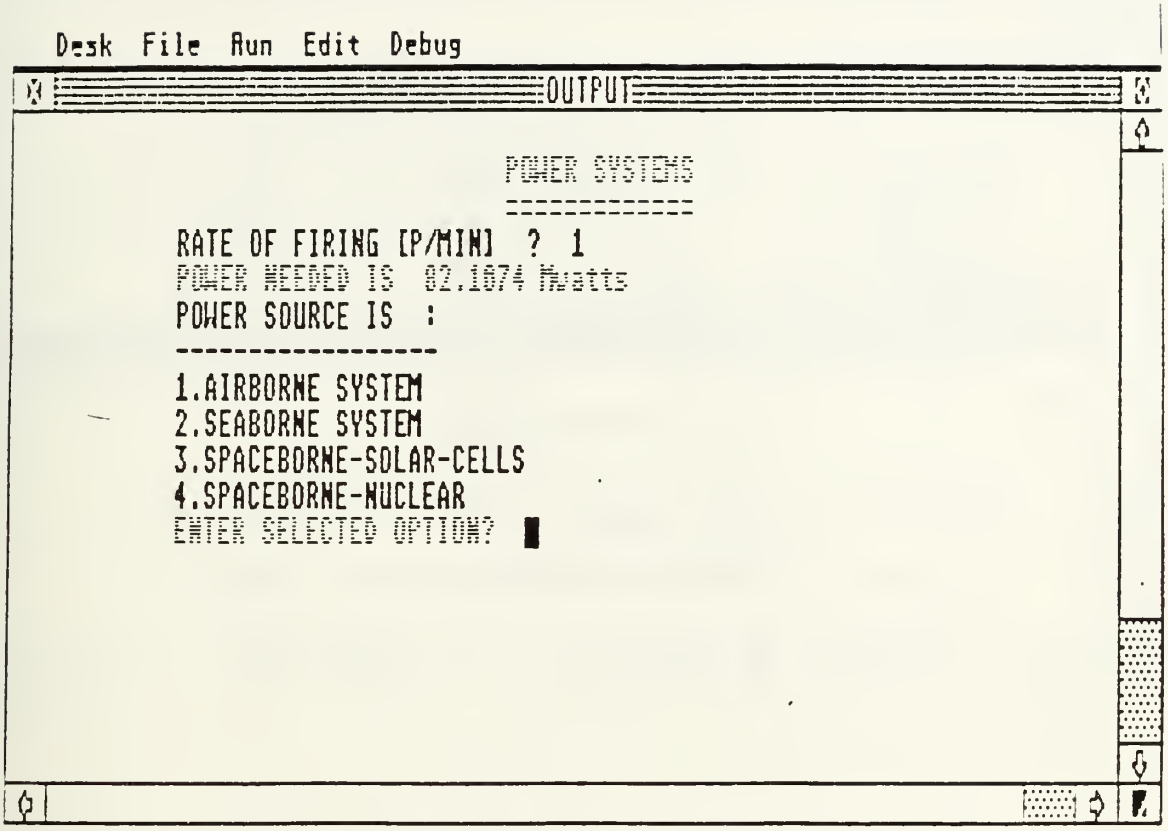

Figure 3.9 Output 3--The Power System

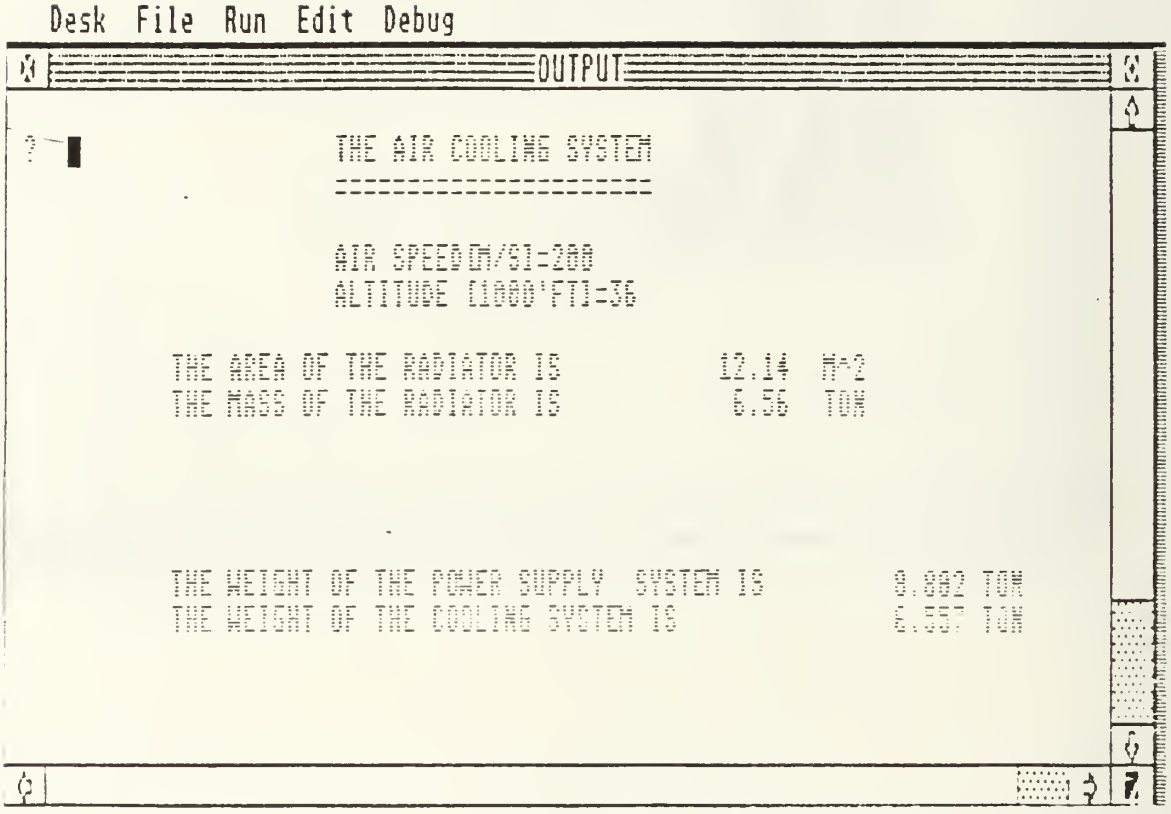
Desk File Run Edit Debug
OUTPUT
? _
THE AIR COOLING SYSTEM
AIR SPEED(M/S)=200
ALTITUDE (1000'FT)=36
THE AREA OF THE RADIATOR IS 12.14 M^2
THE MASS OF THE RADIATOR IS 6.56 TON
THE WEIGHT OF THE POWER SUPPLY SYSTEM IS 9.882 TON
THE WEIGHT OF THE COOLING SYSTEM IS 6.557 TON

Figure 3.10 The Cooling System

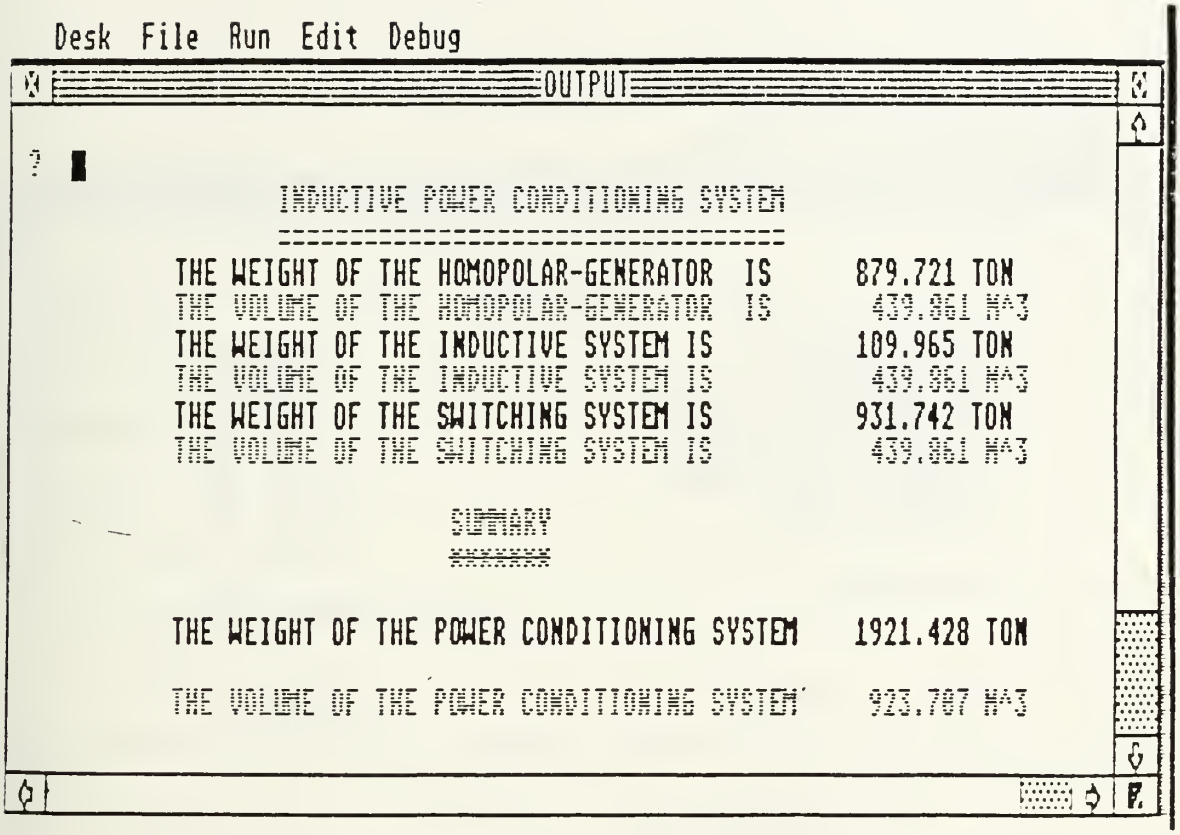
Desk File Run Edit Debug
OUTPUT
?
INDUCTIVE POWER CONDITIONING SYSTEM
THE WEIGHT OF THE HOMOPOLAR-GENERATOR IS 879.721 TON
THE VOLUME OF THE HOMOPOLAR-GENERATOR IS 439.861 M^3
THE WEIGHT OF THE INDUCTIVE SYSTEM IS 189.965 TON
THE VOLUME OF THE INDUCTIVE SYSTEM IS 439.861 M^3
THE WEIGHT OF THE SWITCHING SYSTEM IS 931.742 TON
THE VOLUME OF THE SWITCHING SYSTEM IS 439.861 M^3
SUMMARY
THE WEIGHT OF THE POWER CONDITIONING SYSTEM 1921.428 TON
THE VOLUME OF THE POWER CONDITIONING SYSTEM 923.787 M^3

Figure 3.11 Power Conditioning

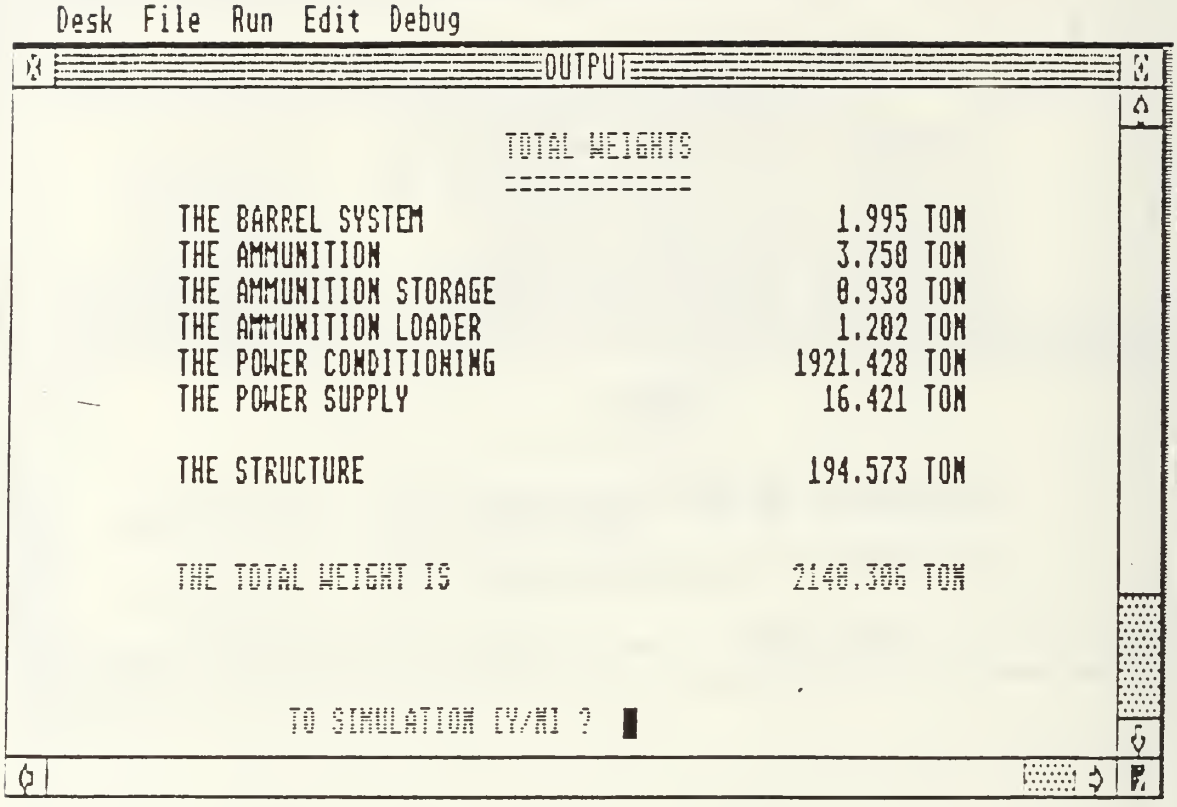
Desk File Run Edit Debug
OUTPUT
TOTAL WEIGHTS
THE BARREL SYSTEM 1.995 TON
THE AMMUNITION 3.750 TON
THE AMMUNITION STORAGE 0.938 TON
THE AMMUNITION LOADER 1.202 TON
THE POWER CONDITIONING 1921.428 TON
THE POWER SUPPLY 16.421 TON
THE STRUCTURE 194.573 TON
THE TOTAL WEIGHT IS 2140.306 TON
TO SIMULATION [Y/N] ?

Figure 3.12 Total Weight and Size

IV. THE FLIGHT SIMULATION MODEL

A. GENERAL

The flight simulation program is the core of this research. It was written in order to simulate a full ballistic flight of a projectile. The program treats separately the three major phases of a ballistic flight, namely:

a) The launch

b) The orbital flight

c) The reentry.

The input to the program includes the parameters of the projectile and the initial conditions at launch.

The output of the program is a time history of the main variables describing the flight. The output may be given either graphically on the monitor screen or as listing of numerical values (either on the screen or by the printer).

The output includes the numerical values of the kinematical variables, the aerodynamic variables and the thermal variables.

The three phases of flight (launch, orbit and reentry) can be run separately in order to permit study of any one of the phases of flight. Ordinarily the program automatically changes from one phase to another when necessary.

B. THE MATHEMATICAL MODEL

1. List of Constants

The list of constants used in this model is given in Table 4.1. The following description is given for each constant:

a) The program code symbol

b) The text symbol

c) The definition

d) The value

e) The units.

TABLE 4.1

LIST OF CONSTANTS

SYMBOLS		MEANING	VALUES	UNITS
Computer Code	Text			
RE	R_e	Radius of earth	6371	Km
PI	π	Pi	3.14	Non Dimen.
hb	H	Scale height	9200	Km
g	g	Gravity acceleration	9.81	m/sec^2
dQdM		Heat of Ablation Carbon-Carbon	28	Mj/kg
DENH0	$\rho_{s.l}$	Air density (S.L)	1.25	Kg/m^3
TCH0	$T_{s.l}$	Temperature (S.L)	15	^oC
PH0	$P_{s.l}$	Pressure (S.L)	1	atm.
MUSL	$\nu_{s.l}$	Kinematic viscosity (S.L)	0.000158	ft^2/sec

2. List of Variables

The list of variables used in this model is given in Table 4.2. The following is given for each variable:

a) The program code symbol

b) The text symbol

c) The definition

d) The units.

TABLE 4.2

LIST OF VARIABLES

SYMBOLS		MEANING	UNITS
Computer Code	Text		
t	t	Time from the start of flight	Sec
Xr	X	Coordinate along X axis	Meter
z	z	Coordinate along y axis	Meter
hr		Altitude	Meter
Vr	V	Velocity of projectile	m/sec
deg	γ	Flight angle above the horizon	Degrees
dar	γ	Flight angle above the horizon	Radians
mp	M_D	Mass of projectile	Kgm
rp	R_p	Radius of the projectile	m
cd	C_d	Drag coefficient	Non Dimen.
ap	A_p	Frontal area of the projectile	m^2

TABLE 4.2 (CONTINUED)

SYMBOLS		MEANING	UNITS
Computer Code	Text		
beta	β	Ballistic factor	N/m^2
vrx	V_{rx}	X component of velocity	m/sec
vry	V_{ry}	Y Component of velocity	m/sec
arx	a_{rx}	X component of acceleration	m/sec^2
ary	a_{ry}	Y component of velocity	m/sec^2
ARAD	θ	Polar coordinate in the orbit plane	Radians
R	R	Radial coordinate in the orbit plane	m
		Elevation angle	Radians
DR1DT1	dR/dt	First time derivative of R	m/sec
DR2DT2	d^2R/dt^2	Second time derivative of R	m/sec^2
DA1DT1	dA/dt	First time derivative of A	Rad/sec
DA2DT2	d^2A/d^2t	Second time derivative of A	Rad/sec^2
DIP	Z_E	Z coordinate of surface of earth	km
dqdt	$\dot{q}$	Rate of heating per unit area	$Watt/cm^2$
qh	q	Total heating per unit area	J/cm^2
eroscm	dl	Depth of erosion	cm
TCH	T_hC	Temperature of the air	Degrees Celsius
TKH	T_hK	Temperature of the air	Degrees Kelvin

TABLE 4.2 (CONTINUED)

SYMBOLS		MEANING	UNITS
Computer Code	Text		
TNOSE	T_o	Temperature at the projectile nose	Degrees Kelvin
SOS	a	Speed of sound	m/Sec
MACH	m	Mach number	Non Dimen.
PNOSE	P_o	Pressure at the projectile nose	Atm
PH	P_h	Pressure of the air	Atm
DENH	ρ_h	Density of the air	Kgm/m^3
MU		Kinematic viscosity of the air	ft^2/sec
LENGTH	L	Typical length	ft
RNRB	R_n/R_b	Ratio of radius	Non-Dimen.
D	D	Aerodynamic drag	Newton
S	S	Reference area	m^2
dm	dm	Mass erosion	Kg
ht	h_t	Total enthalpy	j/Kgm
hw	hw	Carbon-carbon enthalpy	j/Kgm

3. Basic Assumptions and Relations

a. General

The model is divided into three main parts: launch, orbit and reentry. The basic assumptions and relations in each part are described separately.

b. Launch

(1) Equations of Motion. Classical equations of motion were used in this model. It was assumed that the projectile is moving in the same vertical plane. The axes were chosen as follows:

(a) X axis--tangent to the surface of earth at the launch site.

(b) Z axis--in the direction of the local vertical at the instant of launch and pointing upward.

(2) The Earth. A simple model of the earth was selected in which the earth is assumed to be a perfect sphere, with a radius of 6,370 km. It was assumed also that the mass of the earth is equally distributed and the gravitational force is constant and pointing into the (-z) direction.

(3) The Model of the Atmosphere. A simple model of the standard atmosphere was selected. According to this model it is assumed that the temperature (T_h) is decreasing linearly from T = 15° C at sea level to T = -56° C at an altitude of 36,000 ft. At higher altitudes the temperature is constant with a value of T = -56° C.

It was assumed also that the relationship between the air density (ρ_h) and the altitude (h) is exponential and may be represented by the following function:

$$\rho_h = \rho_{s.l} * \exp(h/H) .$$

where $\rho_{s.l}$ is the density of air at sea level ($\rho_{s.l}$ = 1.25 Kgm/m^3) and the scale height (H) is 9.2 Km. This model was found suitable to be used for launch and reentry calculations and was also chosen by NASA technical paper 2614 [Ref. 10] for similar purposes.

(4) The Aerodynamic Model. The aerodynamic model is responsible for producing the values of the aerodynamic forces and the pressures on the projectile.

It was assumed that the stagnation pressure and temperature may be calculated by the isentropic relations for perfect gas:

$$T_o = T_H*(1 + (\gamma-1)/2*M^2)^{\gamma/(\gamma-1)}$$

$$P_o = P_H*(1 + (\gamma-1)/2*M^2)^{\gamma/(\gamma-1)}$$

using the average value of γ = 1.4.

In most cases the projectile velocity is above the speed of sound. In this case it is assumed that the stagnation pressure on the nose tip is related to the stagnation pressure before the shock by the normal shock relation for perfect gas:

$$\frac{P_{02}}{P_{01}} = \left[\frac{((\gamma+1)/2)m^2}{1+((\gamma-1)/2)m^2}\right]^{\gamma/\gamma-1} \left[(2\gamma)/(\gamma+1)m^2 - \frac{(\gamma-1)}{(\gamma+1)}\right]^{1/1-\gamma}$$

Considering the fact that the main region of interest is in the hypersonic domain, the drag on the

projectile was calculated by using the relation:

$$D = 1/2\ \rho_h\ V^2\ S\ C_D$$

The value of C_D is given either as the product of the drag coefficient program or as a direct input by the user.

(5) Heating Analysis. It was assumed that the projectile is coated by a layer of ablation material. For this case a well-established approximation is given by [Ref. 10]:

$$\dot{q} = C\rho^N\ V^M\ \psi$$

At the stagnation point:

$$\psi = \frac{(1+0.72 - [(1+0.72\sigma)^2 - 0.52\sigma^2]^{1/2}}{0.26}$$

where:

$$\sigma = \left(\frac{\text{mol. weight of air}}{\text{mol. weight of the ablative material}}\right)^{1/4} \frac{(h_t - \dot{h}_w)}{\rho}$$

σ, ψ, C, N, M are numerical coefficients.

Here ρ is the effective heat of ablation per unit mass. Therefore the mass of ablation material required per unit area is given by:

$$dm = q/\varepsilon$$

where q is the total accumulated heat load per unit area:

$$q = \int \dot{q}\, dt$$

Knowing the density of the ablative material (ρ_a) the depth of the erosion might be calculated by the relation:

$$d = dm/\rho_a$$

The values of the coefficients C, N and M are defined by the characteristics of the flow and the radius of the projectile. For ρ, V and γ_n given in mks units the value of C is:

$$C = \frac{1.85(10^{-8})}{\sqrt{\gamma_n}} (1 - hw/ht)$$

and q will be in Watt/cm^2.

For laminar convection the values of the constants N and M are: N = 0.5 and M = 3.0.

For turbulent convection the value of M is dependent on the range of speed:

$$M = \begin{cases} 3.7 & \text{for } V > 4 \quad \text{km/s} \\ 3.37 & \text{for } V < 4 \quad \text{km/s} \end{cases}$$

and N = 0.8.

The characteristics of the flow are determined by the Reynolds number. Reynolds number (R_n) is

a function of the velocity (V), typical body dimensions (l) and the kinematic viscosity (ν).

A simplified model for the function of the kinematic viscosity vs. altitude was selected. According to this model the value of the kinematic viscosity is given by:

$$\nu = \nu_{S.L}(\rho_H/\rho_{S.L})$$

where

$\nu_{s.l}$ is the kinematic viscosity at sea level (0.000158 ft^2/sec)

$\rho_H/\rho_{s.l}$ is the ratio between the density at the flight altitude to the density at sea level (standard atmosphere).

In this version of the model it was assumed that the ablative material coating is composed of the state-of-the-art carbon-carbon coat. The heating and density parameters were chosen accordingly.

(6) The Ballistic Factor. The ballistic factor of the projectile was defined and calculated. The ballistic factor measures the ratio between the aerodynamic forces and the inertia of the projectile. Its magnitude in pressure units is equal to the value of the dynamic pressure needed to decelerate the projectile at a rate of 1g (9.82 m/sec^2). So:

$$1g = \frac{\text{aerodynamic forces}}{\text{mass of projectile}} = \frac{1/2\rho V^2 S C_d}{m}$$

or:

$$\beta = 1/2\,\rho V^2 = \frac{mg}{SC_d}$$

It was expected that the ballistic factor (β) would have the major effect on the performance of the projectile both during atmospheric launch and atmospheric reentry.

In this model, as the mks unit system was selected, the units of the ballistic factor (β) are Newtons/m^2.

c. Orbit

(1) The Equations of Motion. The equations of motion for the two body problem in spherical coordinates are as follows:

$$\ddot{r} - r(\dot{\theta}^2 \cos^2\phi + \dot{\phi}^2) = -\mu/r^2$$

$$r\ddot{\theta}\cos\phi + 2\dot{r}\dot{\theta}\cos\phi - 2\dot{r}\dot{\theta}\dot{\phi}\sin\phi = 0$$

where

r is the distance from the earth's center

θ is the azimuth angle

ϕ is the elevation angle

μ is the gravitational constant.

By selecting the orbital plane as the plane of reference, the elevation angle becomes zero. Therefore:

$$\phi = 0$$

and:

$$\cos \phi = 1$$

$$\sin \phi = 0$$

And the equations of motion become:

$$\ddot{r} - r\dot{\theta}^2 = - \mu/r^2$$

$$r\ddot{\theta} + 2\dot{r}\dot{\theta} = 0$$

After transferring this system of differential equations to the equivalent first order system it becomes:

$$\dot{r} = V_r$$

$$\dot{\theta} = \Omega$$

$$\dot{V}_r = - \mu/\gamma^2 + r\Omega^2$$

$$\dot{\Omega} = - 2 \dot{V}_r \Omega/r$$

This form is known as the polar form of the Cowell method. The polar form of the classical Cowell method was applied in this model purposely. This selection permits the use of larger integration step size for the same truncation error.

For greater accuracy the step size (dt) can be reduced. To further the model accuracy, a new method was developed. This method is explained in the appendix.

For this specific model it was assumed that the projectile is moving in the same solar plane. The polar coordinates were chosen so that:

a) The origin is at the center of the earth.

b) The angle is measured from the launch site as the reference point of direction (positive in the direction of the projectile).

(2) The Earth. Again the same model of the earth was selected. According to this model the earth is assumed to be a perfect sphere with a radius of 6,370 km. The mass of the earth is concentrated in its center.

(3) The Space Environment. For this simplified model it was assumed that the density of air in space is negligible and therefore no drag is encountered. As a result the total energy of the projectile (the sum of the kinetic and the potential energy) is constant during the whole phase of orbital flight.

d. Reentry

The reentry model simulates the flight of the projectile from the moment it crosses the h = 100 km altitude line and enters the atmosphere.

Basically the equations are similar to the equations of the launch program. The initial conditions for the reentry program are the final results of the orbital module.

4. Method of Solution

In all three modules of the flight simulation the Euler method was used in order to solve the differential equations.

In order to assure optimal ratio of accuracy to running time, the time step was tailored to the flight conditions. During the launch and the reentry phases shorter time intervals are used. during the orbital flight phase longer time intervals are used because drag effects are negligible.

In addition a special algorithm was developed for solving the orbital module. This algorithm assures accurate results for cases when longer orbital flight is simulated. This method is explained in detail in Reference 11.

C. THE COMPUTER CODE

1. General

The flight simulation program served also as a core for some other programs. The following programs are essentially based on the same mathematical models.

a. Launch

This program simulates only an atmospheric launch of the projectile (altitude less than 100 km).

b. Orbit

This program simulates only an orbital phase of a flight. It assumes zero-drag and therefore can be used only while altitude is above 100 km.

c. Reentry

This program simulates only the reentry phase of a flight. It does take into account the atmospheric drag. Therefore this program is most suitable to simulate the reentry from an altitude of 100 km and below.

d. Full Flight Simulation (Summary Printing Version)

This version of the flight simulation program includes an additional module which is responsible for automatically sending a summary of the results to the printer at the end of each run.

2. Flowchart

The flowchart of this program computer code is shown in Figure 4.1.

D. USING THE PROGRAM

1. Input

The input to the flight simulation program includes the following:

1. Parameters of the projectile:
   a. Mass of the projectile
   b. Coefficient of drag of the projectile
   c. Radius of the projectile

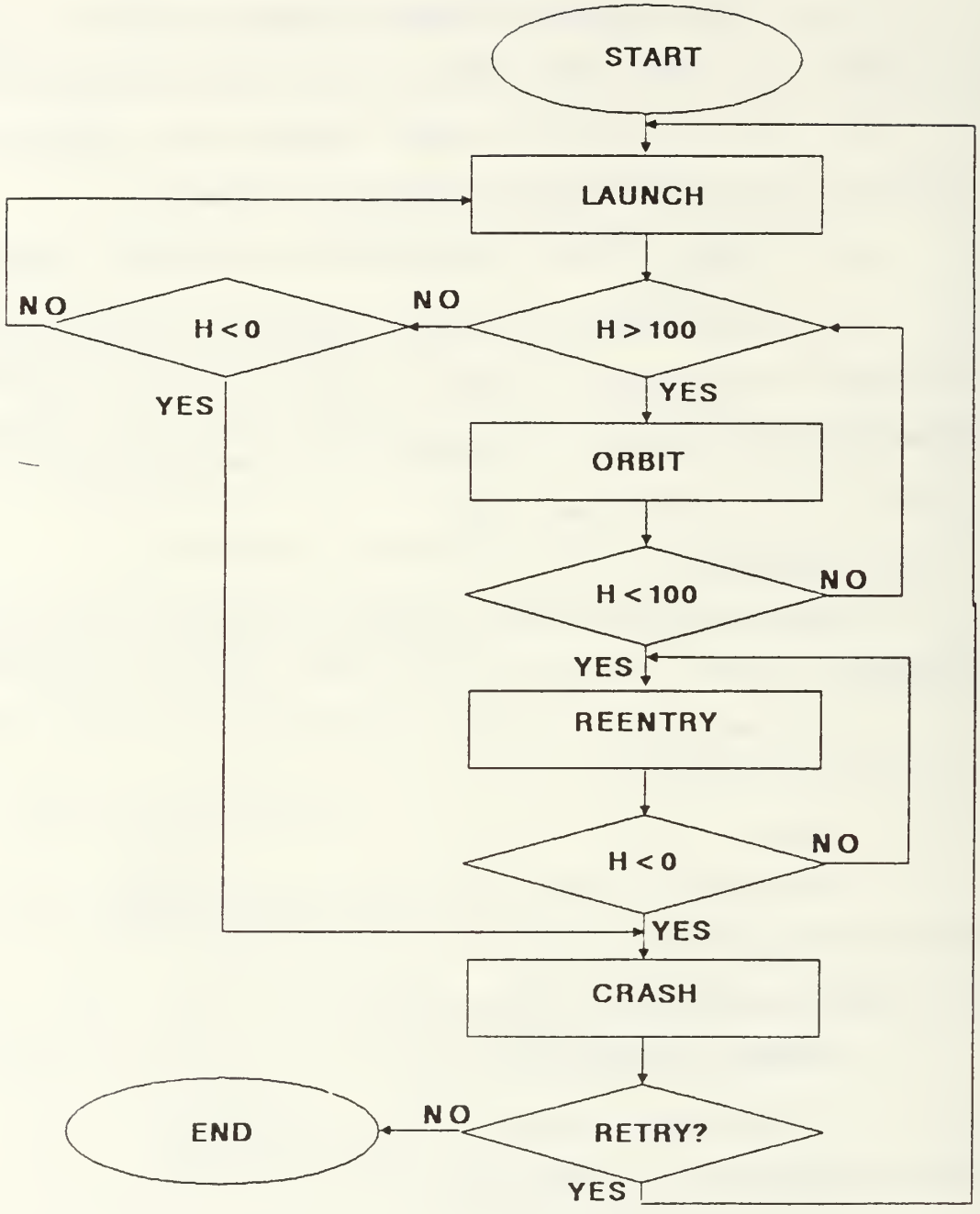

Figure 4.1 Flowchart of Flight simulation Program

2. Initial conditions:

   a. Launch speed

   b. Angle of launch (above horizon)

   c. Altitude of the launcher at the instant of firing.

When the program is rerun, the last set of initial conditions and parameters is used. If the user wishes, he may enter a new set of values or change a selected few , separately.

When chained (or called) by the previous programs, such as the drag estimation code or the railgun simulation, the results of those programs are passed into the flight simulation model as input.

2. Output

   a. General

The graphic output of the program is composed of the following three basic layouts:

1. Launch layout
2. Orbit layout
3. Reentry layout.

When the printer version of the program is run either a listing of selected variables or a summary of the run results is printed.

The summary of the results includes the values of selected variables at the instant of the following events:

1. Launch
2. Entrance to orbit (H = 100 km)
3. Start of reentry (H = 100 km)
4. Ground impact (sea level).

b. Launch Layout

An example of the launch layout is shown in Figure 4.2. The launch layout includes graphic representations and numerical results. The time history of these values may be examined by the user as he follows the development of the graphs and the changes of numerical values during the simulation.

The graphic representation includes the following curves:

1) Speed vs. altitude
2) Deceleration vs. altitude
3) Rate of heating vs. altitude.

A picture of the plane of flight is given on the other side of the screen. The contour of the earth is shown under the projectile location.

The values of the following parameters are shown numerically on the screen and are updated every second:

1) t [sec]--the elapsed time from launch
2) V [km/sec]--speed
3) H [km]--altitude
4) R [Nm]--ground distance from launch site
5) g's--Deceleration

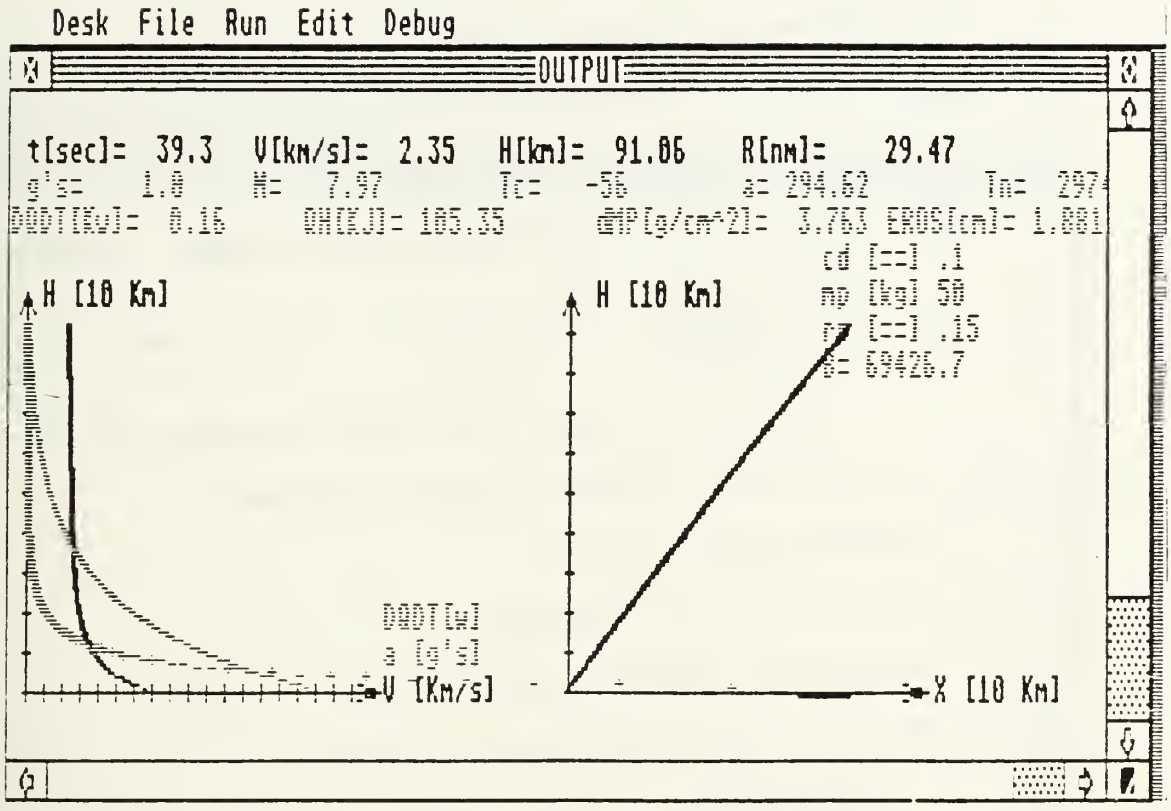

Figure 4.2 Launch Layout

6) M--mach number

7) T_c--ambient temperature [^oC]

8) a--speed of sound [m/sec]

9) T_n--stagnation temperature at the nose tip

10) DQDT [kwatt/cm^2]--rate of heating (at nose tip)

11) QH [kg/cm^2]--accumulated heat (at nose tip)

12) dM_p [q/cm^2]--loss of mass due to thermal erosion (at nose tip)

13) Eros [cm]--depth of erosion (on the carbon-carbon coated nose tip).

In addition the following parameters of the projectile are shown constantly on the screen:

1) C_d--coefficient of drag

2) M_p--mass of the projectile

3) R_p--radius of the projectile base

4) B--the ballistic coefficient [N/m^2].

c. Orbit Layout

(1) General. The orbital layout (Figure 4.3) includes graphical representation and numerical results. The time history of the results may be examined by the user as he follows the development of the curves and the changes of the numerical results during the simulation.

(2) The Graphics. The graphic representation shows the plane of motion of the projectile. The earth and its center are shown in the middle of the screen. The movement of the projectile is shown dynamically on the same scale. The picture is updated about every second.

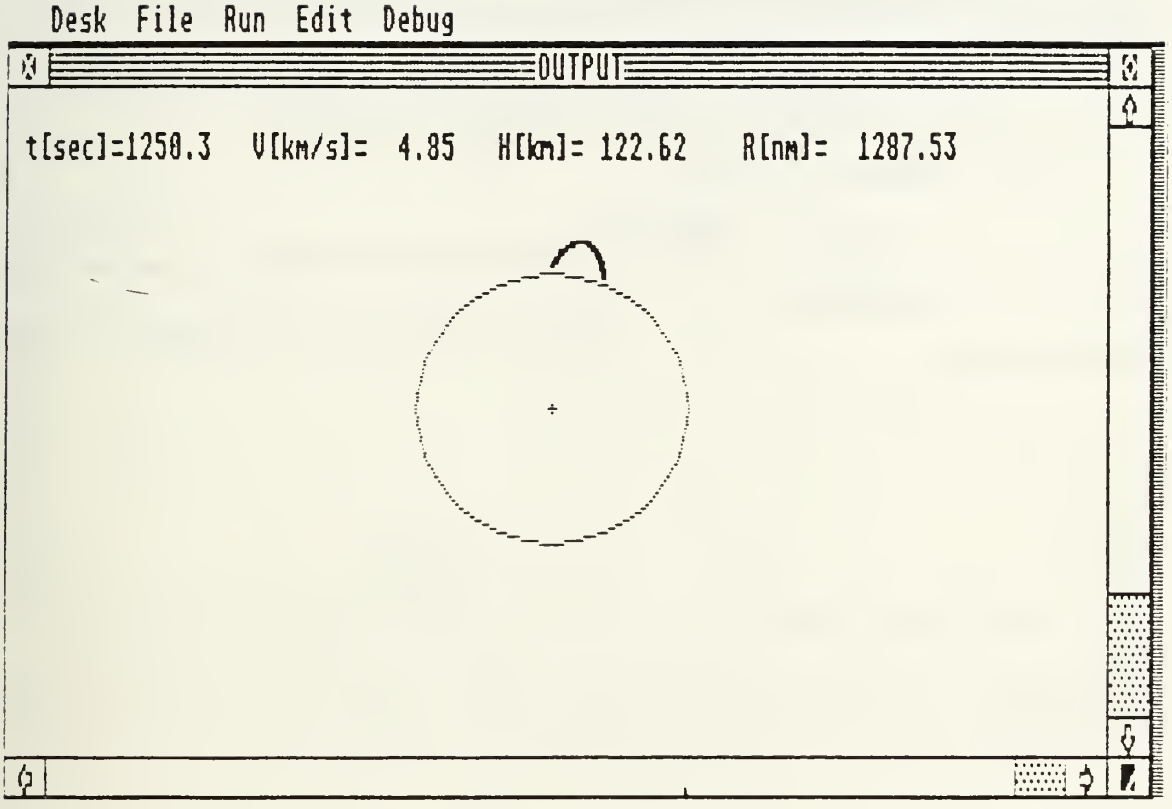

Figure 4.3 Orbit Layout

(3) The Numerical Results. The numerical results of the following variables are shown dynamically on the screen (their values are updated about every second):

1) t [sec]--elapsed time from launch
2) V [km/s]--speed
3) H [km]--altitude (above sea level)
4) R [NM]--ground distance from launch site.

d. Reentry Layout

A typical look of the reentry layout is shown in Figure 4.4. Basically the reentry screen is similar to the launch screen.

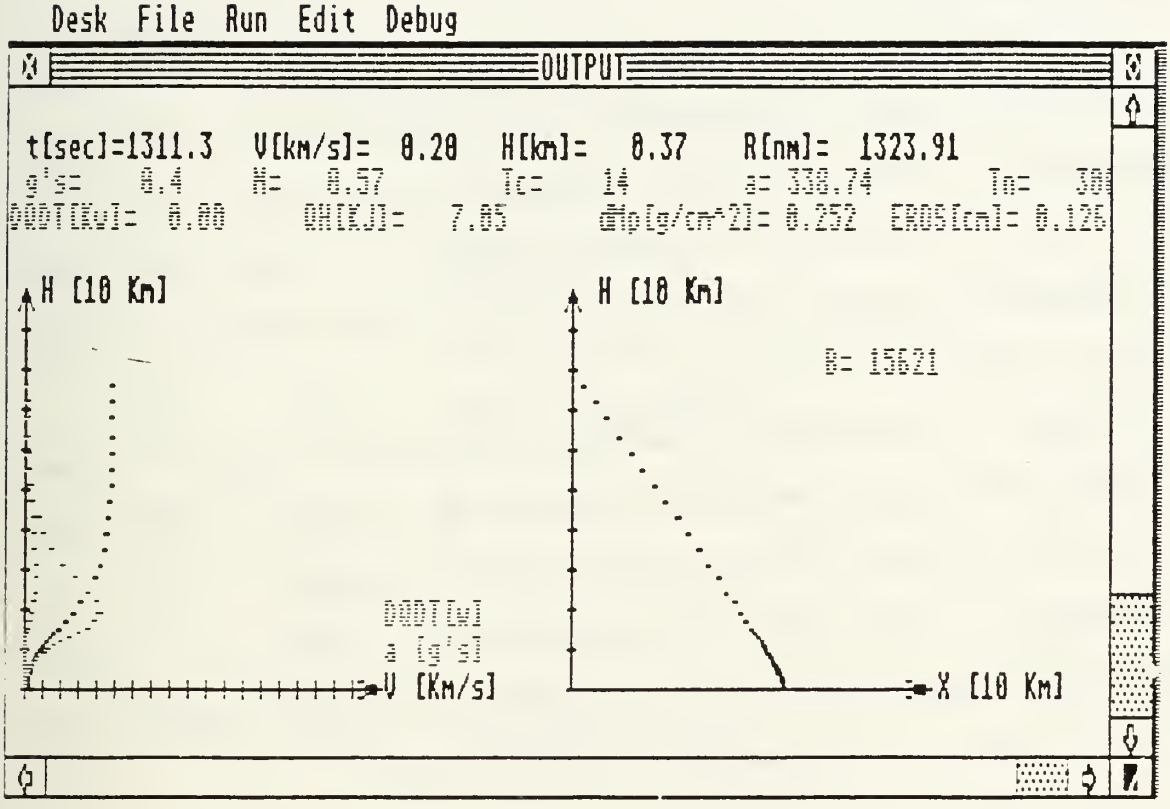

Figure 4.4 Reentry Layout

V. THE GROUND TRACK MODEL

A. GENERAL

The ground track model is based mainly on the orbit module of flight simulation. In addition to the orbit calculation the rotational movement of the earth was taken into account. The results produced by this model are represented as the trace of satellite orbit over the world map as a function of time.

Input to the model includes the initial condition and the parameters of the orbit. Output of the program includes a graphic picture of the track and the scheme of the body movement on the orbital plane. In addition, major characteristic variables of the flight are shown numerically on the screen or are printed by the printer.

B. THE MATHEMATICAL MODEL

1. List of Constants

The list of constants used in this model is given in Table 5.1. The following description is given for each constant:

a) The program code symbol

b) The text symbol

c) The definition

d) The value

e) The units.

TABLE 5.1

LIST OF CONSTANTS

SYMBOLS		MEANING	VALUES	UNITS
Computer Code	Text			
RE	R_e	Radius of earth	6371	Km
PI	π	Pi	3.14	Non Dimen.
hb	H	Scale Height	9200	Km
g	g	Gravity acceleration	9.81	m/sec^2
dQdM	dq/dM	Heat of Ablation Carbon-Carbon	28	Mj/kg
DENHO	$\rho_{s.l}$	Air density (s.l)	1.25	Kg/m^3
TCHO	$T_{s.l}$	Temperature (s.l)	15	^oC
PHO	$P_{s.l}$	Pressure (s.l)	1	atm
MUSL	$\nu_{s.l}$	Kinematic viscosity (s.l)	0.000158	ft^2/sec

2. List of Variables

The list of variables used in this model is given in Table 5.2. The following is given for each variable:

a) The program code symbol

b) The text symbol

c) The definition

d) The units.

TABLE 5.2

LIST OF VARIABLES

SYMBOLS		MEANING	UNITS
Computer Code	Text		
t	t	Time from the start of flight	Sec
VL	V_L	Speed of earth rotation	rad/sec
L	dL	Net eastward movement	rad
NLONG	L_N	New longitude	Degrees
OLONG	L_O	Old longitude	Degrees
TLONG		True longitude	Degrees
DT	dt	Time interval	Sec
Xr	X	Coordinate along X axis	m
z	z	Coordinate along y axis	m
hr		Altitude	m
Vr	V	Velocity of projectile	m/sec
d	γ	Flight angle above the horizon	Degrees
dar	γ	Flight angle above the horizon	radians
mp	M_D	Mass of projectile	Kgm
rp	R_p	Radius of the projectile	m
cd	C_d	Drag coefficient	Non Dimen.
ap	A_p	Frontal area of trhe projectile	m^2
beta	β	Ballistic factor	N/m^2
vrx	V_{rx}	X component of velocity	m/sec

TABLE 5.2 (CONTINUED)

SYMBOLS		MEANING	UNITS
Computer Code	Text		
vry	V_{ry}	Y component of velocity	m/sec
arx	a_{rx}	X component of acceleration	m/sec^2
ary	a_{ry}	Y component of velocity	m/sec^2
ARAD	θ	Polar coordinate in the orbit plane	Radians
R	R	Radial coordinate in the orbit plane	m
ϕ	ϕ	Elevation angle	Radians
DR1DT1	dR/dt	First time derivative of R	m/sec
DR2DT2	d^2R/dt^2	Second time derivative of R	m/sec^2
DA1DT1	dA/dt	First time derivative of A	Rad/sec
DA2DT2	d^2A/dt^2	Second time derivative of A	Rad/sec^2
DIP	Z_E	Z coordinate of surface of earth	km
dqdt	dq/dt	Rate of heating per unit area	$watt/cm^2$
qh	q	Total heating per unit area	J/cm^2
eroscm	dl	Depth of erosion	cm
TCH	T_hC	Temperature of the air	Degrees Celsius
TKH	T_hK	Temperature of the air	Degrees Kelvin

3. Basic Assumptions and Relations

The model is based mainly on the orbit module of the flight simulation program. The solution of Kepler's equations was achieved by Cowell's method. For longer orbital flights or when greater accuracy is needed, the solution of the equations is achieved by an energy approach that was developed as part of this research. The description of this method is given in Reference 11.

Most assumptions and relations described in Chapter II.A.3.c are valid. In addition, the rotation of the earth was introduced. Because of the earth's rotation, the eastward angular movement of a body with respect to the earth's surface is the algebraic difference between the eastward angular movement of the body with respect to the center of the earth and the eastward angular movement of the surface of the earth (on the same latitude) with respect to the same reference point.

The eastward speed (V_L) of the movement of the surface of the earth is given by:

$$V_L = 2\pi/(3600*24) \quad [\text{rad/sec}]$$

In a period of dt, the body moves from the longitude of L_O (old longitude) to longitude of L_N (new longitude). The net movement of the body track with respect to the surface of the earth (the point on the surface under the body location) is given by:

$$dL = (L_N - L_O) - V_L \, dt$$

where:

dL is the net eastward movement

L_N is the new longitude

L_O is the old longitude

V_L is the body eastward velocity

dt is the time interval.

4. Method of Solution

The same methods of solution as for the orbit module of the flight simulation are used here to solve Kepler's equations.

C. THE COMPUTER CODE

1. General

The code of this model is based mainly on the code of the orbit module of the flight simulation. In addition to the solutio of the two body problem, the code includes a module that produces the world map on the screen and a second module that locates the projectile trace on the same map.

2. Flowchart

The flowchart of this program is shown in Figure 5.1.

3. Basic Code

The list of the Basic Code is given in Reference 11.

REPRODUCED AT GOVERNMENT EXPENSE

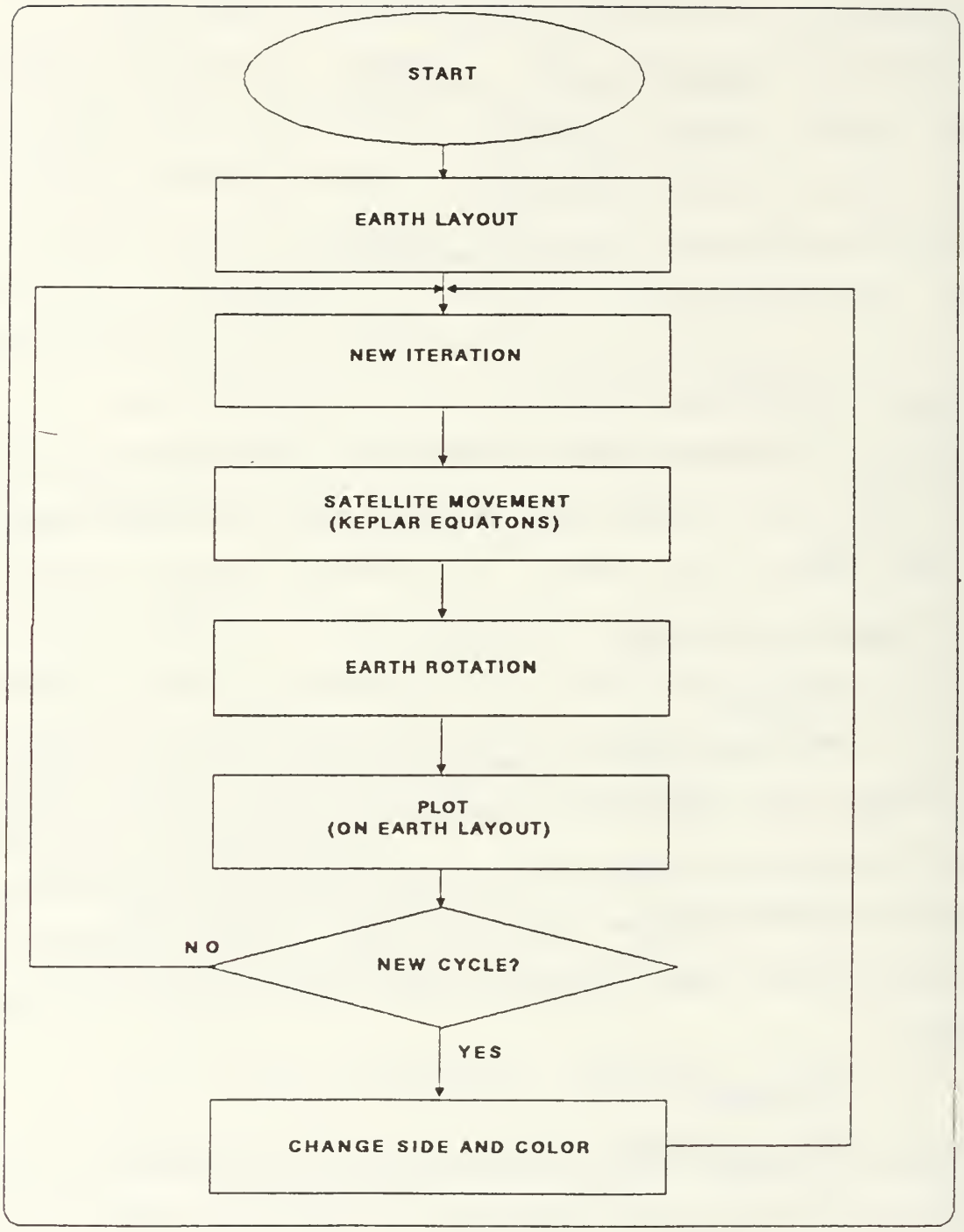

Figure 5.1 Flowchart of Groundtrack Program

D. USING THE MODEL

1. Input

Input to the program includes the following parameters and initial conditions:

a) The initial location of the body in earth coordinates (latitude, longitude, altitude [km])

b) The body speed [km/sec]

c) The body climb angle [degrees]

d) The flight direction [degrees] (flight direction at the equator is equal to the orbit inclination).

2. Output

A typical output of the program is shown in Figure 5.2. The picture on the screen has three parts: numerical results, the world map and the orbital plane.

The values of the following variables are shown continuously on the screen. Their value is updated about every second:

a) Time [sec] is the elapsed time

b) Velocity [km/s]

c) Altitude [km]

d) Latitude [degrees]

e) Longitude [degrees]

In addition, the values of the following parameters are shown as well:

a) Longitude of A.N. [degrees]

b) Initial altitude [km]

c) Inclination.

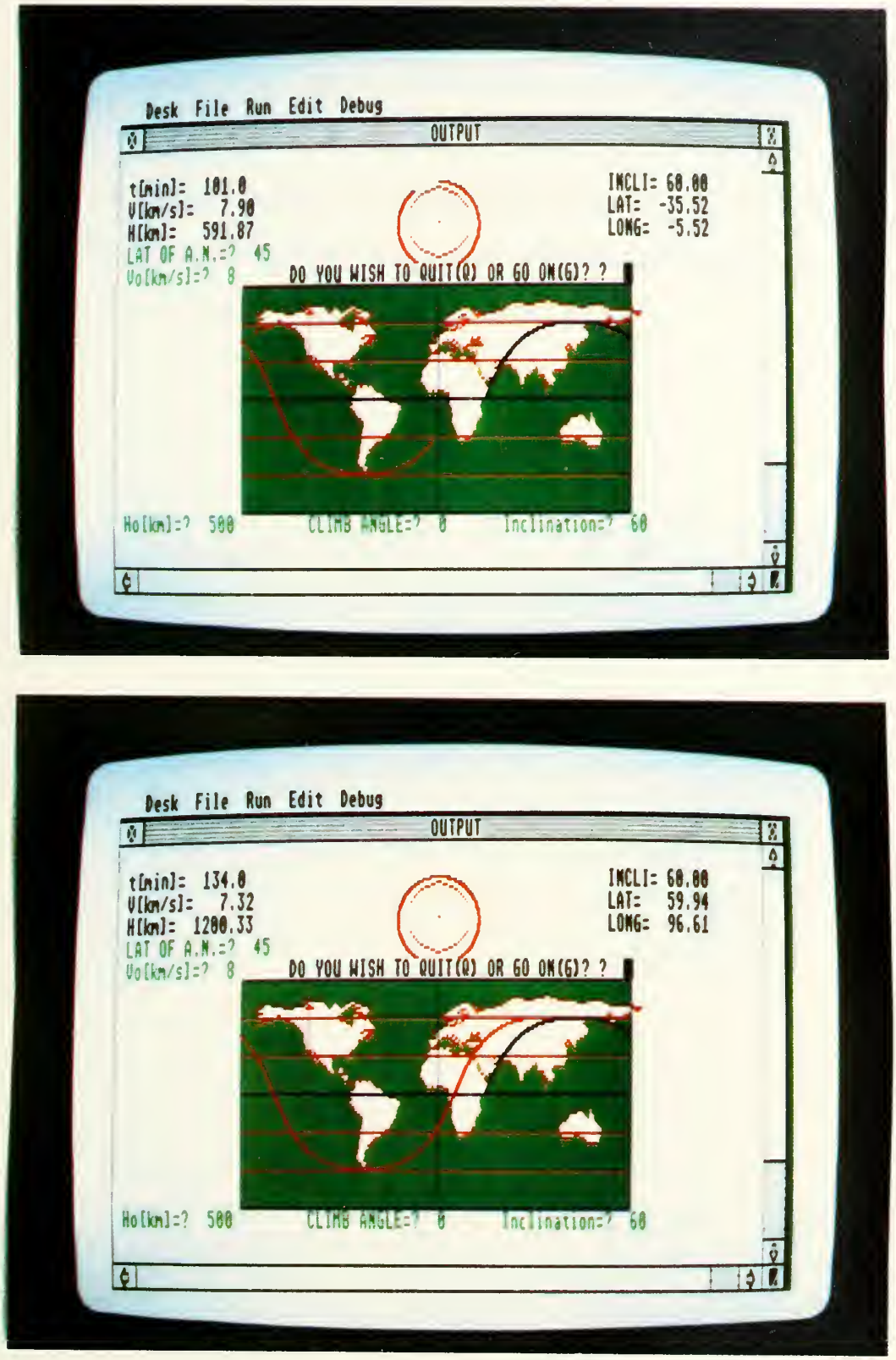

Figure 5.2 Typical Output of the Groundtrack Program

The ground trace of the moving body over the surface of the earth is shown continuously as the simulation advance. Each cycle is shown in a different color.

A small scheme of the orbital plane is shown on the upper part of the screen. This layout permits the user to examine the shape of the orbit clearly.

VI. THE GUIDANCE MODEL

A. GENERAL

The yield of a warhead of any weapon is mainly a function of its mass and volume. In many cases the ability to enlarge the warhead is limited. This is especially true in the case of a railgun where the size and mass of the projectile have to be kept as low as possible.

In order to increase the kill probability of the small railgun projectile, another option than increasing its size has to be examined. The alternative is to achieve greater accuracy.

The goal of increasing the accuracy of any firing system is not an easy task to achieve. The trajectory of the projectile is affected by many factors. Even a slight inaccuracy in the launch conditions, in the projectile size or in the prediction of the weather conditions may result in a significant miss of the target.

Increasing the accuracy of the launching system is not cost effective. Even with considerable efforts, only limited improvement in accuracy would be achieved and the destruction of the target would not be assured.

The tendency therefore is to provide the warhead with some final homing capability. Homing may be achieved by a passive, a semi-active or an active system. It is more likely that railgun projectiles will use a passive system as

their space and weight are very limited. In this model a passive homing system was simulated. A proportional guidance system with variable constants of proportion was selected.

This model may be used, for example, for simulation of a warhead homing towards a target illuminated by a laser designator. The illuminator may be located in space aboard an airplane or on land.

B. THE MATHEMATICAL MODEL

1. List of Constants

The list of constants used in this model is given in Table 6.1. The following description is given for each constant:

a) The program code symbol

b) The text symbol

c) The definition

d) The value

e) The units.

2. List of Variables

The list of variables used in this model is given in Table 6.2. The following is given for each variable:

a) The program code symbol

b) The text symbol

c) The definition

d) The units.

TABLE 6.1

LIST OF CONSTANTS

SYMBOLS		MEANING	VALUES	UNITS
Computer Code	Text			
RE	R_e	Radius of earth	6371	Km
PI	π	Pi	3.14	Non Dimen.
hb	H	Scale Height	9200	Km
g	g	Gravity acceleration	9.81	m/sec^2
dQdM	dq/dm	Heat of Ablation Carbon-Carbon	28	Mj/kg
DEN+10	$\rho_{s.l}$	Air density (s.l)	1.25	Kg/m^3
TC+10	$T_{s.l}$	Temperature (s.l)	15	^oC
PHO	$P_{s.l}$	Pressure (s.l)	1	atm
MUSL	$\nu_{s.l}$	Kinematic viscosity (s.l)	0.000158	ft^2/sec

TABLE 6.2

LIST OF VARIABLES

SYMBOLS		MEANING	UNITS
Computer Code	Text		
t	t	Time from the start of flight	Sec
Xr	X	Coordinate along X axis	Meter
X targ	X_T	Target location	Meter
dX targ	dX	Miss distance	Meter

TABLE 6.2 (CONTINUED)

SYMBOLS		MEANING	UNITS
Computer Code	Text		
ZRMTNEW	N	Vertical bearing of target (New)	Radians
ZRMTOLD	O	Vertical bearing of target (Old)	Radians
KOP	K	Constant of proportional navigation	Non. Dimen.
NP	N_p	Maneuvering acceleration	g's
CDP	C_d	Coefficient of drag	Non Dimen.
CLP	C_L	Coefficient of lift	Non Dimen.
CDO	C_{DO}	Coefficient of parasite drag	Non Dimen.
K	K	Coefficient of induced drag	Non Dimen.
CLP stall	C_{LS}	Coefficient of lift at Stall	Non Dimen.
z	z	Coordinate along y axis	Meter
hr		Altitude	Meter
Vr	V	Velocity of projectile	m/sec
d	γ	Dive angle	Degrees
dar	γ	Dive angle	Radians
mp	M_D	Mass of projectile	Kgm
rp	R_p	Radius of the projectile	m
ap	A_p	Frontal area of the projectile	m^2
beta	β	Ballistic factor	N/m^2
vrx	V_{rx}	X component of velocity	m/sec

TABLE 4.2 (CONTINUED)

SYMBOLS		MEANING	UNITS
Computer Code	Text		
vry	V_{ry}	Y Component of velocity	m/sec
arx	a_{rx}	X component of acceleration	m/sec2
ary	a_{ry}	Y component of velocity	m/sec2
ARAD	θ	Polar coordinate in the orbit plane	Radians
R	R	Radial coordinate in the orbit plane	m
ϕ	ϕ	Elevation angle	Radians
DR1DT1	dR/dt	First time derivative of R	m/sec
DR2DT2	d^2R/dt^2	Second time derivative of R	m/sec^2
DA1DT1	dA/dt	First time derivative of A	Rad/sec
DA2DT2	d^2A/d^2t	Second time derivative of A	Rad/sec^2
DIP	Z_E	Z coordinate of surface of earth	km
dqdt	$\dot{q}$	Rate of heating per unit area	$Watt/cm^2$
qh	q	Total heating per unit area	J/cm^2
eroscm	dl	Depth of erosion	cm
TCH	T_hC	Temperature of the air	Degrees Celsius
TKH	T_hK	Temperature of the air	Degrees Kelvin
TNOSE	T_o	Temperature at the projectile nose	Degrees Kelvin
SOS	a	Speed of sound	m/sec

TABLE 6.2 (CONTINUED)

SYMBOLS		MEANING	UNITS
Computer Code	Text		
MACH	m	Mach number	Non Dimen.
PNOSE	P_o	Pressure at the projectile	Atm
PH	P_h	Pressure of the air	Atm
DENH	ρ_h	Density of the air	Kgm/m^3
MU	μ	Kinematic viscosity of the air	ft^2/sec
LENGTH	L	Typical length	m
RNRB	R_n/R_b	Ratio of radius	Rad
D	D	Aerodynamic drag	Newton
S	S	Reference area	m^2
dm	dm	Mass erosion	Kg
ht	h_t	Total enthalpy	j/Kg
hw	hw	Carbon-carbon enthalpy	j/Kg

3. Basic Assumptions and Relations

a. General

The guidance model was derived from the reentry module of the flight simulation. Most assumptions and relations of that model are applicable here. Additional assumptions and relations are described below.

b. Additional Assumptions and Relations

The construction of this model is based upon the following additional assumptions and relations:

1) The projectile is equipped with some aerodynamic means with which lift can be produced.

2) The relation between the lift coefficient and the drag coefficient may be described in the form:

$$C_D = C_{Do} + KC_L^2$$

where:

C_D = The coefficient of drag of the projectile

C_{Do} = The coefficient of parasite drag (drag at no-lift angle of attack)

C_L = The coefficient of lift

K = The coefficient of induced drag.

3) The projectile flies on a proportional guidance path. For any rate of change in the orientation of the line of sight between the projectile and the target, the projectile reacts in a proportional rate of change of its flight path and in the same direction. The constant of proportion (K_{op}) serves as a parameter and is usually called the navigation ratio.

4) The lift curve is symmetrical for a positive or a negative angle of attack.

5) The projectile responds instantly to any input from the guidance system. Therefore the projectile always follows the desired ideal path of flight.

6) The amount of lift that may be produced by the projectile is limited by the stall angle. Therefore whenever the lift demand to keep the desired path is beyond the maximum lift capability, the model assumes that the projectile is flying at the maximum angle of attack but not beyond.

C. THE COMPUTER CODE

1. General

The guidance model code is based mainly on the code of the reentry module of the flight simulation. In addition the guidance equations were modeled and inserted into the code.

2. Flowchart

The flowchart of this program is given in Figure 6.1.

D. USING THE PROGRAM

1. Input

The input to the guidance program is similar to the input for the reentry module of the flight simulation. In addition the miss distance of the projectile at the moment of acquisition of the target has to be entered. Acquisition of the target by the guidance system is assumed to be reached at an altitude of 95-100 km above sea level.

2. Output

The output of the guidance program is similar to the output of the launch and reentry models of the flight simulations. The only exception is that in order to study the projectile maneuvers the value of q is shown both graphically (it replaces the value of the rate of heating) and numerically on the screen.

A typical layout of results from the guidance program is shown in Figure 6.2.

REPRODUCED AT GOVERNMENT EXPENSE

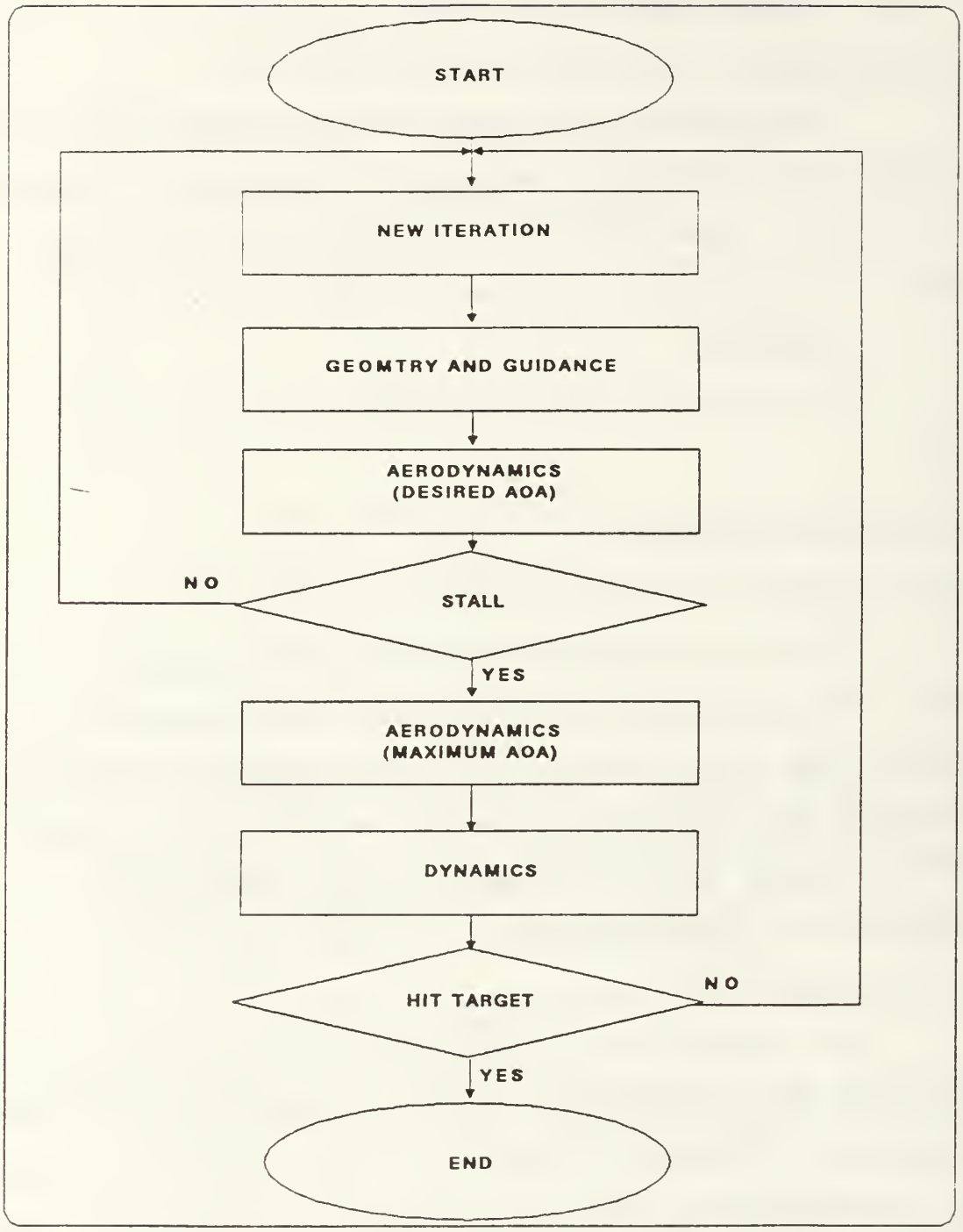

Figure 6.1 Flowchart of Guidance Program

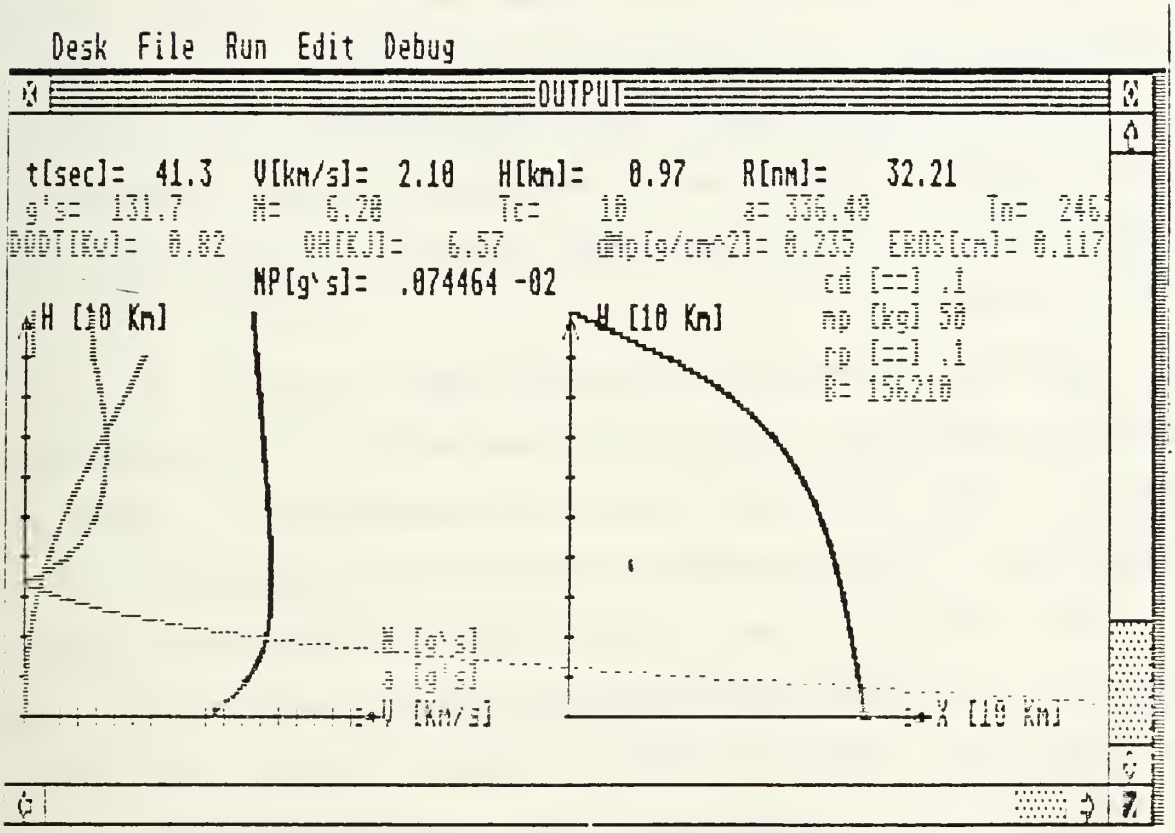

Figure 6.2 Guidance Layout

VII. THE COMPUTER AND THE PROGRAMMING LANGUAGES

A. THE COMPUTERS

The main concept of this research was to create a handy and easy to use tool for preliminary design. The state-of-the-art of microcomputers is so advanced that the powerful CPU, the large memory and the excellent graphic capabilities that most of them offer today, seem to be satisfactory for this purpose.

A decision was made to develop these models on the Atari ST-1040 computer. The cost per performance of this machine was by far superior to any alternative. Technical description of this machine is given in the Appendix.

The new generation of the IBM microcomputers (IBM-2 series) is similar in concept to the Atari-ST. These new machines use the 3.5 inch magnetic discs. The basic language of both machines is very similar as well. As a result the transfer of these models to the new IBM machines is a relatively short and easy process.

B. THE PROGRAMMING LANGUAGE

The models were written initially in ST-Basic. This is a very powerful version of the Basic language. The big advantages of using the ST-Basic language are:

a) The ST-Basic language is an interpreter-based language. Programs may be written or improved and

then be run immediately without the need to make any compilation or linkages.

b) The ST-Basic assures easy and efficient use of the ST-machine and its graphic capability.

In order to accelerate running the programs, after the development of the code was completed, a special version of them was prepared for compilation. Compilation was completed by the LDW compiler. This first version of the software was not yet free from bugs. However, with professional assistance, LDW programmers compiled versions of most modules.

In order to ease the use of the modules, they were packed in one package. A managing program, "INTRODU1" was added. This program loads and runs the different modules upon the user's request. A typical layout of the screen of this program is shown in Figure 7.1.

In order to save time and to prevent the need to transfer relevant results from one module to another, the chaining capabilities of the software were used. A schematic description of the inter-modules chaining is shown in Figure 7.2.

C. RUNNING THE MODEL ON THE MAINFRAME

In order to check and to compare the results of the new suggested method for a solution of the "two body problem" to the existing methods, a Fortran version of the orbit program was created. This program was run on the Naval Postgraduate School's mainframe IBM 370/3033AP computer in order to

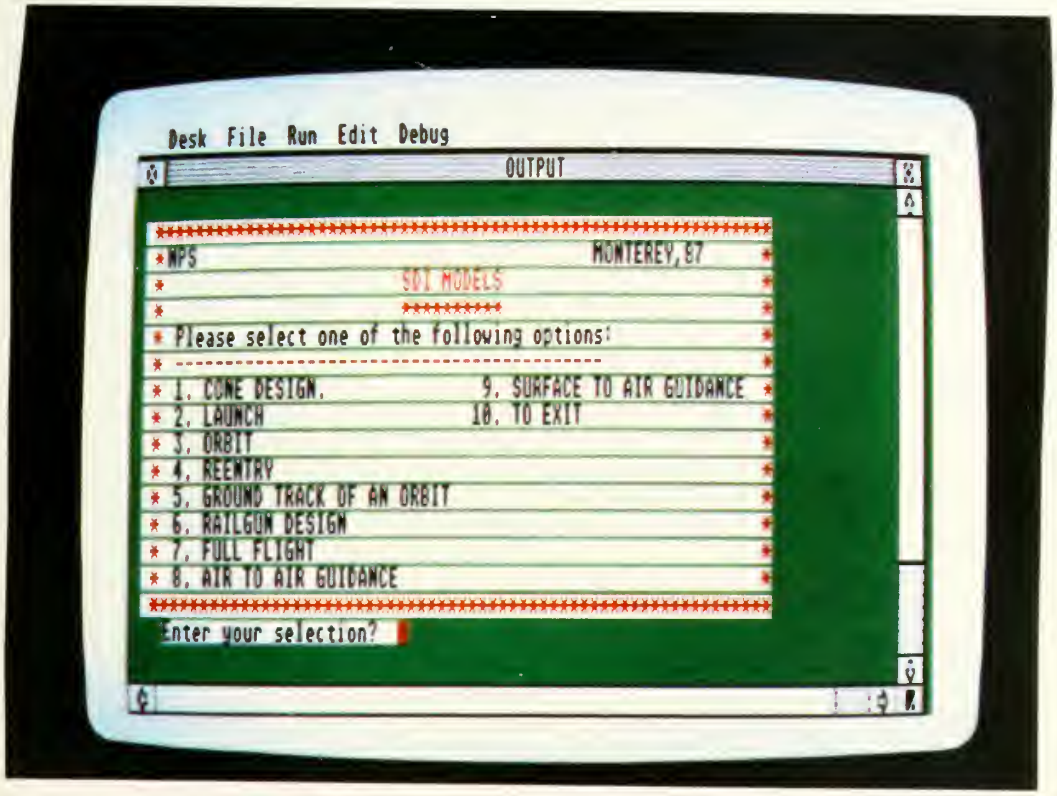

Figure 7.1 Introduction Layout

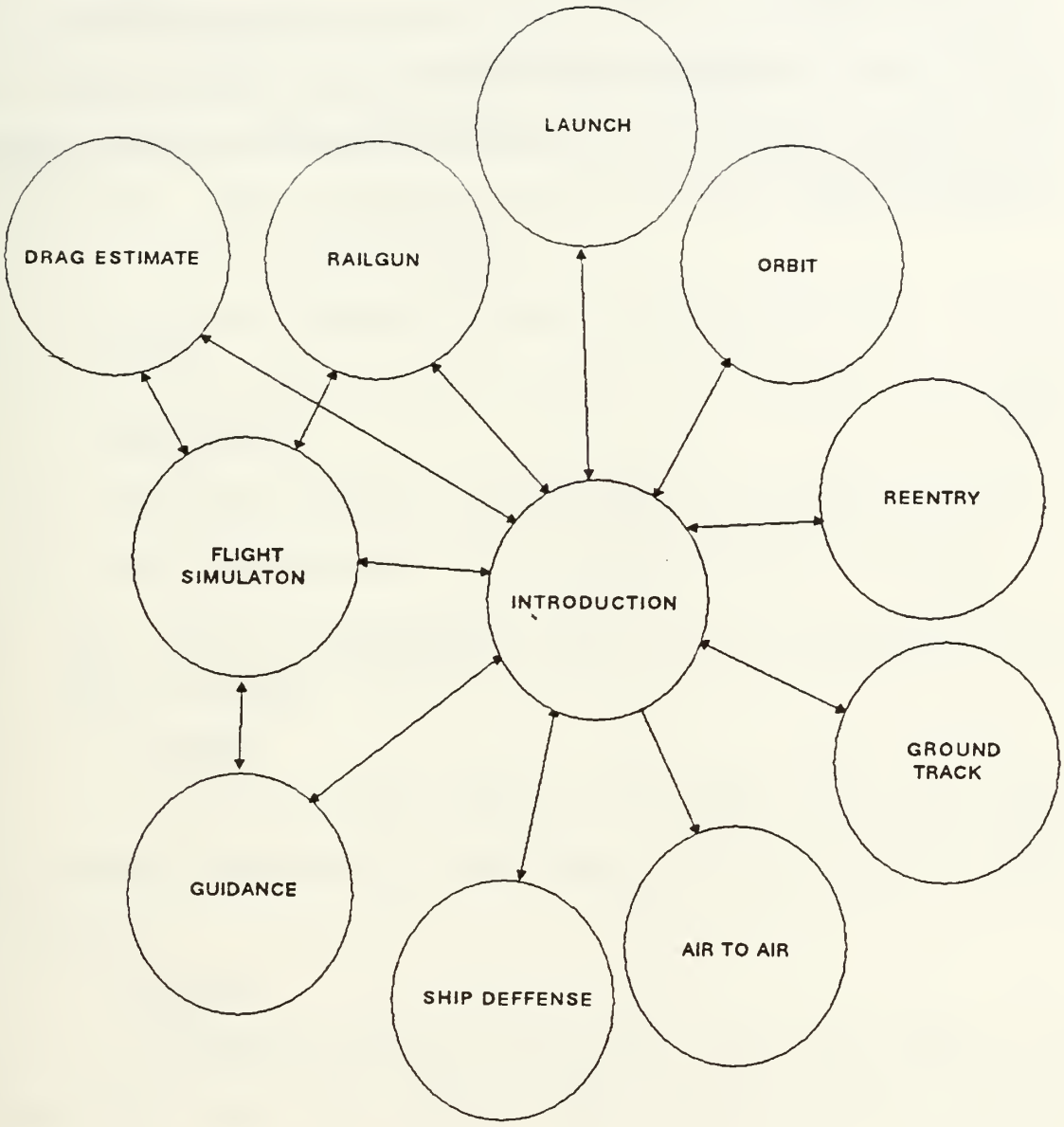

Figure 7.2 Interconnections Between Modules

achieve very long runs. The advantages of the new method are most apparent for long runs.

All other models were written for microcomputers. There is no advantage to run them on the mainframe. In order to achieve the greatest benefit from these models, they have to be run on an Atari-ST or on machines with similar graphics capabilities.

VIII. CASE STUDIES

A. GENERAL

In order to demonstrate the potential use of these models for preliminary design, a few case studies were initiated. The following are the results of a few case studies based on these models:

1) Parametric study of the performance of a railgun system
2) Sensitivity of the range to errors in launch conditions
3) Preliminary design of an airborne railgun system
4) Preliminary design of a seaborne railgun system.

B. CASE STUDY 1--PARAMETRIC STUDY OF THE PERFORMANCE OF A RAILGUN SYSTEM

1. Purpose

The aim of this study is to learn about the effect of relevant parameters on the range of a projectile fired by a railgun.

2. Method

A nominal case was selected. In this example the conditions for the nominal case were selected as the following:

a) Firing of a 50 kg projectile
b) Launch at sea level
c) The projectile with a radius of 0.1 m

d) The projectile with a low drag shape (C_d = 0.1)

e) The projectile was fired at an angle of 50 degrees above the local horizon.

The flight simulation model was run repetitively. In each run a different value of a selected parameter was chosen. All others were kept in their nominal values. The effect of changing each parameter over its full range is shown by graphs.

3. Results

The results of this study are shown in the following figures:

a) Figure 8.1--the effect of the projectile drag coefficient

b) Figure 8.2--the effect of launch speed

c) Figure 8.3--the effect of launch altitude

d) Figure 8.4--the effect of launch angle.

4. Conclusions

The following conclusions were drawn from the study:

a) The coefficient of drag is a key parameter affecting the range performance. For example, reducing the drag coefficient from 0.2 to 0.1 will triple the range.

b) The function of the range vs. the launch speed looks parabolic at the lower speed range (under 7 km/sec in this specific case study) and becomes linear at higher speeds. This means that the system becomes less efficient as the launch speed increases.

c) The range increases linearly with altitude in the majority of the flight altitudes. The rate is approximately 120 NM of range per 1 km of altitude. This means that firing from an airplane flying at typical jet cruise altitude of about 36,000 ft may double the range in comparison with the range achieved by firing at sea level.

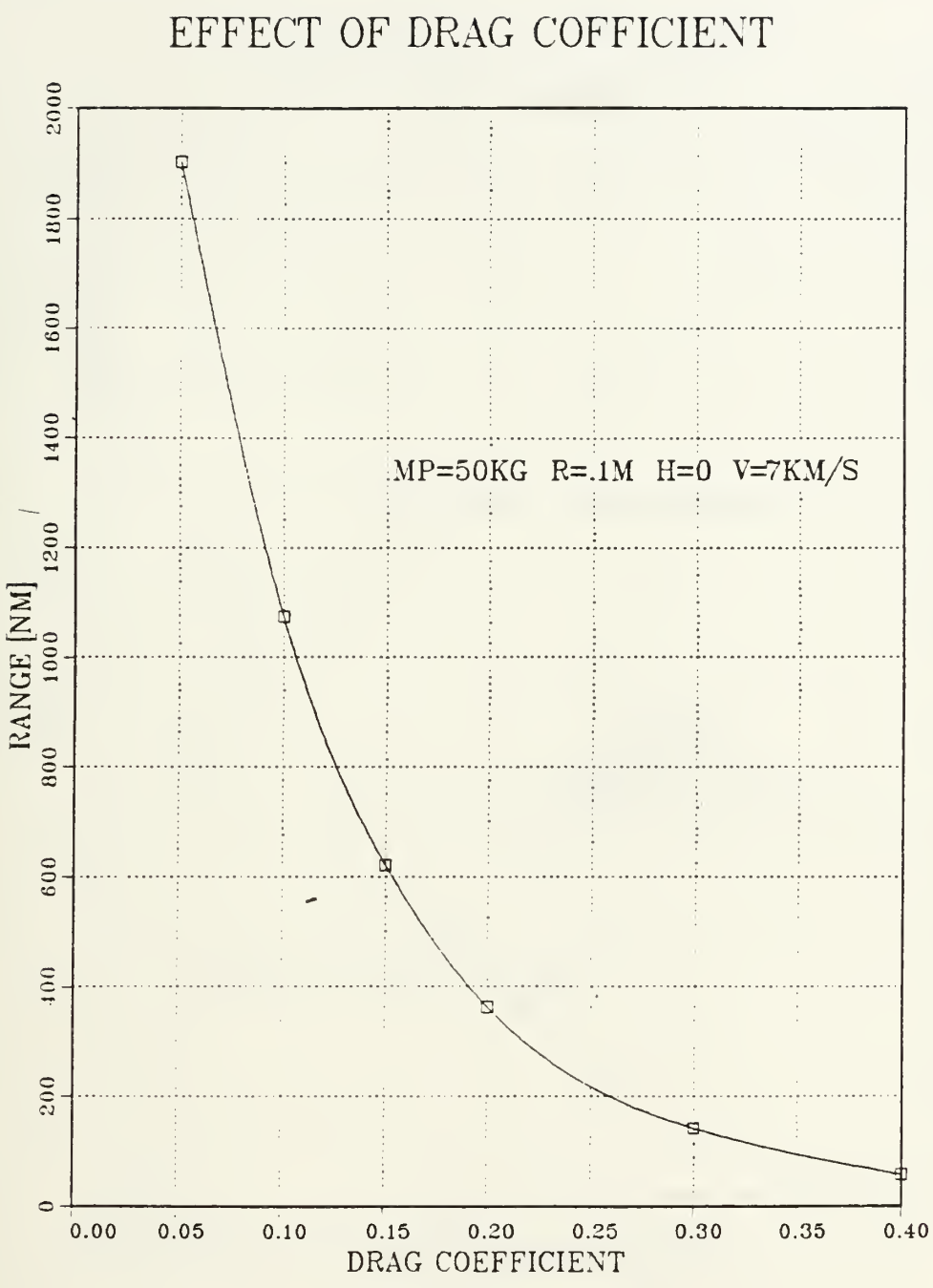

Figure 8.1 The Effect of the Projectile Drag Coefficient

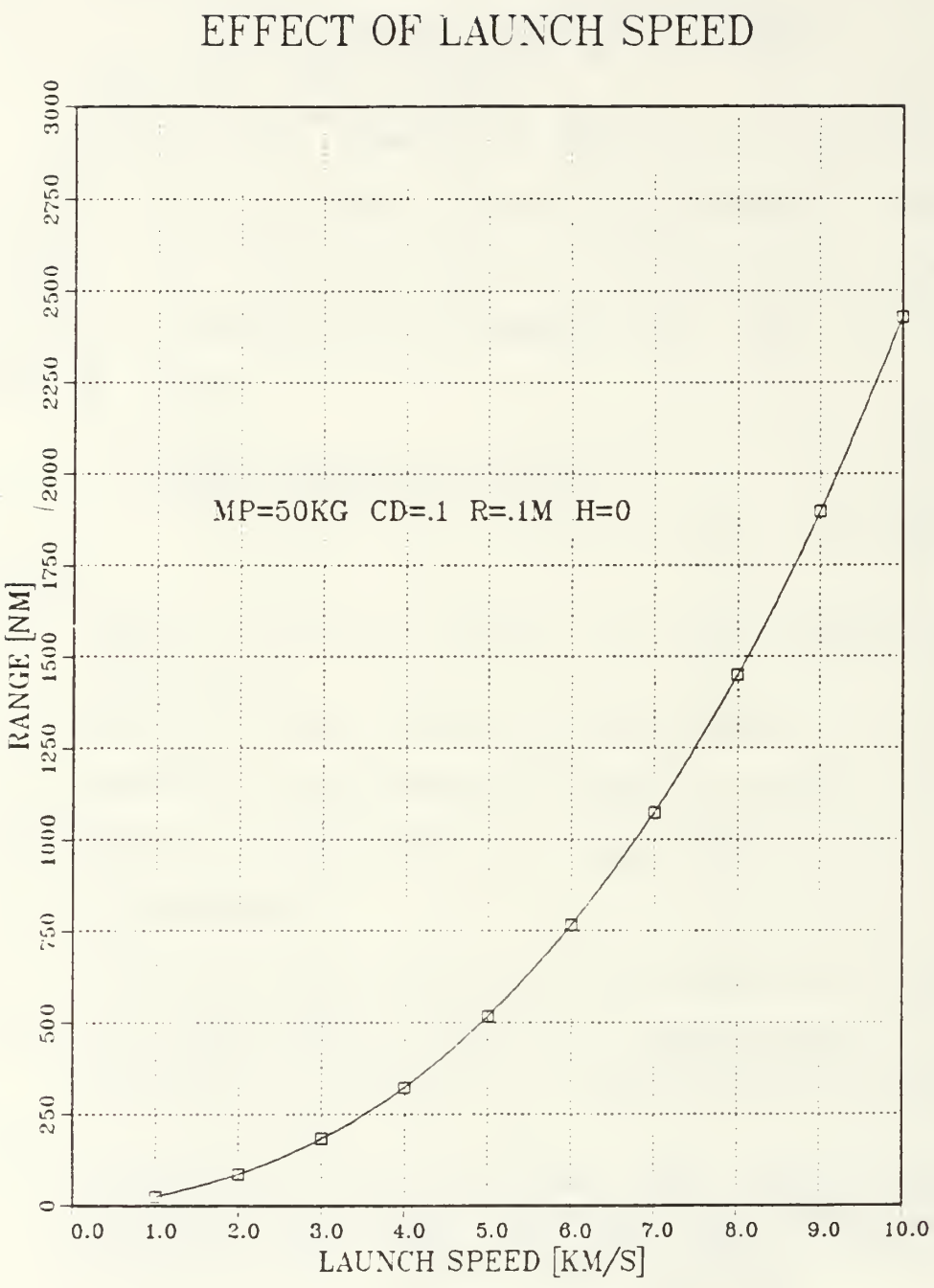

Figure 8.2 The Effect of Launch Speed

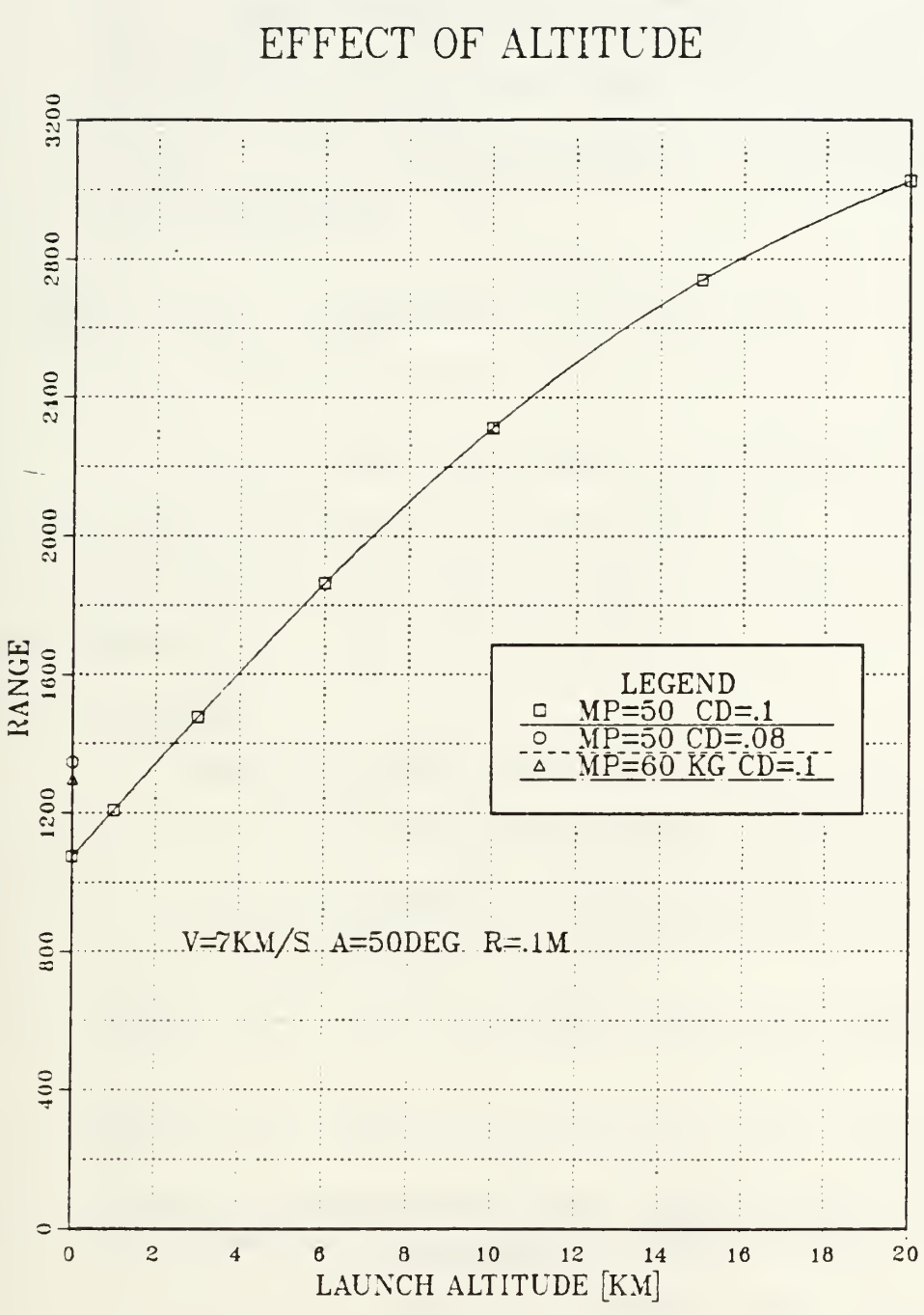

Figure 8.3 The Effect of Launch Altitude

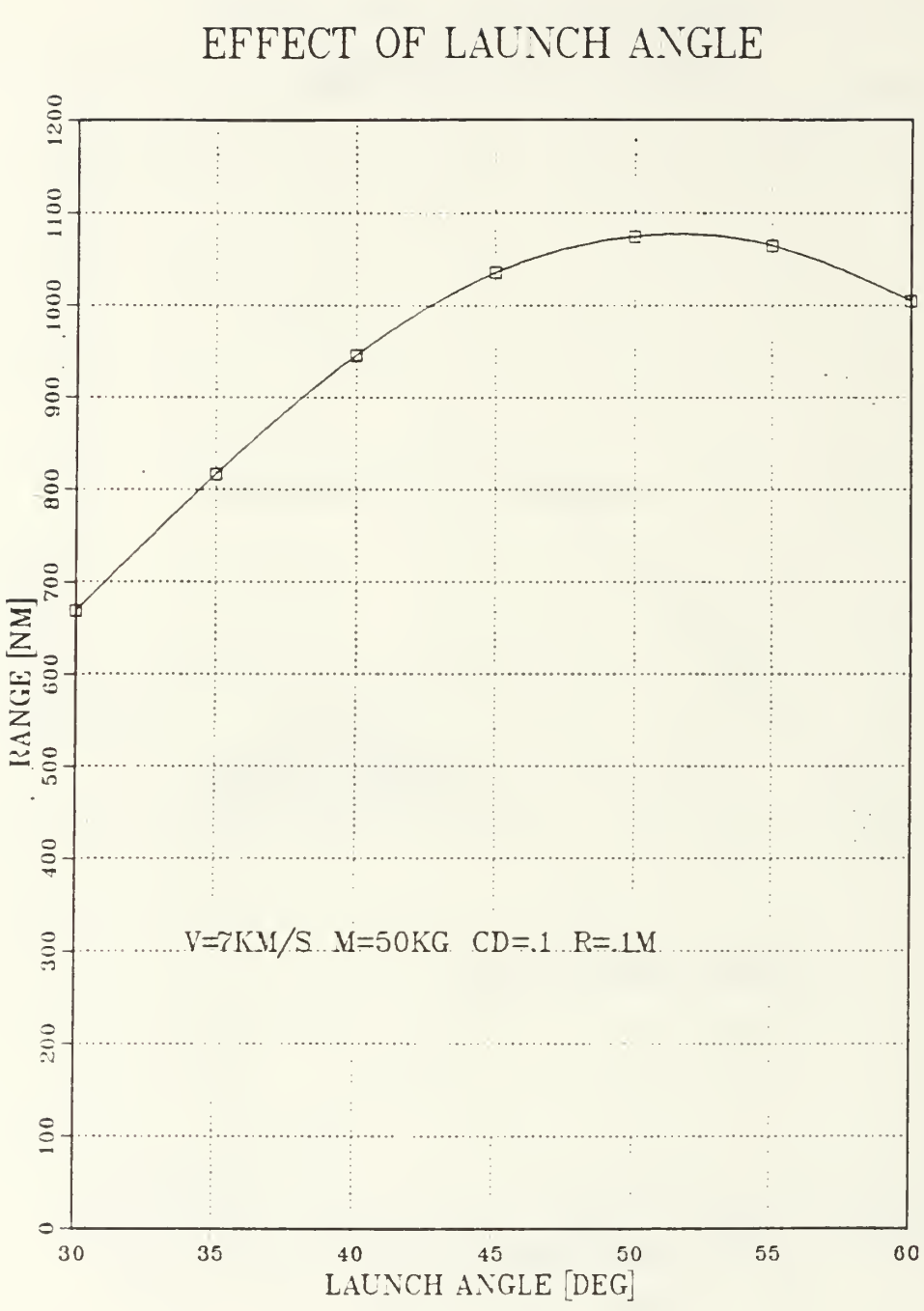

Figure 8.4 The Effect of Launch Angle

d) From the graph of the range vs. launch angle, it can be learned that firing all high angles (above 45^{o}) gives longer ranges. This is caused by the effect of the aerodynamic drag in the atmosphere. Firing at a higher angle results in lengthening the phase of space flight and shortening the phase of atmosphere flight. This is a more efficient use of energy--less kinetic energy is lost to the atmosphere. In this case study, maximum range was achieved at an angle of launch of about 52 degrees.

C. CASE STUDY 2--SENSITIVITY OF THE RANGE TO ERRORS IN LAUNCH CONDITIONS

1. Aim

The aim of this study was to check the sensitivity of the range to errors in launch parameters. In addition, the demands from the guidance system to correct such errors were examined.

2. Method

In order to study the sensitivity of the range to errors in launch parameters, the flight simulation code was run for the following cases:

a) Launch at the nominal condition

b) Launch with a small deviation from the nominal launch angle

c) Launch with a small deviation from the nominal launch speed

d) Launch of a projectile that differs slightly in its coefficient of drag from the nominal value.

In order to study the demands from the guidance system it was assumed that at reentry the guidance system discovers a range error. The measure of the range error was

chosen as the sum of all the errors caused by the deviations from the nominal launch conditions.

The guidance system controlling the flight path of the projectile corrects the range errors. The output from the guidance program includes a graph of the lift forces needed to achieve the desired corrections. The demand for lift may be used to design the lift surfaces and the guidance system of the projectile.

3. Results

The results of this study are summarized in Table 8.1. In this table the sensitivity coefficients of the range to errors in launch conditions and to deviation of the projectile from its design specification are presented. These coefficients were calculated for the following nominal case:

a) Projectile mass (M_p)--50 kg

b) Coefficient of drag (C_d)--0.096

TABLE 8.1

SENSITIVITY COEFFICIENTS

The Cause	Range Error
Deviation of 1 m/s in launch speed	9.15 NM
Deviation of 1 degree in the angle of launch	5.80 NM
Deviation of 0.01 in the drag coefficient	6.09 NM

c) Launch angle--50°

d) Muzzle speed--7 km/s.

To correct such errors the projectile must have a turn capability of 7.5 g's. This is the result of a run made with the guidance model. The run was made for a proportional navigation guidance system with coefficient of proportion of 3.0. Greater refinement in the production of the projectile and less deviation in the launch conditions may ease the demand from the guidance system.

4. Conclusions

In order to achieve greater effectiveness of the railgun weapon system, the warhead has to be brought as close as possible to the target. The measure of accuracy needed is dependent on the type of warhead and its yield.

The range is very sensitive to errors in launch conditions and to inaccuracies in the projectile manufacturing. Increasing the accuracy of the launching system is not cost effective.

Whenever greater accuracy is desired a guidance system is needed. A proportional guidance system may correct these errors and assure high effectiveness of the overall performance of the railgun system.

D. CASE STUDY 3--SEABORNE SYSTEM

1. Purpose

The aim of this study was to check the feasibility and to estimate the performance of a railgun system mounted aboard a naval vessel.

2. Method

By using the flight simulation program the basic parameters of the railgun system were defined in order to assure the desired ranges and effectiveness.

Once the basic parameters (mass and coefficient of drag) were defined, the basic shape of the projectile was identified by using the drag estimation module.

The results of the drag module and the flight simulation were fed into the railgun model. The output of the railgun program included the cross section of the barrel shape and estimates of the overall system weight and volume.

3. Results

The results of this study are presented in the following figures:

a) Figure 8.5--final output of the flight simulation model

b) Figure 8.6--the warhead shape derived by the drag module

c) Figure 8.7--results of the railgun simulation

d) Figure 8.8--the railgun structure

e) Figure 8.9--summary of the power conditioning system

f) Figure 8.10--total weight of the cooling system and its main subsystems

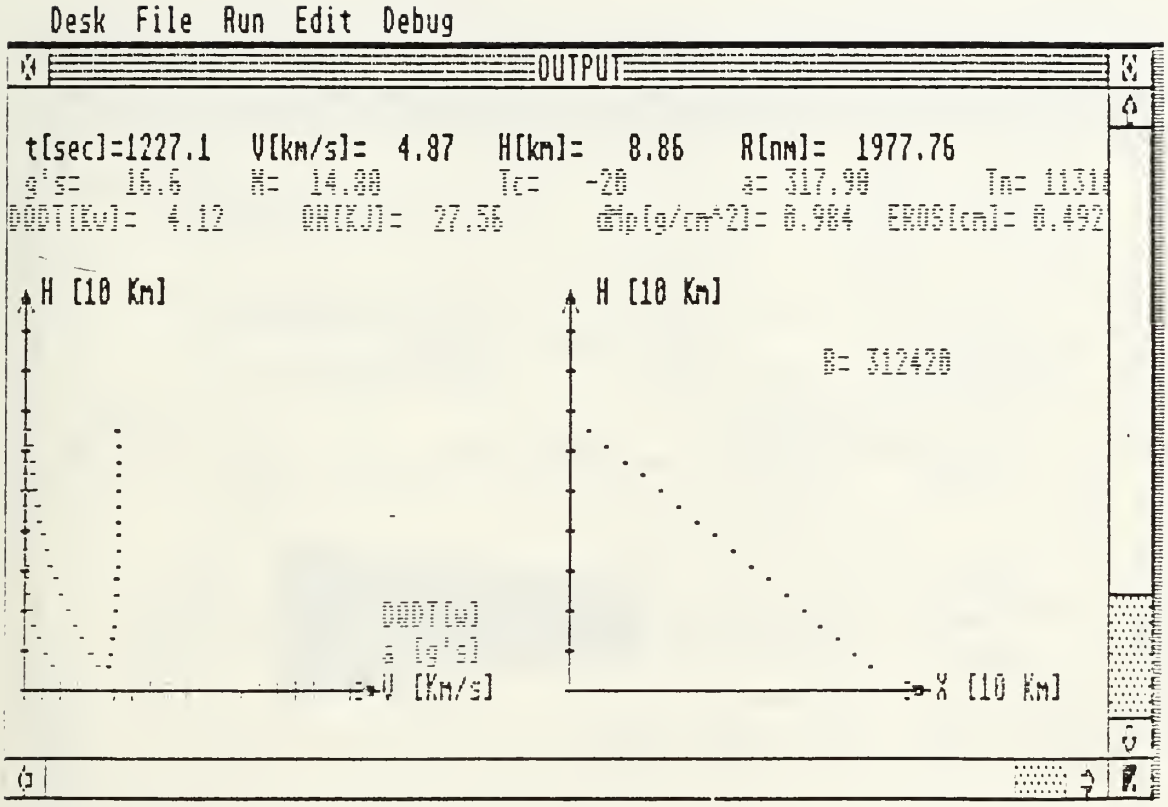

Figure 8.5 Case Study 3--Flight Simulation Results

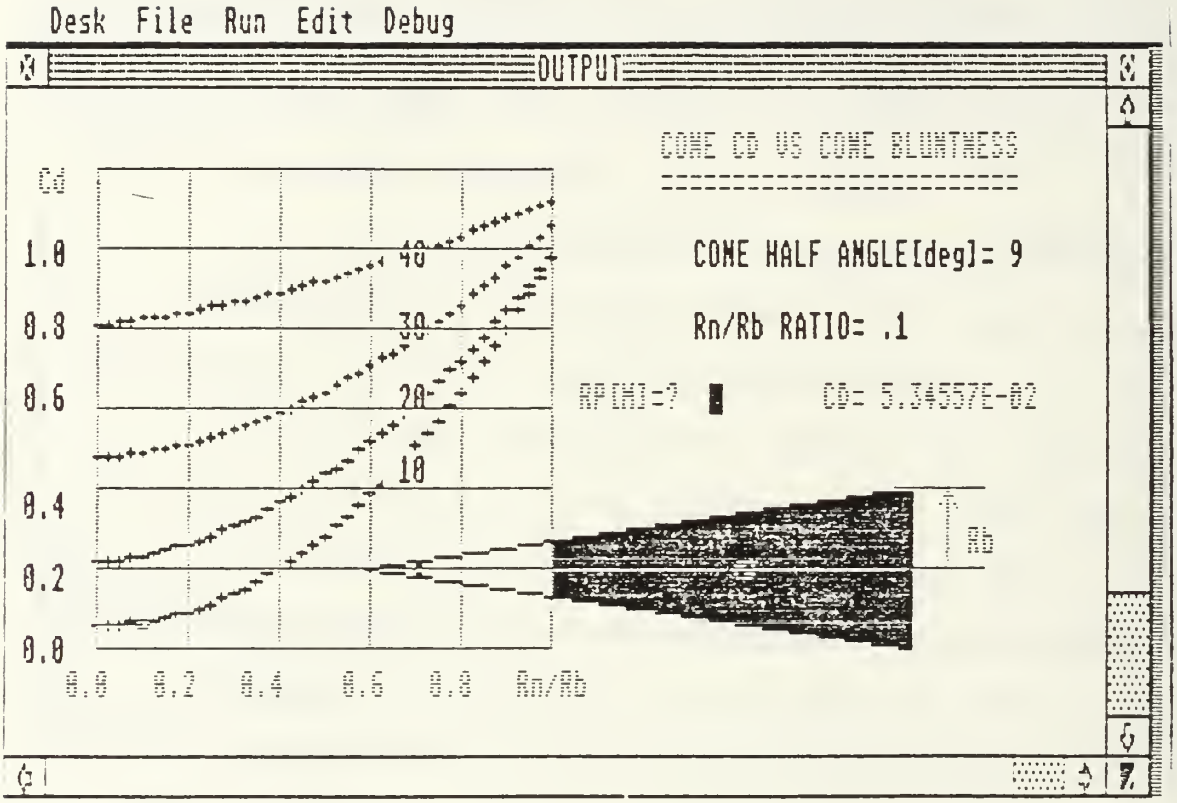

Figure 8.6 Case Study 3--The Warhead Shape

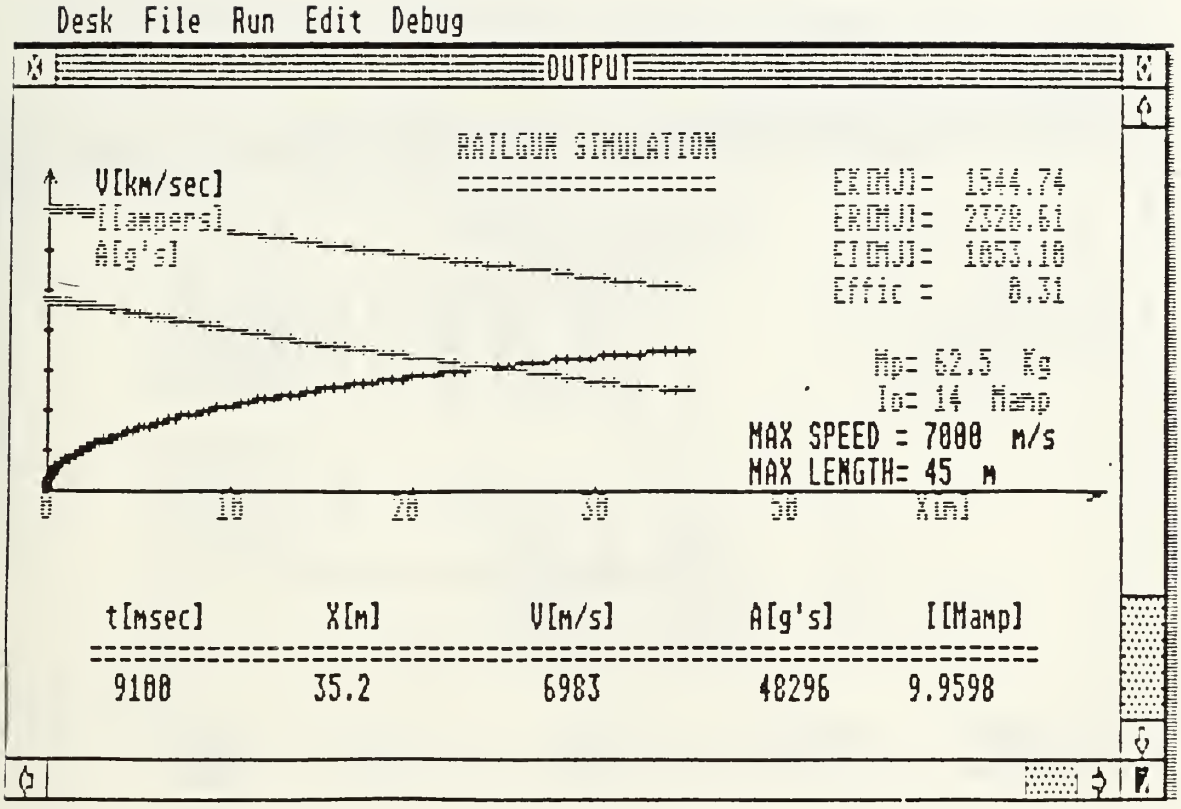

Figure 8.7 Case Study 3--The Railgun Simulation

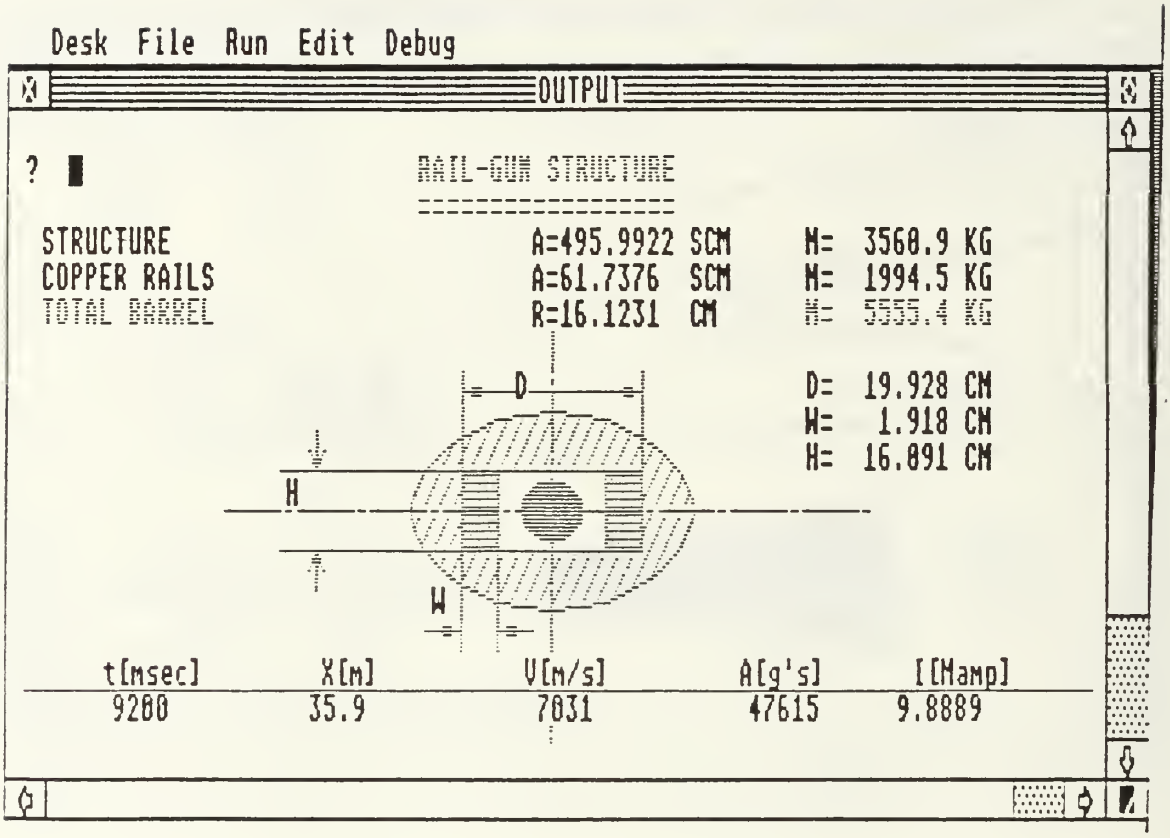

Figure 8.8 Case Study 3--The Railgun Structure

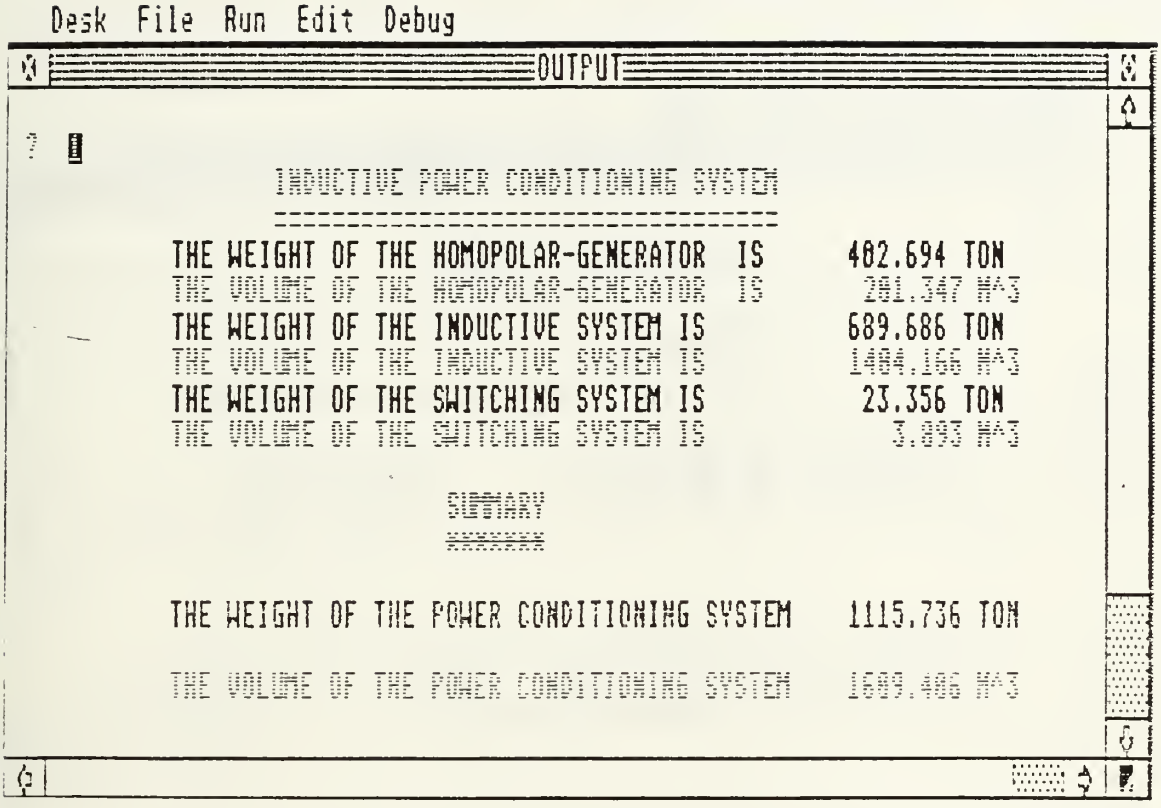
Desk File Run Edit Debug
OUTPUT
?
INDUCTIVE POWER CONDITIONING SYSTEM
THE WEIGHT OF THE HOMOPOLAR-GENERATOR IS 402.694 TON
THE VOLUME OF THE HOMOPOLAR-GENERATOR IS 281.347 M^3
THE WEIGHT OF THE INDUCTIVE SYSTEM IS 689.686 TON
THE VOLUME OF THE INDUCTIVE SYSTEM IS 1484.166 M^3
THE WEIGHT OF THE SWITCHING SYSTEM IS 23.356 TON
THE VOLUME OF THE SWITCHING SYSTEM IS 3.893 M^3
SUMMARY
THE WEIGHT OF THE POWER CONDITIONING SYSTEM 1115.736 TON
THE VOLUME OF THE POWER CONDITIONING SYSTEM 1689.406 M^3

Figure 8.9 Case Study 3--The Power Conditioning

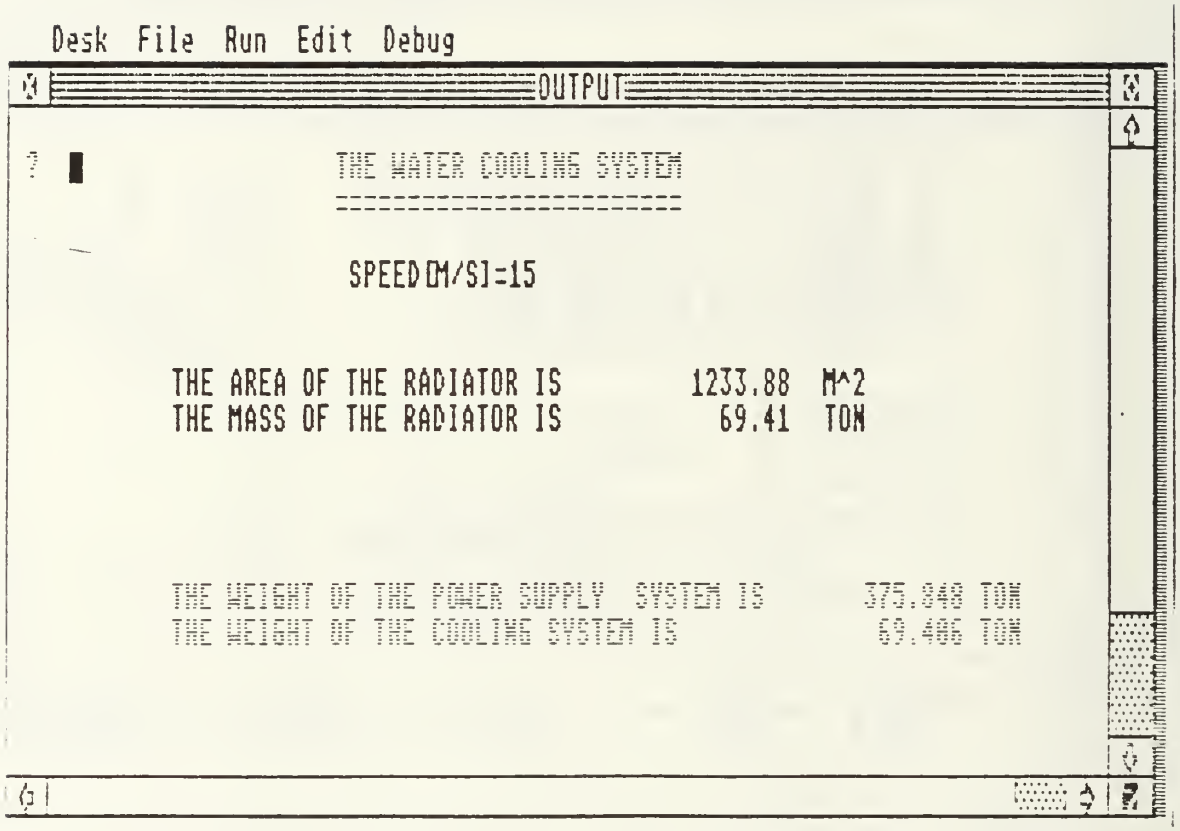
Desk File Run Edit Debug
OUTPUT
? _
THE WATER COOLING SYSTEM
SPEED[M/S]=15
THE AREA OF THE RADIATOR IS 1233.88 M^2
THE MASS OF THE RADIATOR IS 69.41 TON
THE WEIGHT OF THE POWER SUPPLY SYSTEM IS 375.948 TON
THE WEIGHT OF THE COOLING SYSTEM IS 69.406 TON

Figure 8.10 Case Study 3--The Cooling System

g) Figure 8.11--summary of the weight and size of the whole airborne system.

4. Conclusions

The main conclusion from this preliminary examination is that it is feasible to design a railgun system for a naval vessel. Such a system would be capable of firing a 50 kg projectile to a range on the order of 1000 NM. This performance is assured if the value of the drag coefficient is 0.1 or less. This low value can be achieved by proper design of the projectile aerodynamic shape.

The railgun design will be based on a 20 cm (width) rail. The copper rails will have a 2 by 6 cm rectangular cross section. The railgun length has to be at least 8.0 m long.

The inductive power conditioning system will weigh about 1116 tons and its volume will be 1610 cubic meters (Figure 8.9).

E. CASE STUDY 4--AIRBORNE SYSTEM

1. Purpose

The aim of this study was to examine the feasibility and the performance of an airborne railgun system and to obtain an estimate of its weight and size in order to check the capability of airplanes to carry the system.

2. Method

The method of this examination was very similar to the examination of the naval railgun system (Case 3). In

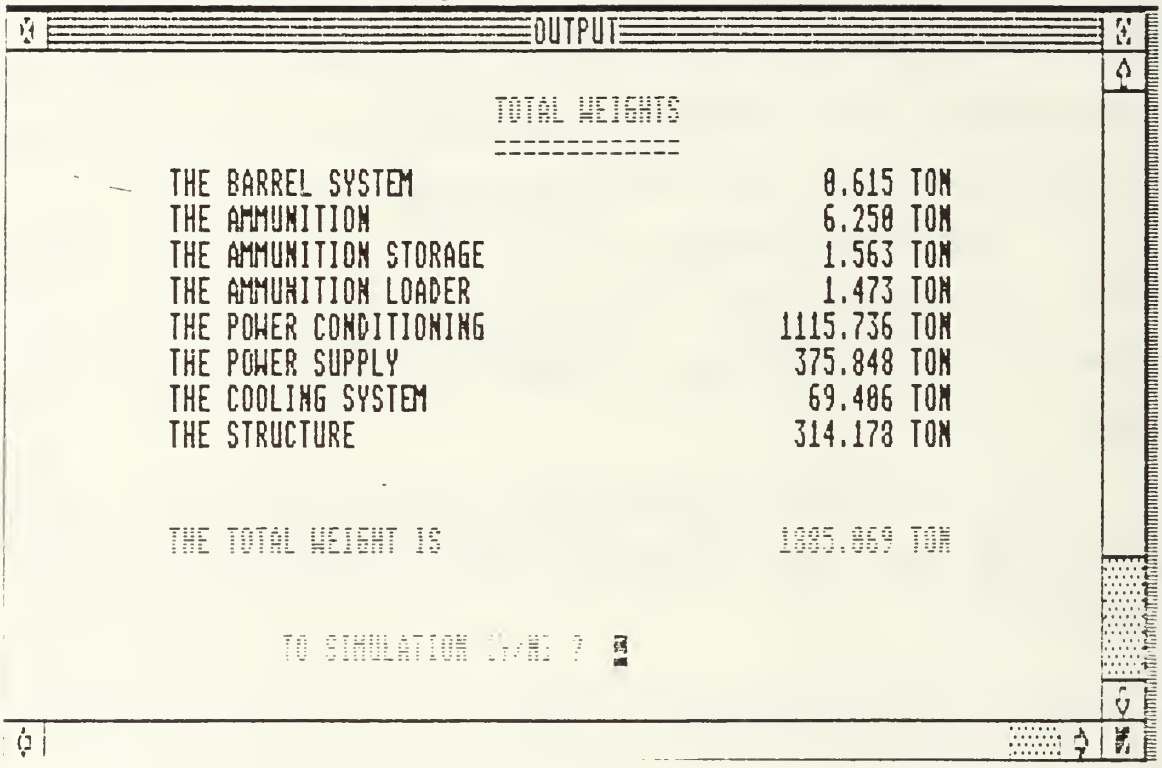
Desk File Run Edit Debug
OUTPUT
TOTAL WEIGHTS
THE BARREL SYSTEM 0.615 TON
THE AMMUNITION 6.250 TON
THE AMMUNITION STORAGE 1.563 TON
THE AMMUNITION LOADER 1.473 TON
THE POWER CONDITIONING 1115.736 TON
THE POWER SUPPLY 375.848 TON
THE COOLING SYSTEM 69.406 TON
THE STRUCTURE 314.178 TON
THE TOTAL WEIGHT IS 1885.869 TON
TO SIMULATION (Y/N) ?

Figure 8.11 Case Study 3--Total Weight and Size

this case typical airborne parameters were used by the airborne modules.

3. Results

The results of this study are presented in the following figures:

a) Figure 8.12--final output of the flight simulation model

b) Figure 8.13--the warhead shape derived by the drag module

c) Figure 8.14--results of the railgun simulation

d) Figure 8.15--the railgun structure

e) Figure 8.16--summary of the power conditioning system

f) Figure 8.17--total weight of the cooling system and its main subsystems

g) Figure 8.18--summary of the weight and size of the whole airborne system.

4. Conclusion

The conclusion of this preliminary study is that it appears feasible to install a railgun system on an existing airplane. This system would be capable of firing a 50 kg projectile to a range on the order of 200 nautical miles (assuming that a c_d of about 0.1 will be achieved by proper design of the aerodynamic shape of the projectile).

The railgun system will be based on 2*16 cm rectangular copper rails with a span of about 20 cm. The inductive power system weights about 70 tons and its volume is about 37 cubic meters.

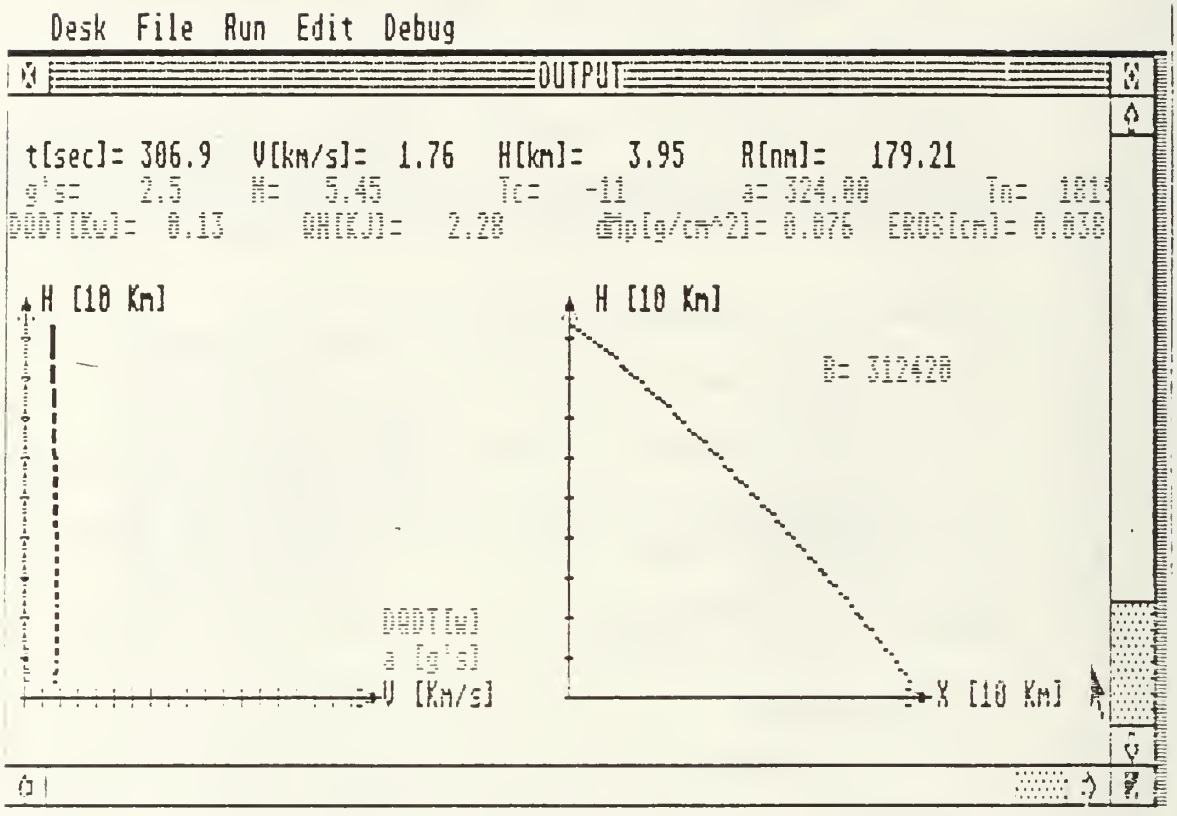
Desk File Run Edit Debug
OUTPUT
t[sec]= 306.9 V[km/s]= 1.76 H[km]= 3.95 R[nm]= 179.21
g's= 2.5 M= 5.45 Tc= -11 a= 324.00 Tm= 181
DADT[km]= 0.13 QH[KJ]= 2.28 ρ[g/cm^2]= 0.076 ERDS[cm]= 0.038
H [10 Km]
DADT[m]
a [g's]
V [Km/s]
H [10 Km]
B= 312420
X [10 Km]

Figure 8.12 Case Study 4--Final Output of the Flight Simulation Program

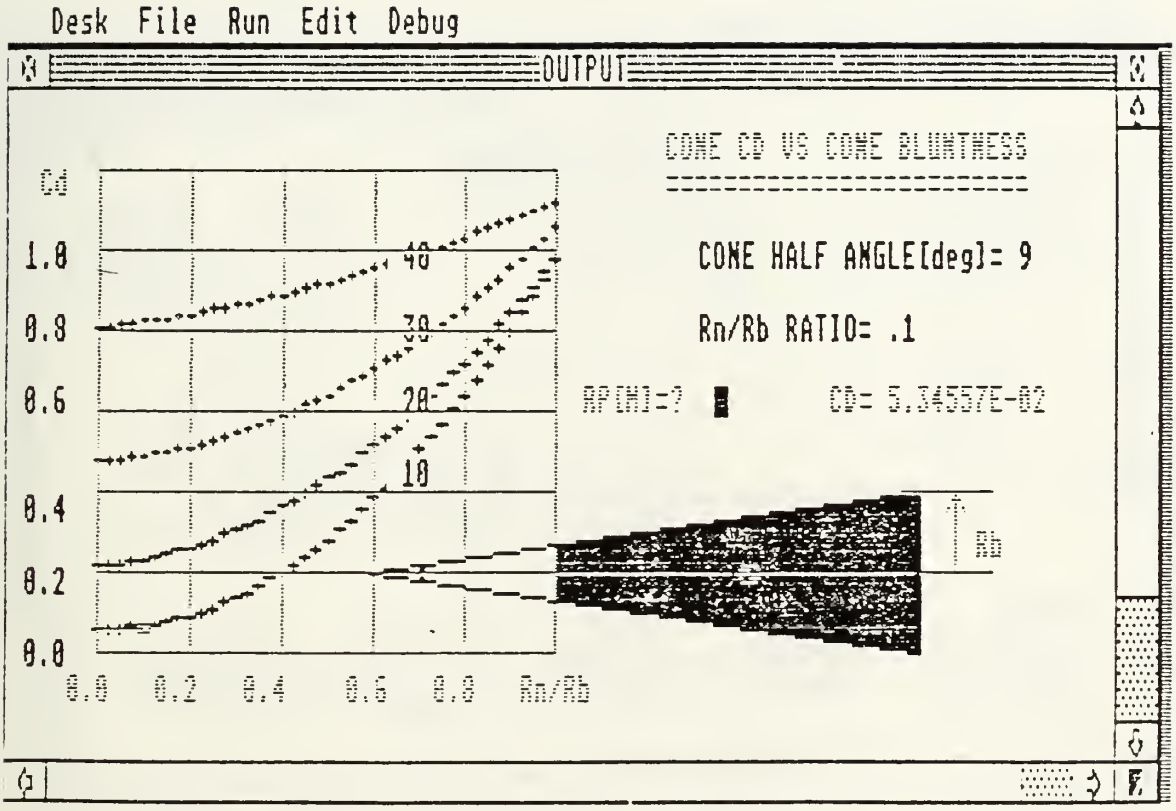

Figure 8.13 Case Study 4--Warhead Weight and Size

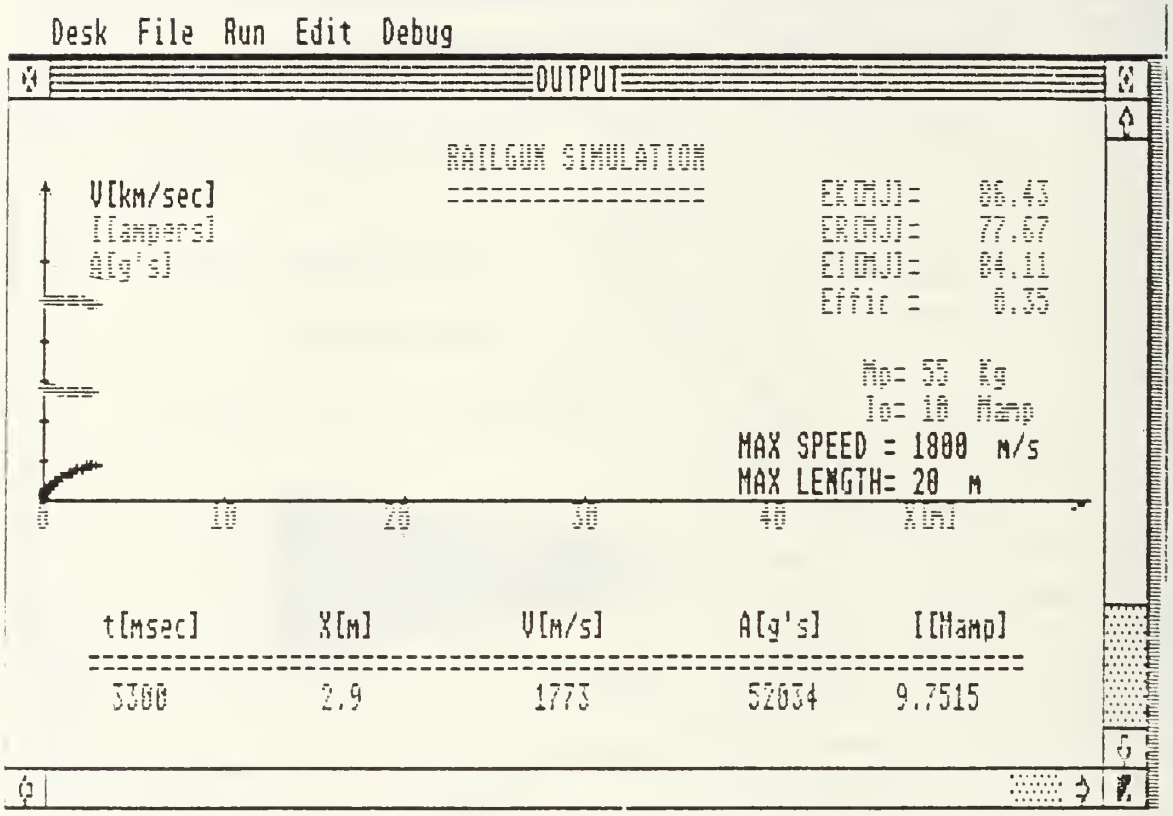

Figure 8.14 Case Study 4--Railgun Simulation

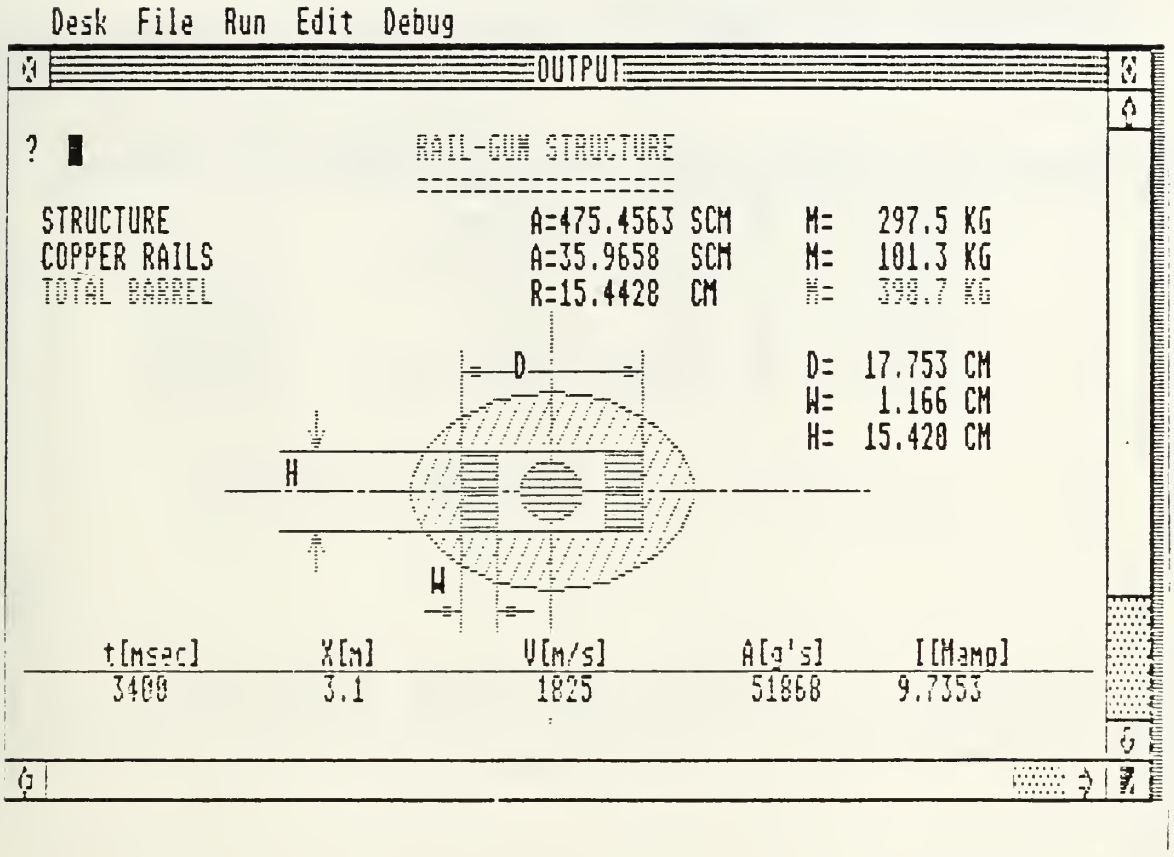

Figure 8.15 Case Study 4--Rail Weight and Size

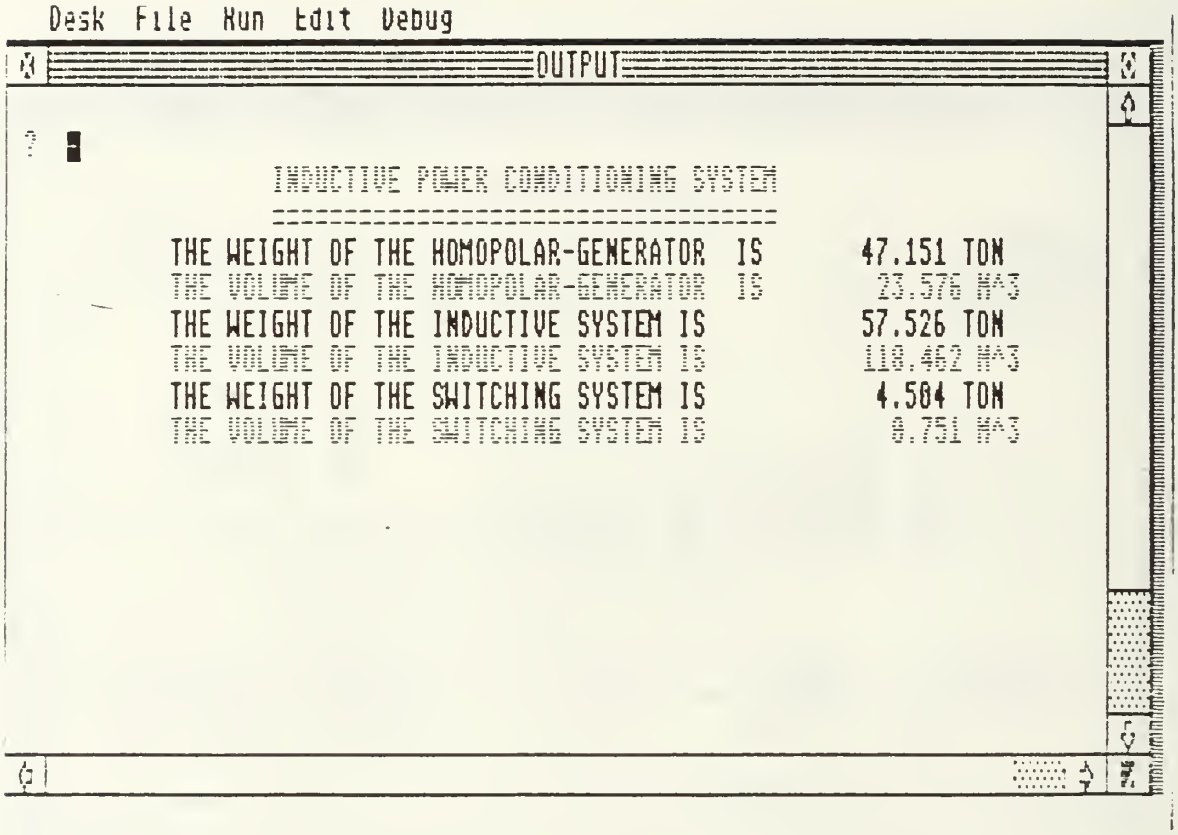
Desk File Run Edit Debug
OUTPUT
? _
INDUCTIVE POWER CONDITIONING SYSTEM
THE WEIGHT OF THE HOMOPOLAR-GENERATOR IS 47.151 TON
THE VOLUME OF THE HOMOPOLAR-GENERATOR IS 23.576 M^3
THE WEIGHT OF THE INDUCTIVE SYSTEM IS 57.526 TON
THE VOLUME OF THE INDUCTIVE SYSTEM IS 118.462 M^3
THE WEIGHT OF THE SWITCHING SYSTEM IS 4.504 TON
THE VOLUME OF THE SWITCHING SYSTEM IS 0.751 M^3

Figure 8.16 Case Study 4--Power Weight and Size

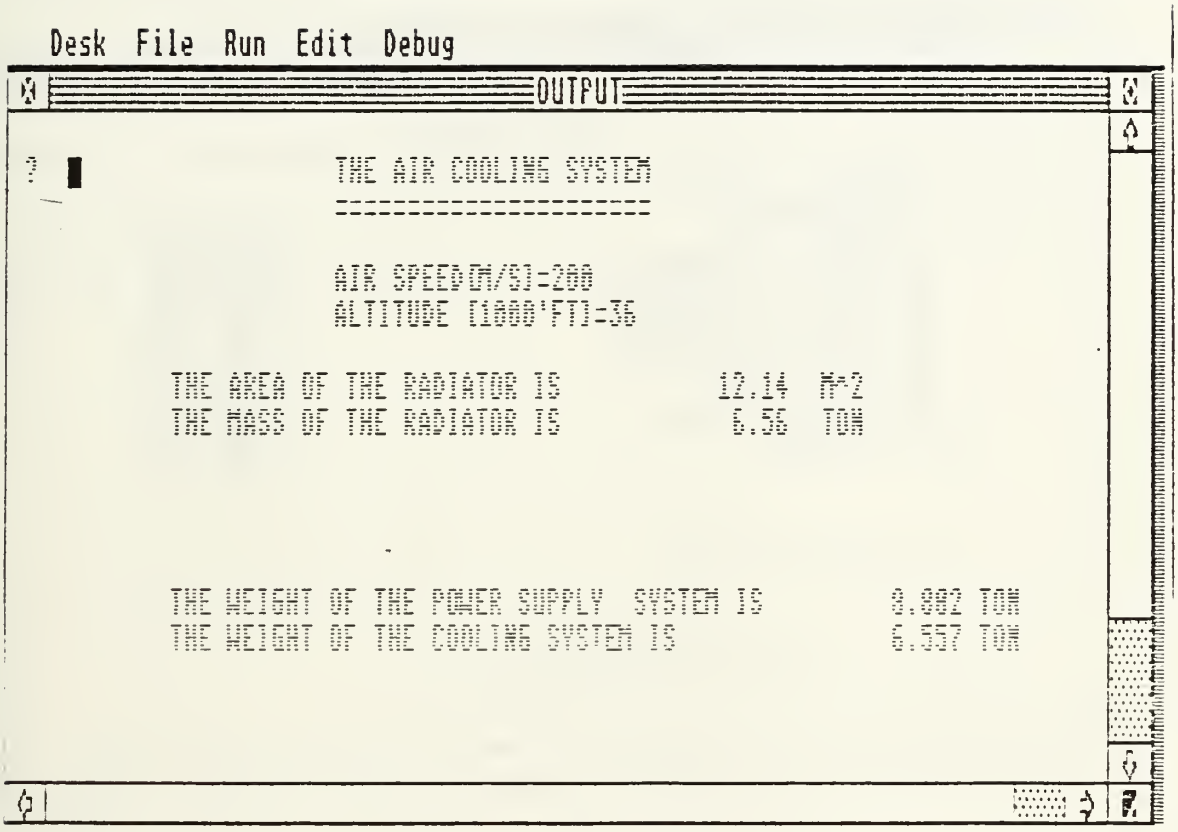
Desk File Run Edit Debug
OUTPUT
?
THE AIR COOLING SYSTEM
AIR SPEED(M/S)=200
ALTITUDE (1000'FT)=36
THE AREA OF THE RADIATOR IS 12.14 M^2
THE MASS OF THE RADIATOR IS 6.56 TON
THE WEIGHT OF THE POWER SUPPLY SYSTEM IS 0.002 TON
THE WEIGHT OF THE COOLING SYSTEM IS 6.557 TON

Figure 8.17 Case Study 4--Cooling Weight and Size

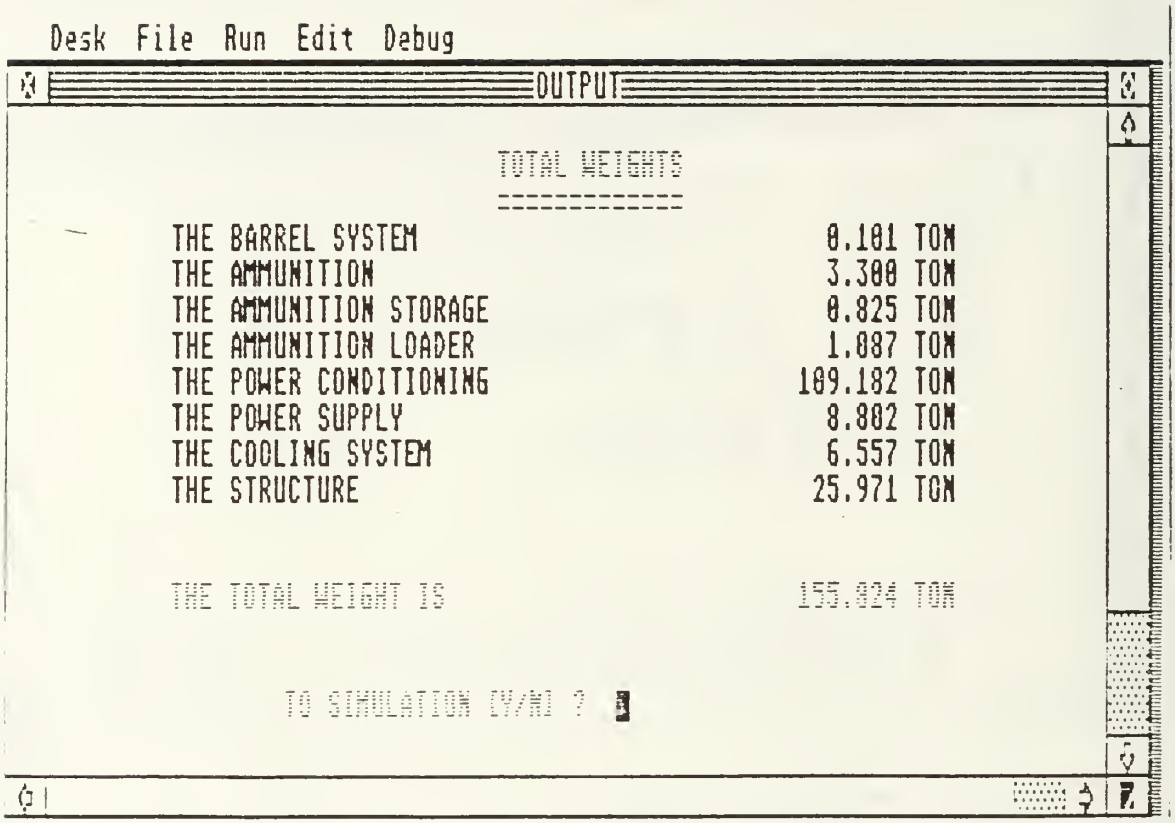
Desk File Run Edit Debug
OUTPUT
TOTAL WEIGHTS
THE BARREL SYSTEM 0.101 TON
THE AMMUNITION 3.300 TON
THE AMMUNITION STORAGE 0.825 TON
THE AMMUNITION LOADER 1.087 TON
THE POWER CONDITIONING 109.182 TON
THE POWER SUPPLY 8.802 TON
THE COOLING SYSTEM 6.557 TON
THE STRUCTURE 25.971 TON
THE TOTAL WEIGHT IS 155.824 TON
TO SIMULATION [Y/N] ?

Figure 8.18 Case Study 4--Total Weight and Size

The overall size and weight of the system is about 90 tons. It appears that a railgun system of this weight and size is suitable to be mounted on an existing airplane. This specific system will require an airplane the size and performance of a Boeing 747. Longer ranges may be achieved if the system is installed on larger planes in the future.

Firing the projectile at a rate of 10 projectiles per minute will demand a power supply on the order of 33.5 Mwatts. The wasted heat will be cooled by large radiators mounted on top of the aircraft. An imaginary picture of such an airplane is shown in Figure 8.19.

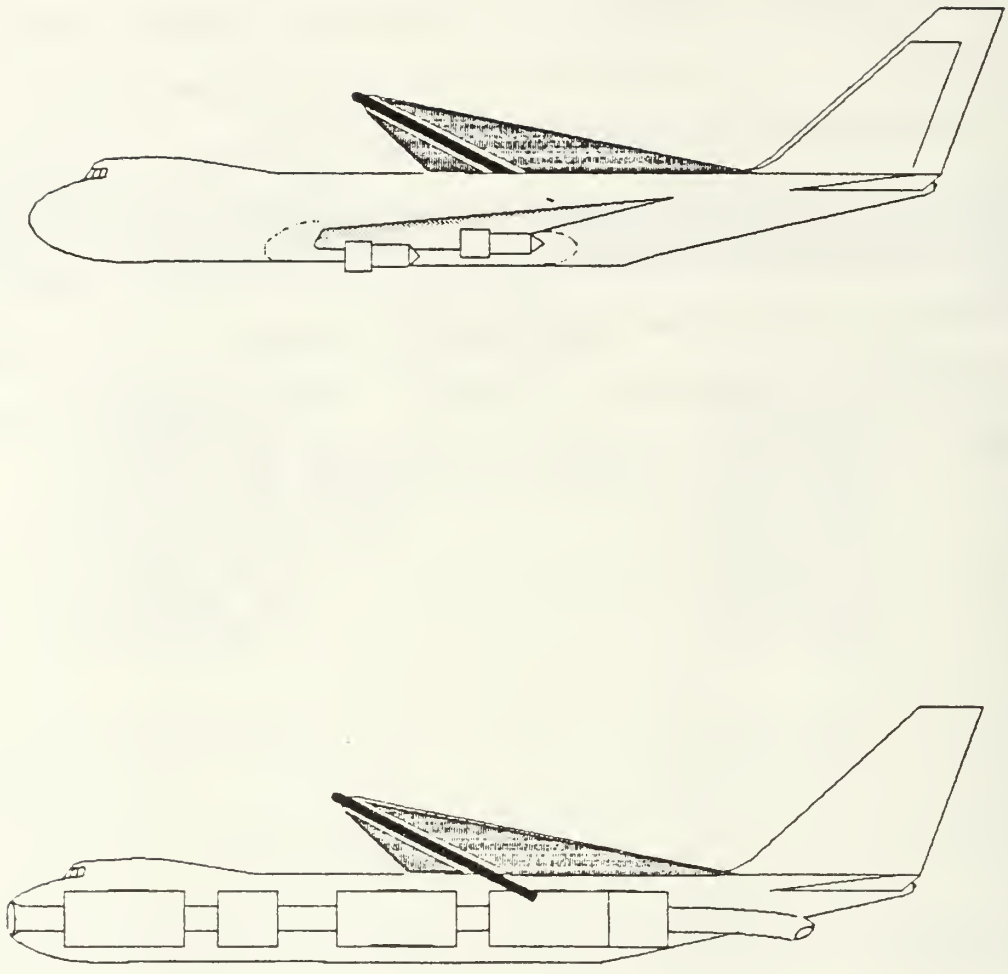

Figure 8.19 Railgun Mounted on Airplane

IX. RECOMMENDATIONS

My attitude in creating this model was to produce an efficient tool for preliminary design. For the purpose of preliminary design fast reaction time is more important than greater accuracy. Other models do exist. Some of them are very sophisticated and take more time to run. It is recommended that a comparison of the results of this model with the results of other models be performed.

The field of railgun and its auxiliary systems is advancing quickly. Many efforts are made to improve the railgun performance and its technology. The intensive research and the various projects in progress may produce new information and data. It is recommended that new information and updated data be continuously implemented into the model.

It is recommended that additional modules will be added to this package. The following topics have to be covered:

a. Weapons:
    1) High energy lasers
    2) Particle beam
    3) Kinetic energy rockets
b. Battle management
    1) Sensors
    2) Tracking

3) Computing

4) Communication

c. Non-SDI missions

1) Anti-aircraft

2) Anti-surface.

APPENDIX

THE ATARI ST-1040 COMPUTER

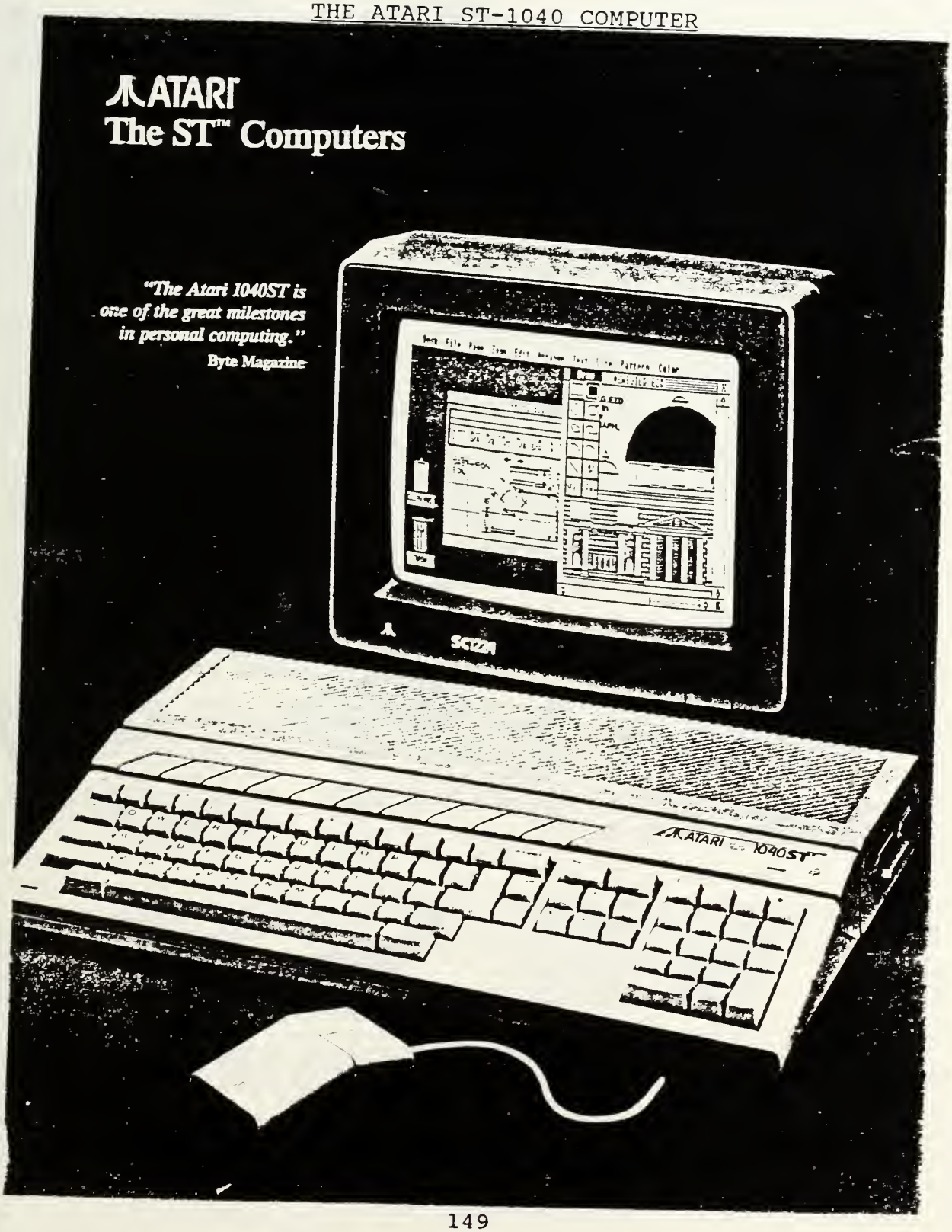

Specifications

	ATARI® 1040ST™	IBM® PC AT™	APPLE® MACINTOSH PLUS™	COMMODORE® AMIGA™
Manufacturers' List Prices*	$999 (mono) $1,199 (color)	$4,675	$2,195	$1,795
Microprocessor	68000	80286	68000	68000
Speed (MHz)	8.0	8.0	7.83	7.16
Standard User-Accessible RAM	1024K	512K	1024K	256K
Cost Per RAM Kilobyte	$0.98	$7.80	$2.14	$7.01
Operating System in ROM	Yes	No	Yes	No
Number of Keys	94	84	78	89
Mouse	Yes	No	Yes	Yes
Floppy Disk Drive	3½"	5¼"	3½"	3½"
Number of Floppy Disk Drives	1	1	1	1
Hard Disk Port	Yes	Yes	Yes	No
Color Video Capability	Yes	Optional	No	Yes
Number of Colors	512	16	None	4096
Screen Resolution: (non-interlaced mode)				
Color	640 x 200	640 x 200	None	640 x 200***
High-Res Monochrome	640 x 400	720 x 350**	512 x 342	None
Built-In MIDI Interface	Yes	No	No	No
Sound Voices	3	1	4	4

*Prices and specifications as of September, 1986. All prices are manufacturers' list prices.
**With optional monochrome board (non bit-mapped).
***Interlaced mode 640 x 400.

(1) The ATARI 520ST offers the same features as the 1040ST, except that it includes 512K RAM and a stand-alone 3½" disk drive, at a suggested retail price of $799 (monochrome monitor) and $999 (color monitor).
(2) The IBM PC is based on the Intel 8088 microprocessor, operates at a slower speed (4.77 MHz) than the PC AT, uses an 84-key keyboard, offers a 320 by 200 unit color screen resolution, and bears a suggested retail price of $2,495. The recently announced IBM PC XT™ 286 is based on the Intel 80286 microprocessor, includes 640K RAM, a 5¼" floppy disk drive and a hard disk drive, and operates at 8.0 MHz, at a suggested retail price of $3,995.
(3) The Apple Macintosh™ offers the same features as the Macintosh Plus, except that it includes 512K RAM and a 59-key keyboard, at a suggested retail price of $1,995. Apple recently announced the 8/16-bit Apple IIgs™, offering 256K RAM (expandable to one megabyte at extra cost), music and voice simulation, graphics, a mouse, and high-resolution monitor (sold separately), at apparent retail prices between $1,600 and $1,900.

Architecture
Central Processing Unit: Motorola 68000 running at 8 MHz.
Memory: 1024K RAM (1040ST); 512K RAM (520ST); 192K ROM; 128K external ROM cartridge.
Data Storage: Built-in 3½" microfloppy disk drive (1040ST), storage capacity 720K (formatted); Built-in microfloppy disk drive port; Second microfloppy disk drive optional; Built-in hard disk (DMA) port; Hard disk drive optional.

Graphics/Sound
Full bit-mapped display.
Monochrome: 640 x 400 pixels.
Color: 640 x 200 pixels x 4 colors; 320 x 200 pixels x 16 colors.
Palette range: 512 colors.
Sound: Three programmable sound channels; Programmable volume, Dynamic envelope shaping; Wave shaping, Programmable attack, decay, sustain, release.

User Interface
Keyboard: Standard QWERTY typewriter format; Separate cursor key cluster; Separate numeric keypad; 94 keys (including 10 function keys); Internal processor; Variable auto-repeat and key-click response
Mouse: Two-button control; High-precision, non-slip ball motion sensor; Removable ball for easy cleaning.

Input/Output Ports (Built-In)
Printer: 8-bit parallel
Modem: RS232C; 50–19,200 baud.
Floppy Disk Drive: 250 Kbits/second
Hard Disk Drive (DMA): 10 Mbits/second.
MIDI (Musical Instrument Digital Interface): MIDI IN; MIDI OUT/THROUGH 31.25 baud; Optically isolated receiver.
Mouse/Joystick: Two ports; Port 0: mouse/joystick. Port 1: joystick.

Operating System
The Operating System (TOS) in ROM.
Hierarchical file structure with subdirectories and path names.
GEM operating environment: Icons; Multiple windows; Window sizing/positioning/scrolling; Drop-down menus (selected with mouse).
GEM virtual device interface.

Standard Software
TOS™ Operating System
GEM™ operating environment
ST BASIC™
Desk Accessories: VT® 52 terminal emulator; Control Panel for system customization; RS232C port configuration control; Install Printer configuration control.

Physical Characteristics
1040ST: Maximum height 2¾"; Width 18¾"; Depth 11½". Internal power supply.
520ST: Maximum height 2½"; Width 18¾"; Depth 9½".

ST Peripherals

SC1224™ RGB Color Monitor & SM124™ High-Resolution Monochrome Monitor

ATARI Monitors provide sharp data displays, along with dazzling graphics. The SC1224 RGB Color Monitor flawlessly displays the ST's 512 colors. The SM124 High-Resolution Monochrome Monitor defines "state-of-the-art" with its crisp and clear video display.

SF314™ & SF354™ MicroFloppy Disk Drives

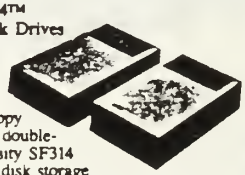

Save and protect all your data with ATARI MicroFloppy Disk Drives. The double-sided, double-density SF314 provides 720K of disk storage capacity, while the SF354 is a single-sided, double-density drive with 360K storage capacity.

SMM804™ Dot Matrix Graphics Printer

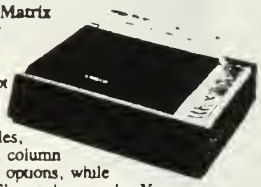

The SMM804 Dot Matrix Graphics Printer offers an array of print styles, character pitches, column widths, and other options, while supporting the ST's graphics mode. You can use the ST Computer's print screen utility to transfer hi-res designs from the computer directly to the printer.

SX212™ Modem

Here's your link to the world! This advanced modem lets your ST communicate via telephone line with other computers. Two modems in one: a low speed (300 baud) and a high speed (1200 baud). And it provides auto dial and auto answer features.

SH204™ Hard Disk Drive

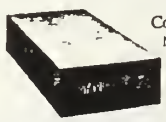

Connecting the SH204 20 megabyte hard disk drive to your system lets you take advantage of the 1040ST's built-in, high-speed DMA channel (hard disk port). Data transfer (read/write) to and from the drive is virtually instantaneous. High-speed data transfers and 20 megabytes of disk storage all at an incredibly low cost.

ATARI

ATARI, SC1224, SF314, SF354, SH204, SM124, SMM804, ST, ST BASIC, SX212, TOS, 520ST, and 1040ST are trademarks of Atari Corporation.
Activision is a trademark of Activision, Inc. Apple and IIgs are trademarks of Apple Computer, Inc. VT is a trademark of Digital Equipment Corporation. GEM is a trademark of Digital Research, Inc. Amiga is a trademark of Commodore-Amiga, Inc. Commodore is a trademark of Commodore Business Machines, Inc. Macintosh and Macintosh Plus are trademarks licensed to Apple Computer, Inc. AT, XT, and IBM are trademarks of International Business Machines Corporation. Microsoft is a trademark of Microsoft Corporation. Spinnaker is a trademark of Spinnaker Software Corporation.
©1986 Atari Corporation. All Rights Reserved. Printed in U.S.A. C034004 Rev. A

LIST OF REFERENCES

1. Regan, F.Y., Re-Entry Vehicles Dynamics, AIEE Series, 1986, Chapter 6.

2. Regan, F.Y., Re-Entry Vehicles Dynamics, AIEE Series, 1986, Chapter 9.

3. Lindsey, G.H. and Redmon., Tactical Missile Design, Department of the Navy, Chapter 9.

4. Barber, Y.P., The Acceleration of Macroparticles in a Hypervelocity Acclerator, Ph.D. Thesis, The Australian National University, 1972.

5. Rice, E.E., Miller, L.A. and Earhart, R.W., "Preliminary Feasibility Assessment for Earth-to-Space electromagnetic Launchers," Columbus Laboratries, June 1982.

6. Prof. Woehler, "The Railgun Class Notes," Naval Postgraduate School, Monterey, California, class notes for Course No. PH 4856, March 1987.

7. Agrawal, B.N., Design of Geosynchronous Spacecraft, Prentice Hall, 1986.

8. IEEE Transactions of Magnetic 3rd Symposium on Electromagnetic Launch Technology, IEEE Magnetic Society, November 1986.

9. Hicks, T.G., Standard Handbook of Engineering Calculations, McGraw-Hill, Second Edition, 1985.

10. Tauber, M.E., Trajectory Characteristics and Heating of Hypervelocity Projectiles Having Large Ballistic Coefficients, NASA Ames, 1986.

11. Neta, B. and Y. Ilan-Lipowski, "A New Conservative Scheme for Solving the Two Body Problem," unpublished manuscript, Naval Postgraduate School, Monterey, California, 1987.

INITIAL DISTRIBUTION LIST

		No. Copies
1.	Defense Technical Information Center Cameron Station Alexandria, Virginia 22304-6145	2
2.	Library, Code 0142 Naval Postgraduate School Monterey, California 93943-5002	2
3.	Professor B. Neta, Code 53Nd Naval Postgraduate School Monterey, California 93943-5000	6
4.	Professor M.F. Platzer, Code 67Pl Naval Postgraduate School Monterey, California 93943-5000	3
5.	Professor H. Woehler, Code 61 Department of Physics Naval Postgraduate School Monterey, California 93943-5000	1
6.	Professor A. Fuhs, Code 67Fu Naval Postgraduate School Monterey, California 93943-5000	1
7.	Dr. D. Parks Naval Surface Weapons Center, K-13 Dahlgren, Virginia 22448	3
8.	Br. General Y. Shanie, Air Attache Israeli Embassy 3514 International Drive Washington, D.C. 20008	2
9.	Y. Ilan-Lipowsky 27 Zimchey Hayehudim str. Tel-Aviv, ISRAEL	6

1M354/7

DUDLEY KNOX LIBRARY
NAVAL POSTGRADUATE SCHOOL
MONTEREY, CALIFORNIA 93943-5002

Thesis
I255
c.1
Ilan-Lipowsky
Mathematical models
for the S.D.I.

Thesis
I255
c.1
Ilan-Lipowsky
Mathematical models
for the S.D.I.

thesl255
Mathematical models for the S.D.I.
3 2768 000 73414 9
DUDLEY KNOX LIBRARY